

¹ **Introduction to the Fractional Distribution Families**

² Stephen Horng-Twu Lihn

³ stevelihn@gmail.com

⁴ Version: Draft 2026-01

⁵ ORFE, Princeton University

⁶ Dedicated to Professor John M. Mulvey for his 80th birthday in 2025.

⁷ (as of January 25, 2026)

Contents

10	Chapter 1. Introduction	1
11	Part 1. Mathematical Functions	
13	2.1. One-Sided Distribution	
15	2.3. Ramanujan's Master Theorem	
17	3.1. Definition	
19	3.3. The M-Wright Functions	
21	3.5. The Elasticity Operator	
23	3.7. Numerical Methods of the M-Wright Functions	
25	4.1. Classic Result	
27	4.3. Ratio Distribution Approach	
29	Chapter 5. Fractional Hypergeometric Functions	
31	5.2. Fractional Gauss Hypergeometric Function	
33	Chapter 6. FG: Fractional Gamma Distribution	
35	6.2. Determination of C	
37	6.4. Mellin Transform	
39	6.6. Inverse Expression of Several Fractional Distributions	
41	Chapter 7. Fractional Chi Distributions	
43	7.2. FCM: Fractional Chi-Mean Distribution	i

44	7.3. FCM Moments	36
45	7.4. FCM Reflection Formula and Negative k	37
46	7.5. FCM2: Fractional Chi-Squared-Mean Distribution	38
47	7.6. FCM2 Mellin Transform	39
48	7.7. FCM2 Moments	39
49	7.8. FCM2 Increment of k	40
50	7.9. Sum of Two Chi-Squares with Correlation	40
51	Chapter 8. Fractional F Distribution	41
52	8.1. Definition	41
53	8.2. PDF at Zero	42
54	8.3. Mellin Transform	42
55	8.4. Moments	42
56	8.5. Sum of Two Fractional Chi-Square Mixtures with Correlation	43
57	8.6. Fractional Adaptive F Distribution	43
58	Chapter 9. The Framework of Continuous Gaussian Mixture	45
59	9.1. The Inverse Chi Distribution	45
60	9.2. The Characteristic Distributions	46
61	9.3. Summary of Gaussian Mixture	47
62	9.4. FCM Extensions	47
63	Part 3. Two-Sided Univariate Distributions	51
64	Chapter 10. SN: The Skew-Normal Distribution - Review	53
65	10.1. Definition	53
66	10.2. The Location-Scale Family	54
67	10.3. Invariant Quantities	54
68	10.4. Mellin Transform	55
69	10.5. Moments	56
70	Chapter 11. GAS: Generalized Alpha-Stable Distribution (Experimental)	59
71	11.1. Definition	59
72	11.2. Limitation	60
73	11.3. Workaround	61
74	11.4. Moments	63
75	Chapter 12. GAS-SN: Generalized Alpha-Stable Distribution with Skew-Normal	65
76	12.1. Definition	65
77	12.2. The Location-Scale Family	66
78	12.3. Mellin Transform	66
79	12.4. Moments	66
80	12.5. Tail Behavior	68
81	12.6. Maximum Skewness and Half GSaS	69
82	12.7. Fractional Skew Exponential Power Distribution	71
83	12.8. Quadratic Form	71
84	12.9. Univariate MLE	71
85	12.10. Examples of Univariate MLE Fits	72
86	Chapter 13. Fractional Feller Square-Root Process	75
87	13.1. Generation of Random Variables for FCM	76

88	13.2. Generation of Random Variables for FCM2	77
89	Part 4. Multivariate Distributions	79
90	Chapter 14. Multivariate SN Distribution - Review	81
91	14.1. Definition	81
92	14.2. The Location-Scale Family	82
93	14.3. Quadratic Form	82
94	14.4. Stochastic Representation	82
95	14.5. Moments	83
96	14.6. Canonical Form	84
97	14.7. 1D Marginal Distribution	84
98	Chapter 15. Multivariate GAS-SN Elliptical Distribution	87
99	15.1. Definition	87
100	15.2. Location-Scale Family	87
101	15.3. Moments	87
102	15.4. Canonical Form	88
103	15.5. Marginal 1D Distribution	88
104	15.6. Quadratic Form	88
105	15.7. Multivariate MLE	89
106	Chapter 16. Multivariate GAS-SN Adaptive Distribution (Experimental)	91
107	16.1. Definition	91
108	16.2. Location-Scale Family	91
109	16.3. Moments	91
110	16.4. Canonical Form	92
111	16.5. Marginal 1D Distribution	92
112	16.6. Quadratic Form	92
113	16.7. 2D Adaptive MLE	92
114	Chapter 17. Fitting SPX-VIX Daily Returns with Bivariate Distributions	95
115	17.1. Elliptical Fit	95
116	17.2. Adaptive Fit	100
117	Appendix A. List of Useful Formula	105
118	A.1. Gamma Function	105
119	A.2. Transformation	105
120	A.3. Half-Normal Distribution	106
121	Bibliography	107

CHAPTER 1

Introduction

In quantitative finance, we often encounter asset return data with prominent skewness and kurtosis. In the domain of portfolio optimization and the market regime model[13, 29, 23], a showcase example is the S&P 500 Index (SPX) and the CBOE Volatility Index (VIX), whose daily prices are publicly available since 1990¹. Such data sets are easy to obtain, but it is difficult to fit them with an existing parametric distribution. Even with many probability distributions available in modern statistical software, such as `scipy.stats`, they do not work well.

In this book, a multivariate elliptical distribution system based on the Wright function[34, 35, 2] is presented. It combines and extends the α -stable distribution[12] with the multivariate skew-t distribution[1]. This super-distribution family can fit real-world data sets with pronounced fat tails more accurately.

In more detail, the daily return distribution of VIX has a high kurtosis of 16, and a skewness of 2.0. Its standardized peak density is approximately 0.55. (see Figure 12.5). Theoretically, the excess kurtosis of the t distribution[31] is $6/(k - 4)$ for $k > 4$. Such kurtosis would put k very close to 4. However, the theoretical standardized peak density is only 0.53 at $k = 4$. The VIX data already push the t distribution to the limit, so to speak.

The daily return distribution of SPX is even more peculiar (see Figure 12.6). In addition to its high kurtosis of 11, its standardized peak density is approximately 0.65. It takes the t distribution of about 3 degrees of freedom ($k \approx 3$) to produce a reasonable fit. However, theoretically, finite kurtosis does not exist until $k > 4$.

These two examples demonstrate mathematical issues when fitting an existing parametric distribution. It is difficult to satisfy both the kurtosis and the peak density simultaneously.

Our new multivariate distribution is able to fit both data sets with satisfactory accuracy while matching empirical skewness, kurtosis, and peak density. Not only is the goodness-of-fit compared in terms of the density function but also how well the tails are captured by the distribution via the quadratic form. We will present these fits in Chapter 17.

The word "fractional" can be roughly understood as adding the Lévy stability index $\alpha \in [0, 2]$ to a known distribution. For example, in the Mellin transform of the PDF of a distribution, $\Gamma(s + c)$ in the classic world becomes $\Gamma(\alpha s + c)$ or $\Gamma(s/\alpha + c)$ in the fractional world. When the coefficient of s is $\frac{1}{2}$, 1, or 2, the fractional distribution subsumes the classic distribution, since the Legendre duplication formula (A.2) becomes applicable.

The change may look simple in the Mellin space. But when it is transformed back to the x space, things become quite complicated. That is what makes it interesting and powerful.

The most important chapters of the book are

- Chapter 12 on the univariate GAS-SN distribution and
- Chapter 15 on the multivariate GAS-SN elliptical distribution.

¹SPX data: Courtesy of S&P Dow Jones Indices LLC, from <https://fred.stlouisfed.org/series/SP500>. VIX data: Courtesy of Chicago Board Options Exchange (CBOE), from <https://fred.stlouisfed.org/series/VIXCLS>). Retrieved from FRED, Federal Reserve Bank of St. Louis. Not for commercial use.

159 The reader can think that the entire book is aimed at developing tools in order to create these two
 160 distributions.

161 The univariate GAS-SN distribution is supposed to be the most flexible two-sided distribution up
 162 to date for statisticians to fit a univariate data set, such as return distributions in finance.

163 The multivariate GAS-SN elliptical distribution is intended to be the most flexible multivariate
 164 distribution to date that extends the multivariate skew-t and skew-normal distributions[1].

165 A reference implementation can be found on Github at: <https://github.com/slihn/gas-impl>

166

167 This book is divided into three parts.

168 Part I describes the mathematical foundation needed for the construction of fractional distribu-
 169 tions. It contains several higher transcendental functions. Several classic special functions are extended
 170 with a fractional parameter.

171 Each distribution has its density function (PDF) and distribution function (CDF). Its Mellin
 172 transform. The squared variable or quadratic forms. Therefore, new mathematical tools are needed
 173 to address them.

174 Part II contains the univariate one-sided fractional distributions that are invented. All of them
 175 have their classic counterparts. For example, the generalized gamma distribution (GG) is upgraded.
 176 All the χ and F related distributions are also upgraded.

177 Part III contains the two-sided univariate fractional distributions. The Azzalini (2013) book is used
 178 as the blueprint[1]. It is integrated with the symmetric distributions developed in my 2024 work[15].

179 This book can be viewed as an integration between the two works, literally going chapter-by-
 180 chapter. The consistency of such integration and harmony speaks volumes.

181 The fourth part contains the multivariate fractional distributions. These distributions are the
 182 super families of Part III. They subsumes and all the SN/ST distributions mentioned in Azzalini's
 183 book.

184 The major strength of fractional distributions integrated with SN is its ability to address a very
 185 wide range of skewness, kurtosis, and peak probability density. This allows a statistician to describe
 186 the statistics of her data set properly.

187 In the modern computer age, large amounts of data are collected in terms of both dimensionality
 188 and the number of samples. Tail behavior becomes more obvious. In the domain of finance, it is
 189 increasingly important to adequately capture the properties of the left tail.

190 An adaptive version of the multivariate distribution is developed to allow each dimension to have
 191 its own set of shape parameters. This distribution is where the rubber means the road. It is used to
 192 fit one of the most difficult data sets in finance: the daily returns from the SPX and VIX indices since
 193 1990. And it works. The methodologies are presented.

194

195 Although the two multivariate distributions present new opportunities to fit the data sets that
 196 were thought impossible formerly, the outcomes post new challenges.

197 On the one hand, the maximum likelihood estimate (MLE) can be implemented in a straightfor-
 198 ward manner for the elliptical distribution. The output (Figures 17.1, 17.2, 17.3) shows a very nice fit
 199 by MLE. But its choice of (α, k) lies in an area near infinite kurtosis when the bivariate distribution
 200 is projected to its two marginal 1D distributions. This behavior is quite puzzling.

201 On the other hand, the adaptive distribution suffers from the curse of dimensionality. A direct
 202 MLE approach is computationally prohibitive. A modified fitting algorithm is used. The output
 203 (Figures 17.4, 17.5, 17.6) is reasonable, but with a few flaws. The SPX marginal near $\alpha = 1, k = 3$
 204 is intrinsically challenging. It is difficult to have a theoretical correlation coefficient that matches the
 205 empirical value (about -0.7). In the absolute term, the former is always lower than the latter. The
 206 quadratic form has not yet a matching F distribution.

207 Hope you enjoy this new statistical and mathematical adventure.

208

Part 1

209

Mathematical Functions

CHAPTER 2

Mellin Transform

210

211 We begin the book with some mathematical foundations. The reader who wishes to dive into the
 212 statistical distributions can skip the next two chapters.

213 The Mellin transform is crucial in the analysis of a statistical distribution. It is named after the
 214 Finnish mathematician Hjalmar Mellin, who first proposed it in 1897[21]. It provides insight into
 215 the inner workings of a statistical distribution and makes it analytically tractable. Once the Mellin
 216 transform of the density function (PDF) is known, the moment formula of the distribution is also
 217 known. In addition, derivatives of the PDF can also be obtained.

218 In particular, the relations between the Wright function, the α -stable distribution, and the frac-
 219 tional χ distribution are best described by their Mellin transforms.

220

221 DEFINITION 2.1. This chapter provides an overview of the Mellin transform. Following the notation
 222 of [19], the Mellin transform of a function $f(x)$ properly defined for $x \geq 0$ is

$$(2.1) \quad f^*(s) := \mathcal{M}\{f(x); s\} = \int_0^\infty f(x) x^{s-1} dx, \quad c_1 < \Re(s) < c_2.$$

223 The role of c_1, c_2 will be explained in the following.

224 If $f^*(s)$ has analytic continuation on the complex plane, the inverse Mellin transform is

$$(2.2) \quad f(x) = \mathcal{M}^{-1}\{f^*(s); x\} = \frac{1}{2\pi i} \int_{C-i\infty}^{C+i\infty} f^*(s) x^{-s} ds, \quad c_1 < C < c_2.$$

225 From (2.1), it is obvious that the Mellin transform is directly related to the moments of a distri-
 226 bution. When $f(x)$ is the PDF of a one-sided distribution, its n -th moment is $\mathbb{E}(X^n|f) = f^*(n+1)$.

227 Hence, by modifying the Mellin transform $f^*(s)$, it is equivalent to constructing a new distribution
 228 based on the original distribution.

229 Introducing the juxtaposition notation $\xleftrightarrow{\mathcal{M}}$, the above expressions, (2.1) and (2.2), are consolidated
 230 to a one-liner: $f(x) \xleftrightarrow{\mathcal{M}} f^*(s)$, with a valid range $c_1 < C < c_2$ for C . This notation is much
 231 more concise. A correct specification for C is required when performing the Mellin integral in (2.2)
 232 numerically. Otherwise, it is irrelevant to the readers most of the time.

233 LEMMA 2.2. The main rules of Mellin transform used in this paper are:

$$(2.3) \quad f(ax) \xleftrightarrow{\mathcal{M}} a^{-s} f^*(s), \quad a > 0$$

$$(2.4) \quad x^k f(x) \xleftrightarrow{\mathcal{M}} f^*(s+k),$$

$$(2.5) \quad f(x^p) \xleftrightarrow{\mathcal{M}} \frac{1}{p} f^*(s/p), \quad p \neq 0$$

and the following ones involving an integral,

$$(2.6) \quad h(x) = \int_0^\infty f(xs)g(s) s ds \xleftrightarrow{\mathcal{M}} h^*(s) = f^*(s)g^*(2-s), \quad (\text{ratio distribution})$$

$$(2.7) \quad \gamma_f(x) = \int_0^x f(x) dx \xleftrightarrow{\mathcal{M}} -s^{-1}f^*(s+1), \quad (\text{lower incomplete function})$$

$$(2.8) \quad \Gamma_f(x) = \int_x^\infty f(x) dx \xleftrightarrow{\mathcal{M}} s^{-1}f^*(s+1). \quad (\text{upper incomplete function})$$

The ratio distribution rule (2.6) is widely used in our fractional distribution system. Notice that the argument of $g^*(s)$ is transformed via $s \rightarrow 2-s$.

For (2.7) and (2.8), the valid range of C is decremented by one: $c_1 - 1 < C < c_2 - 1$. \triangle

238

EXAMPLE 2.3. A simple exercise is the Mellin transform of the standard normal distribution. It starts with

$$e^{-x} \xleftrightarrow{\mathcal{M}} \Gamma(s)$$

via the definition of the gamma function itself.

By applying (2.5) then (2.3), we get

$$(2.9) \quad \mathcal{N}(x) \xleftrightarrow{\mathcal{M}} \mathcal{N}^*(s) = \frac{2^{(s-3)/2}}{\sqrt{\pi}} \Gamma\left(\frac{s}{2}\right)$$

where $\mathcal{N}(x) = \frac{1}{\sqrt{2\pi}} e^{-x^2/2}$ is our notation for the PDF of a standard normal distribution.

EXAMPLE 2.4. A slightly more complicated exercise is the Mellin transform of the PDF of the fractional gamma distribution (FG) in Chapter 6. But we only work out its skeleton here.

Assume we have a function $F_\alpha(x)$ whose Mellin transform is

$$F_\alpha(x) \xleftrightarrow{\mathcal{M}} \frac{\Gamma(s)}{\Gamma(\alpha s)}.$$

It undergoes the following transforms:

$$\begin{aligned} F_\alpha(x^p) &\xleftrightarrow{\mathcal{M}} \frac{1}{|p|} \frac{\Gamma(s/p)}{\Gamma(\alpha s/p)}, \\ x^{d-1} F_\alpha(x^p) &\xleftrightarrow{\mathcal{M}} \frac{1}{|p|} \frac{\Gamma((s+d-1)/p)}{\Gamma(\alpha(s+d-1)/p)}, \end{aligned}$$

which is the prototype of FG before further normalization.

2.1. One-Sided Distribution

When the subject matter is a probability distribution, the two rules of incomplete functions, (2.7) and (2.8), provide a clear path to obtain its distribution function (CDF) while $f(x)$ is associated with its density function (PDF).

For a one-sided distribution denoted f , it is straightforward to define it, since the domain of the distribution $x \geq 0$ is exactly the same as the domain of the Mellin transform. Hence, $f(x)$ is exactly its density function and $\gamma_f(x)$ is its CDF.

By assigning $s = n + 1$, its n -th moment is

$$(2.10) \quad \mathbb{E}(X^n|f) = f^*(n+1)$$

The zeroth moment is the total density that should be normalized to one. That is $f^*(1) = 1$.

The mean of the distribution is $\mathbb{E}(X|f) = f^*(2)$. For a distribution whose mean needs to be determined, for instance, the fractional χ distribution in Chapter 7, this formula is useful.

260

2.2. Two-Sided Distribution

261

When the distribution is two-sided, one more rule is needed.

262

DEFINITION 2.5 (The Reflection Rule). Assume the distribution is two sided, its domain of support is $x \in \mathbb{R}$. The reflection rule requires that its density function $f(x)$ is based on a skew parameter $\beta \in \mathbb{R}$ that satisfies

263

$$(2.11) \quad f(-x; \beta) := f(x; -\beta) \quad \text{for } x > 0.$$

264

Let $c_\beta < 1$ be the one-sided integral of

$$c_\beta = \int_0^\infty f(x; \beta) dx.$$

265

(2.11) leads to $c_{-\beta} + c_\beta = 1$ since $\int_{-\infty}^\infty f(x; \beta) dx = 1$.

2.2.1. Mellin Transform of a Two-sided CDF.

266

LEMMA 2.6. The Mellin transform of the CDF $\Phi(x)$ of a two-sided distribution has two parts.

267

Both can be derived from its density function transform, $f(x; \beta) \xleftrightarrow{\mathcal{M}} f^*(s; \beta)$, in the positive domain.

268

From (2.7), let $\gamma_f(x; \beta) \xleftrightarrow{\mathcal{M}} \Phi^*(s; \beta) := -s^{-1} f^*(s+1; \beta)$. Then for $x > 0$, the Mellin transform of the CDF can be expressed as

$$\begin{aligned} \Phi(x) - \Phi(0) &\xleftrightarrow{\mathcal{M}} \Phi^*(s; \beta), \\ 1 - \Phi(0) - \Phi(-x) &\xleftrightarrow{\mathcal{M}} \Phi^*(s; -\beta). \end{aligned}$$

269

△

PROOF. Note that $\Phi(0) = c_{-\beta} = 1 - c_\beta$. When $x \geq 0$, its CDF is

$$\Phi(x) = \int_{-\infty}^x f(x; \beta) dx = c_{-\beta} + \int_0^x f(x; \beta) dx = \Phi(0) + \gamma_f(x; \beta).$$

270

In the negative domain, its CDF is

$$\begin{aligned} \Phi(-x) &= \int_{-\infty}^{-x} f(x; \beta) dx = \int_x^\infty f(x; -\beta) dx \\ &= 1 - \Phi(0) - \int_0^x f(x; -\beta) dx = 1 - \Phi(0) - \gamma_f(x; -\beta). \end{aligned}$$

271

□

272

The point is that, once the Mellin transform of either the PDF or CDF is known, the other one can be derived by simple algebraic rules.

273

2.2.2. From Mellin Transform to Moments. By assigning $s = n + 1$, it is easy to show that its n -th moment is

$$(2.12) \quad \mathbb{E}(X^n | f) = f^*(n+1; \beta) + (-1)^n f^*(n+1; -\beta)$$

$$(2.13) \quad = -n [\Phi^*(n; \beta) + (-1)^n \Phi^*(n; -\beta)]$$

274

The moment formula is tightly linked to $\Phi^*(n; \beta)$.

275

The Zeroth Moment. The total density can be regarded as the zeroth moment. Hence, c_β can be determined by

$$(2.14) \quad c_\beta = \int_0^\infty f(x; \beta) dx = f^*(1; \beta).$$

276

Its application is in (10.9).

284 **2.3. Ramanujan's Master Theorem**

285 In order to keep things simple, we describe all the distributions via the Mellin transform of their
 286 PDFs. Due to Ramanujan's master theorem[3], not only can the moments be obtained from the Mellin
 287 transform but also all the derivatives of the PDF at $x = 0$. We get its series representation "for free",
 288 so to speak.

289 LEMMA 2.7 (Ramanujan's master theorem). If $f(x)$ has an expansion of the form

$$(2.15) \quad f(x) = \sum_{n=0}^{\infty} \frac{\varphi(n)}{n!} (-x)^n$$

290 then its Mellin transform is given by

$$(2.16) \quad f(x) \xleftrightarrow{\mathcal{M}} f^*(s) = \Gamma(s) \varphi(-s)$$

291 △

292 Assume that $g^*(s) := f^*(s)/\Gamma(s)$ exists on the complex plane, $s \in \mathbb{C}$. Its connection to the
 293 derivatives of the PDF at $x = 0$ is as follow.

294 LEMMA 2.8. The Taylor series of $f(x)$ is

$$f(x) = \sum_{n=0}^{\infty} \frac{f^{(n)}(0)}{n!} x^n$$

295 where $f^{(n)}(0)$ is the n -th derivative of $f(x)$ at $x = 0$.

296 Then $f^{(n)}(0)$ can be obtained from $g^*(s)$ by

$$(2.17) \quad f^{(n)}(0) = (-1)^n g^*(-n)$$

297 At $x = 0$, we have $f(0) = g^*(0)$.

298

299 △

300 The power of the master theorem is that, once the Mellin transform is known, the Taylor series is
 301 also known immediately. We provide a contrived example from next chapter as a showcase.

302 EXAMPLE 2.9. The Mellin transform of the Wright function from (3.5) is $f(-x) \xleftrightarrow{\mathcal{M}} f^*(s) =$
 303 $\Gamma(s)/\Gamma(\delta - \lambda s)$. Then its $g^*(s) = 1/\Gamma(\delta - \lambda s)$.

304 According to Lemma 2.8, its Taylor series should be

$$f(-x) := \sum_{n=0}^{\infty} \frac{(-1)^n g^*(-n)}{n!} x^n = \sum_{n=0}^{\infty} \frac{g^*(-n)}{n!} (-x)^n$$

305 Replace $-x$ with z , and plug in $g^*(-n)$, we have

$$f(z) := \sum_{n=0}^{\infty} \frac{z^n}{n! \Gamma(\lambda n + \delta)}$$

306 This is the series representation (3.1) where we essentially "derived" it from the master theorem.

307 The major application in this book is in Chapter 11. In the experimental construction of the
 308 generalized α -stable distribution, the theorem is used to remedy the discontinuity of the PDF in
 309 $x = 0$.

310 2.3.1. Distribution Function. The form of the Mellin transform in (2.16) has an important
 311 implication when $f(x)$ is a density function.

LEMMA 2.10. Assume $x > 0$, its complimentary distribution function $\Gamma_f(x) := \int_x^\infty f(x) dx$ has the series representation of

$$(2.18) \quad \Gamma_f(x) = \sum_{n=0}^{\infty} \frac{\varphi(n-1)}{n!} (-x)^n$$

314 △

PROOF. From (2.8), the Mellin transform of $\Gamma_f(x)$ is

$$\Gamma_f(x) = \int_x^\infty f(x) dx \xrightarrow{\mathcal{M}} s^{-1} f^*(s+1)$$

316 which can be simplified to

$$s^{-1}f^*(s+1) = s^{-1}\Gamma(s+1)\varphi(-s-1)$$

$$= \Gamma(s)\varphi(-s-1).$$

³¹⁷ This is still in the form of (2.16), with a transformation rule of $s \rightarrow s + 1$ in the function $\varphi(-s)$.

318 Applying the master theorem of (2.15), we get (2.18).

We use the CDF of the M-Wright function from (3.16) as an example.

LEMMA 2.11. The goal is to show

$$(2.19) \quad \int_x^\infty M_\alpha(t) dt = W_{-\alpha,1}(-x).$$

PROOF. We start with the Mellin transform of $M_\alpha(x)$ from (3.13),

$$M_\alpha(x) \xleftrightarrow{\mathcal{M}} M_\alpha^*(s) = \frac{\Gamma(s)}{\Gamma((1-\alpha)+\alpha s)}$$

³²⁴ which yields $\varphi(-s) = 1/\Gamma((1-\alpha)+\alpha s)$.

Therefore, its $\Gamma_f(x)$ should be

$$\Gamma_f(x) = \sum_{n=0}^{\infty} \frac{1}{n! \Gamma((1-\alpha) - \alpha(n-1))} (-x)^n = \sum_{n=0}^{\infty} \frac{1}{n! \Gamma(-\alpha n + 1)} (-x)^n$$

which is $W_{-\alpha,1}(-x)$ according to (3.1).

327

CHAPTER 3

328

The Wright Function

329

3.1. Definition

330 The Wright function is the most basic building block in our fractional distribution system. It was
 331 proposed by E. M. Wright in the 1930s[34, 35]. Bateman recorded this function together with the
 332 Mittag-Leffler function in the 1930s[2].

333 Its importance was gradually noticed since the late 1980's, especially through the works of F.
 334 Mainardi, who proposed the M-Wright function $M_\alpha(x)$. $M_\alpha(x)$ is considered the fractional extension
 335 of the exponential function e^{-x} . Such logic appears in many places of this book. This chapter provides
 336 an overview.

337 DEFINITION 3.1. The series representation of the Wright function is

$$(3.1) \quad W_{\lambda,\delta}(z) := \sum_{n=0}^{\infty} \frac{z^n}{n! \Gamma(\lambda n + \delta)} \quad (\lambda \geq -1, z \in \mathbb{C})$$

338

339 Its shape parameters are pairs (λ, δ) . The apparent limit is $W_{0,1}(z) = e^z$.

340 The author used four variants extensively. The first group of two are

- $M_\alpha(z) := W_{-\alpha,1-\alpha}(-z)$
- $F_\alpha(z) := W_{-\alpha,0}(-z)$

343 where $\alpha \in [0, 1]$. They are related to each other by $M_\alpha(z) = F_\alpha(z)/(\alpha z)$.

344 In particular, $M_\alpha(z)$ is called *the M-Wright function* or simply *the Mainardi function*[16, 20, 17].
 345 See Section 3.3 for further details. Conceptually, *fractional extension* of a classic exponential-based
 346 function is based on two important properties: $M_0(z) = \exp(-z)$ and $M_{\frac{1}{2}}(z) = \frac{1}{\sqrt{\pi}} \exp(-z^2/4)$.

347 The second group of the two are

- $W_{-\alpha,-1}(-z)$
- $-W_{-\alpha,1-2\alpha}(-z)$

350 The author discovers their usefulness. They are associated with the derivatives of $F_\alpha(z)$ and $M_\alpha(z)$,
 351 for the generation of random variables, such as in (3.18) and Section 11 of [15]. In some cases, they
 352 lead to beautiful polynomial solutions.

353

3.2. Classic Results

354 The recurrence relations of the Wright function are (Chapter 18, Vol 3 of [2])

$$(3.2) \quad \lambda z W_{\lambda,\lambda+\mu}(z) = W_{\lambda,\mu-1}(z) + (1-\mu)W_{\lambda,\mu}(z)$$

$$(3.3) \quad \frac{d}{dz} W_{\lambda,\mu}(z) = W_{\lambda,\lambda+\mu}(z)$$

355 The moments of the Wright function are (See (1.4.28) of [20])

$$(3.4) \quad \mathbb{E}(X^{d-1}) = \int_0^\infty x^{d-1} W_{-\lambda,\delta}(-x) dx = \frac{\Gamma(d)}{\Gamma(d\lambda + \delta)}$$

356 The way it is written is in fact its Mellin transform:

$$(3.5) \quad W_{\lambda,\delta}(-x) \xleftrightarrow{\mathcal{M}} W_{\lambda,\delta}^*(s) = \frac{\Gamma(s)}{\Gamma(\delta - \lambda s)}$$

357 $W_{\lambda,\delta}(z)$ has the following Hankel integral representation:

$$(3.6) \quad W_{\lambda,\delta}(z) = \frac{1}{2\pi i} \int_H dt \frac{\exp(t + z t^{-\lambda})}{t^\delta}$$

358 Prodanov[27] derived an integral form of the Wright function. We focus on the branch of $\lambda < 0$
359 and $\delta \leq 1$ from Theorem 1 there, such that

$$(3.7) \quad W_{\lambda,\delta}(z) = \frac{1}{\pi} \int_0^\infty \frac{dr}{r^\delta} \sin(\sin(\lambda\pi)w + \delta\pi) e^{\cos(\lambda\pi)w - r}, \quad \text{where } w = z r^{-\lambda}.$$

360 This integral can be calculated by the tanh-sinh quadrature with a reasonable speed.

361 The four-parameter Wright function is defined as

$$(3.8) \quad W_{\lambda, \mu}^{[a, b]}(z) := \sum_{n=0}^{\infty} \frac{z^n}{\Gamma(n+1)} \frac{\Gamma(an+b)}{\Gamma(\lambda n + \mu)}$$

362 This function is a higher-order Wright function. It was used seriously for the first time by the
363 author[15].

3.3. The M-Wright Functions

364 Mainardi has introduced two auxiliary functions of Wright type (see F.2 of [16]). Assume $\alpha \in [0, 1]$,

$$(3.9) \quad F_\alpha(z) := W_{-\alpha,0}(-z) \quad (z > 0)$$

$$(3.10) \quad M_\alpha(z) := W_{-\alpha,1-\alpha}(-z) = \frac{1}{\alpha z} F_\alpha(z) \quad (z > 0)$$

366 The relation between $M_\alpha(z)$ and $F_\alpha(z)$ in (3.10) is an application of (3.2) by setting $\lambda = -\alpha, \mu = 1$.

367 $F_\alpha(z)$ has the following Hankel integral representation:

$$(3.11) \quad F_\alpha(z) = \frac{1}{2\pi i} \int_H dt \exp(t - z t^\alpha)$$

368 Both functions have simple Mellin transforms from (3.5):

$$(3.12) \quad F_\alpha(x) \xleftrightarrow{\mathcal{M}} F_\alpha^*(s) = \frac{\Gamma(s)}{\Gamma(\alpha s)}$$

$$(3.13) \quad M_\alpha(x) \xleftrightarrow{\mathcal{M}} M_\alpha^*(s) = \frac{\Gamma(s)}{\Gamma((1-\alpha)+\alpha s)}$$

369 $F_\alpha(z)$ is used to define fractional one-sided distributions. But its series representation isn't very
370 useful computationally. It requires many more terms to converge to a prescribed precision.

371 On the other hand, $M_\alpha(z)$ has a more computationally friendly series representation, especially
372 for small α 's:

$$(3.14) \quad M_\alpha(z) = \sum_{n=0}^{\infty} \frac{(-z)^n}{n! \Gamma(-\alpha n + (1-\alpha))} = \frac{1}{\pi} \sum_{n=1}^{\infty} \frac{(-z)^{n-1}}{(n-1)!} \Gamma(\alpha n) \sin(\alpha n \pi) \quad (0 < \alpha < 1)$$

373 $M_\alpha(z)$ also has very nice analytic properties at $\alpha = 0, 1/2$, where $M_0(z) = \exp(-z)$ and $M_{\frac{1}{2}}(z) =$
374 $\frac{1}{\sqrt{\pi}} \exp(-z^2/4)$. $M_\alpha(0) = 1/\Gamma(1-\alpha)$ is monotonically decreasing from 1 to 0 as α increases from 0 to
375 1.

376 $M_\alpha(z)$ can be computed to high accuracy when properly implemented with arbitrary-precision
377 floating point library, such as the mpmath package[22]. In this regard, it is much more "useful" than
378 $F_\alpha(z)$.

379 This is particularly important in working with large degrees of freedom and extreme values of
 380 α , mainly close to 0 and 1. The typical 64-bit floating-point algorithm suffers from overflow and/or
 381 underflow. See Section 3.7 for more details.

382 $M_\alpha(z)$ has the asymptotic representation in the *generalized gamma* (GG) style: (see F.20 of [16])

$$(3.15) \quad M_\alpha\left(\frac{x}{\alpha}\right) = A x^{d-1} e^{-B x^p}$$

where $p = 1/(1 - \alpha)$, $d = p/2$, $A = \sqrt{p/(2\pi)}$, $B = 1/(\alpha p)$.

383 Additional correction terms in the asymptotic expansion have been derived up to the order $x^{-6/(1-\alpha)}$ [26].
 384 This formula is important in guiding (3.14) to high precision for large x , where the series representation
 385 often fails to converge.

386 $M_\alpha(x)$ can be used as the density function of a one-sided distribution [17], because $\int_0^\infty M_\alpha(x)dx =$
 387 1 and $M_\alpha(x)$ for $x \geq 0$. Its CDF is another Wright function:

$$(3.16) \quad \int_0^x M_\alpha(t)dt = 1 - W_{-\alpha,1}(-x).$$

388 This is proved in Lemma 2.11.

389 The absolute moments of $M_\alpha(x)$ in \mathbb{R}^+ are

$$(3.17) \quad \int_0^\infty t^n M_\alpha(t)dt = \frac{\Gamma(n+1)}{\Gamma(n\alpha+1)}, \quad n > -1.$$

390 Hence, its mean is located at $1/\Gamma(\alpha+1)$, which is equal to 1 when $\alpha = 0, 1$. Its variance is $2/\Gamma(2\alpha+1) - 1/\Gamma(\alpha+1)^2$. The variance becomes zero when $\alpha = 1$, consistent with $M_1(x) = \delta(x-1)$.

392 Differentiating $M_\alpha(z)$, and from (3.14), we get

$$(3.18) \quad \frac{d}{dz} M_\alpha(z) = -W_{-\alpha,1-2\alpha}(-z) = \frac{-1}{\pi} \sum_{n=2}^{\infty} \frac{(-z)^{n-2}}{(n-2)!} \Gamma(\alpha n) \sin(\alpha n \pi)$$

393 Note that $\frac{d}{dz} M_\alpha(0) = -\frac{1}{\pi} \Gamma(2\alpha) \sin(2\alpha\pi)$. This also indicates that

$$(3.19) \quad \frac{d}{dz} F_\alpha(z) = \alpha \left(1 + z \frac{d}{dz} \right) M_\alpha(z)$$

394 which can be implemented from $M_\alpha(z)$ through (3.14) and (3.18). These differential forms lead to the
 395 concept of elasticity in Section 3.5 and below.

396 3.4. The Fractional Gamma-Star Function

397 The so-called γ^* function is documented in 8.2.6 and 8.2.7 of DLMF [6]. It is defined as follows:

$$\gamma^*(s, x) := \frac{1}{\Gamma(s)} \int_0^1 t^{s-1} e^{-xt} dt = \frac{x^{-s}}{\Gamma(s)} \gamma(s, x)$$

398 The finite integral in $t \in [0, 1]$ is transformed from the incomplete gamma function, which takes the
 399 form of $\gamma(s, x) = \int_0^x t^{s-1} e^{-t} dt$.

400 $\gamma^*(s, x)$ can be extended fractionally in a straightforward manner. It is used to calculate the CDF
 401 of the FG in Chapter 6. See (6.7) for details.

402 DEFINITION 3.2 (The fractional γ^* function). It is defined by replacing e^{-xt} with $M_\alpha(xt)$ such
 403 that

$$(3.20) \quad \gamma_\alpha^*(s, x) := \frac{\Gamma((1-\alpha)+\alpha s)}{\Gamma(s)} \int_0^1 dt t^{s-1} M_\alpha(xt)$$

The $\alpha \rightarrow 0$ limit of $\gamma_\alpha^*(s, x)$ subsumes the classic γ^* function, that is, $\gamma_0^*(s, x) = \gamma^*(s, x)$. This is reflected in the simple fact that $M_0(xt) = \exp(-xt)$.

The γ^* function is a subset of the fractional confluent hypergeometric function in Lemma 5.4.

The supplementary γ_α^* function is defined as

$$(3.21) \quad \Gamma_\alpha^*(s, x) := \frac{\Gamma((1-\alpha)+\alpha s)}{\Gamma(s)} \int_1^\infty dt t^{s-1} M_\alpha(xt)$$

LEMMA 3.3. It has an analytic relation such as

$$(3.22) \quad \Gamma_\alpha^*(s, x) = x^{-s} - \gamma_\alpha^*(s, x)$$

△

PROOF. The total integral of $t \in \mathbb{R}$ has an analytic solution due to (3.17):

$$\begin{aligned} \Gamma_\alpha^*(s) &:= \frac{\Gamma((1-\alpha)+\alpha s)}{\Gamma(s)} \int_0^\infty dt t^{s-1} M_\alpha(xt) \\ &= \frac{\Gamma((1-\alpha)+\alpha s)}{\Gamma(s) x^s} \int_0^\infty dz z^{s-1} M_\alpha(z) \\ &= x^{-s}. \end{aligned}$$

Split the integral into two parts: \int_0^1 and \int_1^∞ . We obtain (3.22). □

The identity formula is

$$(3.23) \quad x^s \Gamma_\alpha^*(s, x) + x^s \gamma_\alpha^*(s, x) = 1$$

This identity is critical in understanding how to use γ_α^* versus Γ_α^* when calculating the CDF of a FG distribution.

Numerically, it is better to use γ_α^* when $x \leq 1$ and to use Γ_α^* when $x > 1$.

3.5. The Elasticity Operator

In (3.18) and (3.19), we encountered an important mathematical structure called "elasticity" which will be used in Chapter 13. It provides an elegant view of the inner structure of the FG density functions.

DEFINITION 3.4 (The elasticity operator). Assume $f(x)$ is differentiable for $x \in \mathbb{R}$. The elasticity of $f(x)$ is defined as

$$(3.24) \quad \mathcal{L} f(x) := \frac{x}{f(x)} \frac{d}{dx} f(x)$$

$$(3.25) \quad = \frac{d \log f(x)}{d \log x}, \quad \text{when } x > 0 \text{ and } f(x) > 0.$$

The second line can be interpreted as the percentage change of $f(x)$ over a percentage change of x . This is often used in statistics and economics. (It is an extension of the Euler dilation operator, $x \frac{d}{dx}$.)

To illustrate its property, if $f(x) \sim x^k$ locally, then $\mathcal{L} f(x) \approx k$. It informs *local degree of homogeneity* in the scaling analysis.

More generally, some algebraic rules of \mathcal{L} are

- $\mathcal{L}[f(x)g(x)] = \mathcal{L}f(x) + \mathcal{L}g(x)$; multiplication becomes addition.
- $\mathcal{L}[f(g(x))] = \mathcal{L}g(x) \times [\mathcal{L}f](g(x))$; composition becomes multiplication.
- $\mathcal{L}(x^k) = k$; the trivial case is $\mathcal{L}(x) = 1$.
- $\mathcal{L}(e^{-x}) = -x$;

- 432 • \mathcal{L} (constant) is zero;

433 As an application, it is a good exercise to derive $\mathcal{L}[f((x/\sigma)^p)] = p[\mathcal{L}f]((x/\sigma)^p)$.

434 The recurrence relations of the Wright function, (3.2) and (3.3), can be rewritten using the \mathcal{L} operator.
435 They become two expressions of the elasticity of the Wright function.

436 Define the ratio of two Wright functions as

$$(3.26) \quad Q_{\lambda,\mu,\delta}(z) = \frac{W_{\lambda,\mu+\delta}(z)}{W_{\lambda,\mu}(z)}.$$

437 It follows immediately that (3.2) becomes

$$(3.27) \quad \lambda z Q_{\lambda,\mu,\lambda}(z) = Q_{\lambda,\mu,-1}(z) + 1 - \mu.$$

438 LEMMA 3.5. The elasticity of the Wright function is expressed by the following ratios:

$$(3.28) \quad \mathcal{L} W_{\lambda,\mu}(z) = \frac{1}{\lambda} Q_{\lambda,\mu,-1}(z) + \frac{1-\mu}{\lambda},$$

$$(3.29) \quad \mathcal{L} W_{\lambda,\mu}(z) = z Q_{\lambda,\mu,\lambda}(z).$$

439 △
440 PROOF. The second line is straightforward from (3.3). The first line is derived from the second
441 line by replacing the $z Q_{\lambda,\mu,\lambda}(z)$ term on the RHS with (3.27).
442 □

444 3.6. The Elasticity of the M-Wright Functions

445 What we are most interested in is the elasticity of $M_\alpha(x)$:

$$(3.30) \quad \mathcal{L} M_\alpha(x) = [\mathcal{L} W_{-\alpha,1-\alpha}](-x)$$

446 which is from (3.10). Note that $\mathcal{L} F_\alpha(x)$ is trivial if $\mathcal{L} M_\alpha(x)$ is known. This is due to (3.19), we have

$$(3.31) \quad \mathcal{L} F_\alpha(x) = \mathcal{L} M_\alpha(x) + 1.$$

447 However, $\mathcal{L} F_\alpha(x)$ has a representation that is more friendly to FCM. From (3.28),

$$(3.32) \quad \mathcal{L} F_\alpha(x) = [\mathcal{L} W_{-\alpha,0}](-x) = \frac{1}{\alpha} Q_\alpha(x) - \frac{1}{\alpha},$$

$$(3.33) \quad \text{where } Q_\alpha(x) := -Q_{-\alpha,0,-1}(-x) = -\frac{W_{-\alpha,-1}(-x)}{W_{-\alpha,0}(-x)}.$$

448 It follows that $Q_\alpha(x) = \alpha \mathcal{L} M_\alpha(x) + (1 + \alpha)$.

449 The following lemma converts the elasticity of the FG PDF to either $\mathcal{L} M_\alpha(x)$ or $Q_\alpha(x)$.

450 LEMMA 3.6. Let $\mathfrak{N}(x)$ represent the functional form of FG PDF (6.1) where $\mathfrak{N}(x) = x^{d-1} F_\alpha \left(\left(\frac{x}{\sigma} \right)^p \right)$
451 (apart from a constant multiplier). The elasticity of $\mathfrak{N}(x)$ is

$$(3.34) \quad \mathcal{L} \mathfrak{N}(x) = p [\mathcal{L} M_\alpha]((x/\sigma)^p) + (d + p - 1).$$

452 Alternatively, a useful ratio form for the FCM where p/α is a constant is

$$(3.35) \quad \mathcal{L} \mathfrak{N}(x) = \frac{p}{\alpha} Q_\alpha \left(\left(\frac{x}{\sigma} \right)^p \right) - \frac{p}{\alpha} + (d - 1).$$

453 We observe that the role of the degrees of freedom d is very simple in $\mathcal{L} \mathfrak{N}(x)$. It shifts the constant
454 level, but it does not affect the shape of $\mathcal{L} \mathfrak{N}(x)$.
455 △

457 $\mathcal{L} M_\alpha(x)$ has simple behaviors in a few cases. For example,

$$\begin{aligned}\mathcal{L} M_0(x) &= -x; \\ \mathcal{L} M_{1/2}(x) &= -x^2/2.\end{aligned}$$

458 When $x \rightarrow 0$,

$$(3.36) \quad \mathcal{L} M_\alpha(x) \sim -b_1 x, \quad \text{where } b_1 := \frac{\Gamma(1-\alpha)}{\Gamma(1-2\alpha)}.$$

459 When $\alpha \in [0, 1/2]$, $\mathcal{L} M_\alpha(x) < 0$ for all $x > 0$. It is a monotonically decreasing function for $x \in [0, \infty)$.

460 When $x \rightarrow \infty$, the GG-style asymptotic form in (3.15) leads to

$$(3.37) \quad \mathcal{L} M_\alpha(x) \sim -\alpha^{\alpha/(1-\alpha)} x^{1/(1-\alpha)} + \frac{\alpha-1/2}{1-\alpha},$$

461 in which the first term is dominant. It leads to the asymptotic limit of second-order elasticity:

$$(3.38) \quad \lim_{x \rightarrow \infty} \mathcal{L}[-\mathcal{L} M_\alpha](x) \rightarrow \frac{1}{1-\alpha}.$$

462 It follows immediately from (3.29) that (with $z \rightarrow -x$)

$$(3.39) \quad \mathcal{L} M_\alpha(x) = -x \frac{W_{-\alpha,1-2\alpha}(-x)}{W_{-\alpha,1-\alpha}(-x)} = -x Q_{-\alpha,1-\alpha,-\alpha}(-x)$$

463 where the series form of the numerator is in (3.18). We can compute the numerator and denominator individually, then take the ratio. Or we can derive its series representation as follows.

LEMMA 3.7. The series representation of $\mathcal{L} M_\alpha(x) = -x Q_{-\alpha,1-\alpha,-\alpha}(-x)$ is

$$\mathcal{L} M_\alpha(x) = \sum_{k=1}^{\infty} c_k x^k$$

465 where

$$(3.40) \quad c_k = \frac{(-1)^k}{(k-1)!} b_k + \sum_{j=1}^{k-1} \frac{(-1)^{(j+1)}}{j!} b_j c_{k-j}, \quad k \geq 1;$$

$$(3.41) \quad b_n = \frac{\Gamma(1-\alpha)}{\Gamma(1-\alpha(n+1))}, \quad n \geq 1.$$

466

△

PROOF. From (3.14), we have

$$M_\alpha(x) = \sum_{n=0}^{\infty} a_n x^n, \quad a_n = \frac{(-1)^n}{n! \Gamma(1-\alpha(n+1))}.$$

Then (3.18) can be written as

$$\frac{d}{dx} M_\alpha(x) = -W_{-\alpha,1-2\alpha}(-x) = \sum_{n=1}^{\infty} n a_n x^{n-1}.$$

And

$$x \frac{M'_\alpha(x)}{M_\alpha(x)} = \frac{\sum_{n \geq 1} n a_n x^n}{\sum_{n \geq 0} a_n x^n}.$$

The coefficients satisfy the standard recurrence of series divisions, which becomes

$$c_k = \frac{1}{a_0} \left(k a_k - \sum_{j=1}^{k-1} a_j c_{k-j} \right), \quad k \geq 1.$$

467 With $a_0 = \frac{1}{\Gamma(1-\alpha)}$, and $\frac{a_n}{a_0} = \frac{(-1)^n}{n!} b_n$, it leads to (3.40) and (3.41).

468 \square

REMARK 3.8. The first three coefficients are explicitly derived as follows.

$$c_1 = -b_1 = -\frac{\Gamma(1-\alpha)}{\Gamma(1-2\alpha)},$$

$$c_2 = b_2 - b_1^2 = \frac{\Gamma(1-\alpha)}{\Gamma(1-3\alpha)} - \left(\frac{\Gamma(1-\alpha)}{\Gamma(1-2\alpha)} \right)^2,$$

$$c_3 = -\frac{1}{2}b_3 + \frac{3}{2}b_2b_1 - b_1^3 = -\frac{\Gamma(1-\alpha)}{2\Gamma(1-4\alpha)} + \frac{3}{2} \frac{\Gamma(1-\alpha)^2}{\Gamma(1-2\alpha)\Gamma(1-3\alpha)} - \left(\frac{\Gamma(1-\alpha)}{\Gamma(1-2\alpha)} \right)^3.$$

The small- x expansion up to the x^3 term is

$$\mathcal{L} M_\alpha(x) = \left[-\frac{\Gamma(1-\alpha)}{\Gamma(1-2\alpha)} \right] x + c_2 x^2 + c_3 x^3 + O(x^4).$$

3.7. Numerical Methods of the M-Wright Functions

470 To properly compute the subsequent special functions and distributions in this book, we need a
 471 very robust numerical implementation of $F_\alpha(x)$ and $M_\alpha(x)$ for the entire range of $\alpha \in [0, 1]$ and $x \geq 0$.
 472 Since $F_\alpha(x) = \alpha x M_\alpha(x)$, we can easily compute one from the other in most cases. It is a matter of
 473 which approach is faster, more convenient, and precise.

474 **3.7.1. Handling alpha for zero and one.** When $\alpha = 0$, we should use $M_0(x) = e^{-x}$. $\lim_{\alpha \rightarrow 0} F_\alpha(x)$
 475 should be handled carefully in the fractional gamma distribution.

476 When $\alpha = 1$, we could use a normal distribution to simulate the delta function: $M_1(x) =$
 477 $\mathcal{N}(x; 1, \sigma^2)$ where $\sigma = 0.001$. This is to ensure that $\int_0^\infty M_1(x) dx = 1$.

478 **3.7.2. Using scipy.stats.levy-stable.** Both functions can be derived from the one-sided α -
 479 stable distribution $L_\alpha(x)$ of Section 4.2, which is implemented in `scipy.stats.levy_stable` package[33].

480 For example, $M_\alpha(x)$ can be computed using $L_\alpha(x) = \alpha x^{-\alpha-1} M_\alpha(x^{-\alpha})$ where $x > 0$. On the other
 481 hand, for $\beta > 1/2$, we can also use $M_\beta(x) = \alpha L_\alpha^{\alpha-2}(x)$ where $\beta = 1/\alpha$.

482 These two numerical methods are good for the bulk of α and x . However, they begin to lose
 483 precision for small $\alpha < 0.08$ and large $\alpha > 0.99$. They are also not good enough for small $x < 0.01$.

484 **3.7.3. Using the series sum in numpy.** Based on (3.14), we define the sum of the series of
 485 finite terms as

$$(3.42) \quad M_\alpha^{(m)}(x) = \frac{1}{\pi} \sum_{n=1}^m \frac{(-x)^{n-1}}{(n-1)!} \Gamma(\alpha n) \sin(\alpha n \pi). \quad (0 < \alpha < 1)$$

486 This method implemented in `numpy` and `scipy` is good for several scenarios. First, to cover the small
 487 x area ($x < 0.01$), use $M_\alpha^{(7)}(x)$ if $\alpha < 0.9$.

488 Otherwise, we could use $M_\alpha^{(80)}(x)$ for $\alpha \leq 0.998$ and $x < 0.85$. The sum of 80 terms takes more
 489 time to compute. But it is a necessary path when `scipy.stats.levy_stable` approach loses precision.

490 **3.7.4. Using the series sum in mpmath.** $M_\alpha^{(m)}(x)$ implemented in `mpmath` is our de facto
 491 implementation to calibrate the precision of other approaches. In order to make it a good baseline
 492 implementation, we must carefully choose `mp.prec` and m to use.

493 After rigorous testing, it was found that `mp.prec >= 64` provides sufficient precision. Therefore,
 494 `mp.prec = 128` is more than abundant up to three decimal points in α . `mpmath` is smart about handling
 495 summing many small terms, especially with large amount of cancellation due to the $\sin(\alpha n\pi)$ factor
 496 in (3.42).

497 The more crucial choice is m , where $m = 40,000$ is enough for $\alpha < 0.9$. Much larger m ($m =$
 498 $80,000$) is needed for α very close to 1 ($\alpha = 0.998$). Obviously, a very large m makes the series
 499 sum more compute-intensive. This can be used during the calibration phase, but not for the actual
 500 numpy-style implementation.

501 This will be elaborated on in the next section.

502 **3.7.5. Using the asymptotic approximation.** Paris et al. [26] derived a more refined asymptotic formula, where (3.15) is simply its first term. Theorem 2.2 of that paper is recaptured in the
 503 following.

504 LEMMA 3.9.

$$(3.43) \quad M_\alpha(x) \sim \frac{A(\alpha)}{2\pi} X^{\alpha-1/2} e^{-X} \sum_{n=0}^{\infty} c_j(\alpha) (-X)^{-j}. \quad (0 < \alpha < 1)$$

505 where $c_j(\alpha)$ is in its (2.4) up to $j = 6$. Other parameters are $A(\alpha) = \sqrt{\frac{2\pi}{\alpha}} \left(\frac{\alpha}{\kappa}\right)^\alpha$ and $X = \kappa(hx)^{1/\kappa}$
 506 with $\kappa = 1 - \alpha$ and $h = \alpha^\alpha$.

507 \triangle

508 When $M_\alpha(x)$ is small, (3.43) could be very precise with an error as small as 10^{-5} . Our strategy
 509 is to use other implementations to get $M_\alpha(x)$ to a small number, e.g. 10^{-6} in most cases, and at least
 510 10^{-3} in some difficult cases. Then use (3.43) for larger x up to infinity (the maximum 64-bit float).

511 This right-tail strategy works for the bulk of α from 0.1 to 0.9. The transition interval (defined as
 512 $M_\alpha(x) \in [10^{-5}, 10^{-6}]$) could be precomputed by the faster (3.15).

513 For α from 0.9 to 0.99, the `mpmath` version of $M_\alpha^{(m)}(x)$ is more precise to determine the transition
 514 interval.

515 For α from 0.001 to 0.1, the asymptotic form is adjusted to

$$(3.44) \quad M_\alpha(x) \sim A'(\alpha) e^{-B'(\alpha)X'}, \quad \text{where } X' = x^{1/\kappa}.$$

516 $A'(\alpha)$ and $B'(\alpha)$ are obtained from a linear regression in the transition interval: $\log M_\alpha(x) \sim \log A'(\alpha) -$
 517 $B'(\alpha)X'$.

518 **3.7.6. Using the integral form.** For α from 0.99 to 0.998, the `scipy` version of $M_\alpha(x)$ loses
 519 precision very quickly in the right tail. We use (3.7) to supplement this deficiency for this range of α
 520 as long as $M_\alpha(x) > 10^{-3}$.

521 The numerical difficulty arises in the integral when the target $M_\alpha(x)$ is very small. The integrand
 522 in (3.7) becomes fast oscillating and is non-zero only in a very small range of r^δ . It is hard for
 523 existing integration algorithms to detect this small range, capture these oscillations, and perform the
 524 cancellation properly. A more sophisticated quadrature integration algorithm is needed. It is left for
 525 future research.

526 For $M_\alpha(x) < 10^{-3}$ at large x , we still use (3.43) asymptotically. This equation is fine for large α ,
 527 as long as the numeric overflow is handled properly.

CHAPTER 4

528

The Alpha-Stable Distribution - Review

529 The two-sided distributions in this book are based on the α -stable distribution, which was published
530 in the seminal 1925 book of Paul Lévy[12]. These distributions have a major parameter, among others,
531 called *the stability index* $\alpha \in (0, 2]$. We call it the *fractional* parameter.

532 In this chapter, we provide a review of the α -stable distribution based on the Mellin transform
533 framework. This framework lays the foundation for further generalization in subsequent chapters.

534 The ratio distribution approach for its density function in Section 4.3 is invented by the author.

535

4.1. Classic Result

536 The α -stable distribution has two shape parameters. There are many parametrizations that have
537 been studied (see p.5 of [24]). We are primarily concerned with Feller's (α, θ) parametrization[8, 9],
538 where α is called the stability index with a range of $0 < \alpha \leq 2$, and θ is an angle that injects skewness
539 to the distribution when it is not zero.

540 An innovative approach is to study its Mellin transform. This presentation is used because it is
541 *simpler* and provides great insight into its structure.

542 LEMMA 4.1. The Mellin transform of its PDF is

$$(4.1) \quad L_\alpha^\theta(x) \xrightarrow{\mathcal{M}} \epsilon \frac{\Gamma(s)\Gamma(\epsilon(1-s))}{\Gamma(\gamma(1-s))\Gamma(1-\gamma+\gamma s)} \\ \text{where } \epsilon = \frac{1}{\alpha}, \gamma = \frac{\alpha-\theta}{2\alpha}.$$

543 where $0 < C < 1$ implicitly. This is defined for $x \geq 0$. The reflection rule is used for $x < 0$ such that
544 $L_\alpha^\theta(x) := L_\alpha^{-\theta}(-x)$.

△

546 This result was first derived in 1986 by Schneider[28], then rediscovered in 2001 by Mainardi et
547 al.[18], and summarized by Mainardi and Pagnini in (2.8) of [19], from which we quote.

548 In (4.1), instead of using (α, θ) directly, it uses a different representation, which we call the (ϵ, γ)
549 representation. In the Mellin transform space, such representation is often more elegant.

550 The constraint on θ in the Feller parameterization: $|\theta| \leq \min\{\alpha, 2 - \alpha\}$, is called the "Feller-
551 Takayasu diamond". In the (ϵ, γ) parametrization, the constraint becomes (a) $0 \leq \gamma \leq 1$ when $\epsilon > 1$;
552 and (b) $1 - \epsilon \leq \gamma \leq \epsilon$ when $\epsilon \leq 1$.¹

553 **4.1.1. The Reflection Rule.** Note that the reflection of $\theta \rightarrow -\theta$ in the (α, θ) parametrization
554 is equivalent to the reflection of $\gamma \rightarrow 1 - \gamma$ in the (ϵ, γ) parametrization.

555 Since we often mingle the two parameterizations, this alternative view can be very helpful in
556 certain scenarios. For example, the total density in the positive domain is $\int_0^\infty L_\alpha^\theta(x) = \gamma$. By the
557 reflection rule, $\int_0^\infty L_\alpha^{-\theta}(x) = 1 - \gamma$. Hence, the total density $\int_{-\infty}^\infty L_\alpha^\theta(x) = \gamma + (1 - \gamma) = 1$.

¹Conversely, if γ is fixed, (b) puts a constraint on the largest α allowed: $\alpha \leq \min\{1/\gamma, 1/(1 - \gamma)\}$.

558 **4.2. Extremal Distributions**

559 There are two types of the so-called "extremal distributions", where θ is pushed to the limit, so
 560 to speak. They are especially intriguing because the M-Wright functions, $F_\alpha(x), M_\alpha(x)$ in Section 3.3,
 561 can be derived from them.

562 They can be understood from (4.1). The first kind of extremal distribution lies in $\gamma = 0$ or $\gamma = 1$
 563 when $\theta = \pm\alpha \leq 1$. Due to the reflection rule, we only need to study the case of $\theta = -\alpha$, that is, $\gamma = 1$.

564 This defines the one-sided α -stable distribution:

$$L_\alpha(x) := L_\alpha^{-\alpha}(x) \xleftrightarrow{\mathcal{M}} \epsilon \frac{\Gamma(\epsilon(1-s))}{\Gamma(1-s)}$$

565 Apply three manipulations of Mellin transform on $F_\alpha(x)$: First, $x \rightarrow x^\alpha$; second, multiply x ; third,
 566 $x \rightarrow x^{-1}$. We obtain the classic result of

$$(4.2) \quad L_\alpha(x) = x^{-1} F_\alpha(x^{-\alpha}) \quad (x \geq 0 \text{ and } 0 < \alpha \leq 1)$$

567 and $L_1(x) = \delta(x-1)$ is the upper bound of this relation.

568 $L_\alpha(x)$ can be computed via `scipy.stats.levy_stable[33]` using 1-Parameterization with `beta=1`,
 569 `scale=cos(alpha*pi/2)^1/alpha` for $0 < \alpha < 1$.² It might seem somewhat peculiar that we can use the existing
 570 implementation of $L_\alpha(x)$ to develop all the new fractional distributions for proof of concept.

571 The second kind of extremal distribution (but not necessarily one-sided) occurs when $\theta = \alpha - 2$,
 572 which leads to $\epsilon = \gamma = 1/\alpha$ and

$$L_\alpha^{\alpha-2}(x) \xleftrightarrow{\mathcal{M}} \epsilon \frac{\Gamma(s)}{\Gamma(1-\epsilon+\epsilon s)}$$

573 Compare it to (3.13), we get the classic result of (e.g. see (F.49) of [16])

$$(4.3) \quad L_\alpha^{\alpha-2}(x) = \frac{1}{\alpha} M_{1/\alpha}(x) \quad (x \in \mathbb{R} \text{ and } 1 < \alpha \leq 2)$$

574 Notice that it extends the M-Wright function to $x < 0$ because $L_\alpha^{\alpha-2}(x)$ is two-sided.

575 **4.3. Ratio Distribution Approach**

576 Important insight can be obtained by interpreting (4.1) as a ratio distribution (2.6). We split (4.1)
 577 into two components:

$$(4.4) \quad L_\alpha^\theta(x) \xleftrightarrow{\mathcal{M}} \epsilon \left[\frac{\Gamma(s)}{\Gamma(1-\gamma+\gamma s)} \right] \left[\frac{\Gamma(\epsilon(1-s))}{\Gamma(\gamma(1-s))} \right]$$

578 The first bracket is the Mellin transform of the M-Wright function (3.13).

579 The second bracket comes from the Mellin transform of the PDF of the fractional χ -mean distri-
 580 bution (FCM) at $k = 1$:

$$(4.5) \quad \bar{\chi}_{\alpha,1}^\theta(x) \xleftrightarrow{\mathcal{M}} \bar{\chi}_{\alpha,1}^{\theta,*}(s) \\ = \epsilon \gamma^{\gamma(s-1)-1} \frac{\Gamma(\epsilon(s-1))}{\Gamma(\gamma(s-1))}$$

581 According to the Mellin transform rule of a ratio distribution, s should be replaced by $2-s$ in
 582 $\bar{\chi}_{\alpha,1}^{\theta,*}(s)$. Therefore, $s-1$ in the second line of (4.5) becomes $1-s$ in the second bracket of (4.4).

²See Chapter 1 of [24] for more detail on different parameterizations. We would not go into the issue of stable parameterizations.

583 **4.3.1. Rescaled M-Wright Function.** Additionally, a small nuance here is to deal with scaling
 584 factors. Define the rescaled M-Wright function

$$(4.6) \quad \tilde{M}_\gamma(x) := \gamma^{1-\gamma} M_\gamma(x/\gamma^\gamma)$$

585 such that it matches the standard normal distribution: $\tilde{M}_{1/2}(x) = \frac{1}{\sqrt{2\pi}} e^{-x^2/2}$ of $\mathcal{N}(0, 1)$. And
 586 $\int_0^\infty \tilde{M}_\gamma(x) dx = \gamma$ since $\int_0^\infty M_\gamma(x) dx = 1$.

587 Notice that, according to the reflection rule, $\int_0^\infty \tilde{M}_\gamma(-x) dx = \int_0^\infty \tilde{M}_{1-\gamma}(x) dx = 1 - \gamma$. We get
 588 $\int_{-\infty}^\infty \tilde{M}_\gamma(x) dx = 1$. Hence, $\tilde{M}_\gamma(x)$ is a valid two-sided density function.

589 According to (2.3), the rescaling of PDF modifies the Mellin transform from (3.13) to

$$(4.7) \quad \begin{aligned} \tilde{M}_\gamma(x) &\xrightarrow{\mathcal{M}} \tilde{M}_\gamma^*(s) \\ &= \gamma^{1-\gamma+\gamma s} \frac{\Gamma(s)}{\Gamma(1-\gamma+\gamma s)} \end{aligned}$$

590 from which the $\gamma^{1-\gamma+\gamma s}$ term cancels out its counterpart in $\bar{\chi}_{\alpha,1}^\theta(2-s)$ nicely.

591 Therefore, we find a new method to construct the α -stable distribution using the following integral.

592 LEMMA 4.2 (The ratio-distribution representation of the α -stable distribution). The Mellin trans-
 593 form of the PDF (4.1) becomes

$$(4.8) \quad L_\alpha^\theta(x) \xrightarrow{\mathcal{M}} \tilde{M}_\gamma^*(s) \bar{\chi}_{\alpha,1}^\theta(2-s)$$

594 from which the PDF can be written in a ratio distribution form of

$$(4.9) \quad L_\alpha^\theta(x) := \int_0^\infty \tilde{M}_\gamma(xs) \bar{\chi}_{\alpha,1}^\theta(s) s ds \quad (x \geq 0)$$

595 Since the Mellin integral is only valid for $x > 0$, it is supplemented with *the reflection rule*:

$$(4.10) \quad L_\alpha^\theta(-x) := L_\alpha^{-\theta}(x)$$

△

596 This construction places $\bar{\chi}_{\alpha,1}^\theta$ in the central role. We define it at one degree of freedom $k = 1$. In
 597 Chapter 7, we will add *degrees of freedom* k to it and make it $\bar{\chi}_{\alpha,k}^\theta$, which is the fractional extension
 600 of the classic χ distribution.

601 Subsequently, in Chapter 11, we will add *degrees of freedom* k to the α -stable distribution and
 602 merge it with Student's t distribution.

603 4.4. SaS

604 Note that $\theta = 0$ is equivalent to $\gamma = 1/2$. The distribution is symmetric, with the nickname of
 605 "SaS", which stands for "Symmetric α -Stable".

606 Its Mellin transform is simplified to

$$(4.11) \quad \begin{aligned} L_\alpha^0(x) &\xrightarrow{\mathcal{M}} \epsilon \left[\frac{\Gamma(s)}{\Gamma((1+s)/2)} \right] \left[\frac{\Gamma(\epsilon(1-s))}{\Gamma((1-s)/2)} \right] \\ &= \epsilon \left[\frac{2^{s-1}}{\sqrt{\pi}} \Gamma\left(\frac{s}{2}\right) \right] \left[\frac{\Gamma(\epsilon(1-s))}{\Gamma((1-s)/2)} \right]. \end{aligned}$$

607 The first bracket is the Mellin transform of a normal distribution (2.9) with a scale. The second bracket
 608 is $\bar{\chi}_{\alpha,1}^0(2-s)$ from above.

609 Hence, the PDF of SaS is

$$(4.12) \quad L_{\alpha}^0(x) = \int_0^{\infty} \mathcal{N}(xs) \bar{\chi}_{\alpha,1}^0(s) s ds.$$

610 This is one of the foundations of GAS-SN in (12.1).

611 **4.4.1. Method of Normal Mixture.** SaS in (4.12) will be generalized to GSaS in (12.3) in
 612 Chapter 12. Both integrals are in the normal mixture structure (9.1) that enjoys several nice properties
 613 described in Chapter 9.

614 The classic exponential power distribution (Section 3.11.1 of [24]) is the characteristic function
 615 transform in Lemma 9.2.

CHAPTER 5

Fractional Hypergeometric Functions

616 In this chapter, we extend both the confluent hypergeometric function ${}_1F_1(a, b; x)$ or $M(a, b; x)$ (Chapter 13, DLMF[6]); and the Gauss hypergeometric function ${}_2F_1(a, b, c; x)$ (Chapter 15 of DLMF).

619 The former occurs when dealing with the CDF of the FG and FCM distributions. The latter
620 occurs when handling the CDF of the GSaS and F distributions.

621 The reader who is not interested in the hypergeometric functions can safely skip this chapter
622 without losing direction.

623 To clear up the situation, we first recite the DLMF formulas and convert them to our convention
624 according to (2.2).

625 From DLMF 13.2.4 and 13.4.16, the Mellin transform of the Kummer function is

$$M(a, b; -x) = \frac{\Gamma(b)}{2\pi i \Gamma(a)} \int_{C-i\infty}^{C+i\infty} \frac{\Gamma(a-s)\Gamma(s)}{\Gamma(b-s)} x^{-s} ds,$$

626 where $a \neq 0, -1, -2, \dots$

627 From DLMF 15.1.2 and 15.6.6, the Mellin transform of the Kummer function is

$${}_2F_1(a, b, c; -x) = \frac{\Gamma(c)}{2\pi i \Gamma(a)\Gamma(b)} \int_{C-i\infty}^{C+i\infty} \frac{\Gamma(a-s)\Gamma(b-s)\Gamma(s)}{\Gamma(c-s)} x^{-s} ds,$$

628 where $a, b \neq 0, -1, -2, \dots$

629 Use our Mellin transform notation, they become

$$(5.1) \quad M(a, b; -x) \xleftrightarrow{\mathcal{M}} M^*(a, b; s) = \frac{\Gamma(b)}{\Gamma(a)} \frac{\Gamma(a-s)\Gamma(s)}{\Gamma(b-s)},$$

$$(5.2) \quad {}_2F_1(a, b, c; -x) \xleftrightarrow{\mathcal{M}} {}_2F_1^*(a, b, c; s) = \frac{\Gamma(c)}{\Gamma(a)\Gamma(b)} \frac{\Gamma(a-s)\Gamma(b-s)\Gamma(s)}{\Gamma(c-s)}.$$

630 Now let us add the fractional components to them!

5.1. Fractional Confluent Hypergeometric Function

632 The fractional confluent hypergeometric function (FCHF) is the union of the Kummer function
633 and the Wright function. It allows us to extend many classic functions to their fractional forms.

634 We start with its Mellin transform. And we follow with the integral and series representations.

635 DEFINITION 5.1. The Mellin transform of the FCHF is

$$(5.3) \quad M_{\lambda, \delta}(a, b; -x) \xleftrightarrow{\mathcal{M}} M_{\lambda, \delta}^*(a, b; s) = \frac{\Gamma(b)}{\Gamma(a)} \frac{\Gamma(a-s)\Gamma(s)}{\Gamma(\delta - \lambda s)\Gamma(b-s)}$$

636 where the $\Gamma(\delta - \lambda s)$ term is from the Wright function (3.5).

637 LEMMA 5.2. The integral representation from DLMF 13.4.1 is extended to

$$(5.4) \quad M_{\lambda, \delta}(a, b; z) = \frac{\Gamma(b)}{\Gamma(a)\Gamma(b-a)} \int_0^1 W_{\lambda, \delta}(zt) t^{a-1} (1-t)^{b-a-1} dt$$

638 The obvious limit $W_{0,1}(zt) = e^{zt}$ restores it to the classic DLMF formula.

639

△

640 PROOF. Replace the Wright function in (5.4) with its Hankel integral (3.6),

$$M_{\lambda,\delta}(a, b; z) = \frac{\Gamma(b)}{2\pi i \Gamma(a)} \int_0^1 \int_{H_a} \left(\frac{e^{s+zt}s^{-\lambda}}{s^\delta} ds \right) t^{a-1} (1-t)^{b-a-1} dt$$

641 which can be simplified to

$$M_{\lambda,\delta}(a, b; z) = \frac{1}{2\pi i} \int_{H_a} (s^{-\delta} e^s ds) M(a, b; -z s^{-\lambda})$$

642 Substitute the Mellin integral from (5.1) to it,

$$\begin{aligned} M_{\lambda,\delta}(b, c; -z) &= \frac{1}{2\pi i} \int_{H_a} (s^{-\delta} e^s ds) \frac{\Gamma(b)}{2\pi i \Gamma(a)} \int_{C-i\infty}^{C+i\infty} \frac{\Gamma(b-t)\Gamma(t)}{\Gamma(c-t)} (z s^{-\lambda})^{-t} dt \\ &= \frac{\Gamma(b)}{2\pi i \Gamma(a)} \int_{C-i\infty}^{C+i\infty} \left[\frac{1}{2\pi i} \int_{H_a} s^{\lambda t-\delta} e^s ds \right] \frac{\Gamma(b-t)\Gamma(t)}{\Gamma(c-t)} z^{-t} dt \\ &= \frac{\Gamma(b)}{2\pi i \Gamma(a)} \int_{C-i\infty}^{C+i\infty} \left[\frac{1}{\Gamma(\delta-\lambda t)} \right] \frac{\Gamma(b-t)\Gamma(t)}{\Gamma(c-t)} z^{-t} dt \end{aligned}$$

643 which is the Mellin transform in (5.3).

644 From the second line to the third line, we use the well-known Hankel integral of the reciprocal
645 gamma function:

$$\frac{1}{2\pi i} \int_{H_a} s^{-z} e^s ds = \frac{1}{\Gamma(z)}$$

646

□

647 LEMMA 5.3. The series representation is

$$(5.5) \quad M_{\lambda,\delta}(a, b; z) := \sum_{n=0}^{\infty} \left[\frac{(a)_n}{(b)_n \Gamma(\lambda n + \delta)} \right] \frac{z^n}{n!}$$

648 where $(a)_n, (b)_n$ are Pochhammer symbols.

649

△

650 PROOF. Take (5.3) and apply Ramanujan's master theorem from Section 2.3. This produces
651 $(M_{\lambda,\delta}^*(a, b; s)/\Gamma(s))|_{s=-n}$, which is equal to the bracket term, since $(x)_n = \Gamma(x+n)/\Gamma(x)$. □

652 **5.1.1. FCHF Subsumes the Kummer Function.** It is obvious that $M_{0,1}(a, b; x) = M(a, b; x)$.

653 **5.1.2. FCHF Subsumes the M-Wright Function.** By using the same setting from (3.10), we
654 get

$$M_\alpha(z) = M_{-\alpha, 1-\alpha}(c, c; -z) \quad (c \neq 0)$$

655 **5.1.3. FCHF Subsumes Fractional Gamma-Star Function.** An important variant of FCHF
656 is the fractionalization of the incomplete gamma function. The reader is referred to Sections 8 and 13
657 of DLMF[6] and Wikipedia for background information.

658 We are mainly concerned with the following setup:

$$M_{-\alpha, 1-\alpha}(c, c+1; -x) = c \int_0^1 M_\alpha(xt) t^{c-1} dt$$

659 This integral is found in (3.20). Hence, we obtain -

660 LEMMA 5.4. The fractional γ^* function (3.20) has the following FCHF representation:

$$(5.6) \quad \gamma_\alpha^*(s, x) = \frac{\Gamma(\alpha s - \alpha + 1)}{\Gamma(s + 1)} M_{-\alpha, 1-\alpha}(s, s + 1; -x)$$

661 △

662 The fractional γ^* function is the basis for expressing the CDF of the fractional gamma distribution
663 in Section 6.5. In fact, this was the main motivation to enrich the classic confluent hypergeometric
664 function.

665

666 **5.2. Fractional Gauss Hypergeometric Function**

667 The fractional Gauss hypergeometric function (FGHF) arises from the ratio distribution between
668 an elementary function and FCM2 ($\hat{\chi}_{\alpha,k}^2$) in Section 7.5.

669 When $\alpha = 1$, the Mellin transform of FCM2 is reduced from a fractional form to a classic form in
670 (7.27). The ratio distribution is reduced to a Gauss hypergeometric function ${}_2F_1$. Hence, we consider
671 the general form of such a ratio distribution as fractional ${}_2F_1$.

672 We start by modifying the Mellin transform from (5.2) (DLMF 15.6.6). Then we derive the integral
673 and series representations from it.

674

675 DEFINITION 5.5. The Mellin transform of the fractional Gauss hypergeometric function is

$$(5.7) \quad {}_2F_1(a, b, c, \epsilon; -x) \xrightarrow{\mathcal{M}} {}_2F_1^*(a, b, c, \epsilon; s) \\ = [M^*(a, c; s)] \left[\frac{B(k/2, 1/2)}{\Gamma(1/2)} \hat{\chi}_{\alpha,k}^{2*}(3/2 - s) \right]$$

676 where $\epsilon = 1/\alpha$ is the convention from (4.1), and $b = (k + 1)/2$. $M^*(a, c; s)$ is from (5.1), and $\hat{\chi}_{\alpha,k}^{2*}(s)$
677 is from (7.26) (we jump ahead). And $B(x, y)$ is the beta function.

678 This structure is a fractional form of the generalized hypergeometric function ${}_3F_2$ (DLMF 16.5.1,
679 replace s with $-s$). To see this, expand (5.7) and we get

$$(5.8) \quad {}_2F_1^*(a, b, c, \epsilon; s) = \left[\frac{\Gamma(c)}{\Gamma(a)} \frac{\Gamma(a - s)\Gamma(s)}{\Gamma(c - s)} \right] \left[2^{2s-1} \frac{B(k/2, 1/2)}{\Gamma(1/2)} \frac{\Gamma((k - 1)/2)}{\Gamma(\epsilon(k - 1))} \frac{\Gamma(2\epsilon(k/2 - s))}{\Gamma(k/2 - s)} \right].$$

680 There are five gamma functions that contain s : three in the numerator, two in the denominator. And
681 the $\Gamma(2\epsilon(k/2 - s))$ term is fractional.

682 **5.2.1. FGHF Subsumes the Gauss Hypergeometric Function.**

683 LEMMA 5.6. When $\epsilon = 1$,

$${}_2F_1^*(a, b, c, \epsilon = 1; s) = {}_2F_1^*(a, b, c; s)$$

684 △

685 PROOF. Let $\epsilon = 1$, the second bracket becomes

$$(5.9) \quad \frac{B(k/2, 1/2)}{\Gamma(1/2)} \frac{\Gamma(k/2 + 1/2 - s)}{\Gamma(k/2)} = \frac{\Gamma(k/2 + 1/2 - s)}{\Gamma(k/2 + 1/2)} = \frac{\Gamma(b - s)}{\Gamma(b)}.$$

686 Hence, (5.7) is reduced to the classic limit of ${}_2F_1^*(a, b, c; s)$ in (5.2). □

687 **5.2.2. The Integral Form.**

688 LEMMA 5.7. The integral form of FGHF is

$$(5.10) \quad {}_2F_1(a, b, c, \epsilon; -x) := \frac{B(k/2, 1/2)}{\Gamma(1/2)} \int_0^\infty M(a, c; -x\nu) \hat{\chi}_{\alpha, k}^2(\nu) \sqrt{\nu} d\nu$$

689 where $\epsilon = 1/\alpha$ and $b = (k+1)/2$. $M(a, c; x)$ is the Kummer function (Chapter 13, DLMF). $\hat{\chi}_{\alpha, k}^2(x)$
690 is from (7.18).

△

691 PROOF. We use the generalized convolution formula:

$$h(x) = \int_0^\infty f(xs)g(s) s^p ds \xrightarrow{\mathcal{M}} h^*(s) = f^*(s)g^*(1+p-s),$$

693 Clearly f is M , and g is $\hat{\chi}_{\alpha, k}^2$. Substitute $p = 1/2$ due to the $\sqrt{\nu}$ term. The Mellin transform of (5.10)
694 is

$${}_2F_1(a, b, c, \epsilon; -x) \xrightarrow{\mathcal{M}} \frac{B(k/2, 1/2)}{\Gamma(1/2)} M^*(a, c; s) \hat{\chi}_{\alpha, k}^{2*}(3/2 - s)$$

695 This is exactly (5.7).

□

697 **5.2.3. Relation between FGHF and Real-World Usage.** This section addresses a broader
698 issue. How does FGHF relate to FCM and GAS (and GAS-SN) in general? The reader can skip this
699 section and come back later after she read the later chapters.

700 This topic is important. In an abstract sense, most of the univariate PDFs in their ratio distribution
701 forms can be understood by the integral form of FGHF.

702 Let us make (5.10) more abstract, by ignoring some cumbersome parameters. Assume $F(-x) :=$
703 ${}_2F_1(a, b, c, \epsilon; -x)$ and $M(-x) := M^*(a, c; -x)$ ($x \geq 0$), then (5.10) becomes

$$(5.11) \quad F(-x) := B \int_0^\infty M(-x\nu) \bar{\chi}_{\alpha, k}^2(\nu; \sigma = 1/4) \sqrt{\nu} d\nu$$

704 where we employ the notation $\bar{\chi}_{\alpha, k}^2(x) = \bar{\chi}_{\alpha, k}^2(x; \sigma = \frac{1}{4})$ from (7.18), and $B := B(\frac{k}{2}, \frac{1}{2})/\Gamma(\frac{1}{2})$.

705 LEMMA 5.8. Let $F'(-x)$ be the scaled FGHF, which is more closely related to real-world use cases.
706 The following ratio-distribution integrals can be converted to F' such as

$$(5.12) \quad \left. \begin{aligned} & \int_0^\infty M(-xs) \bar{\chi}_{\alpha, k}^2(s) \sqrt{s} ds \\ & \int_0^\infty M(-xs^2) \bar{\chi}_{\alpha, k}(s) s ds \end{aligned} \right\} = F'(-x) := \frac{2\sqrt{\pi} \sigma_{\alpha, k}}{B(\frac{k}{2}, \frac{1}{2})} F(-4\sigma_{\alpha, k}^2 x)$$

707 Or use the full FGHF notation explicitly:

$$(5.13) \quad \left. \begin{aligned} & \int_0^\infty M(a, c; -xs) \bar{\chi}_{\alpha, k}^2(s) \sqrt{s} ds \\ & \int_0^\infty M(a, c; -xs^2) \bar{\chi}_{\alpha, k}(s) s ds \end{aligned} \right\} = F'_{\alpha, k}(a, c; -x) := \frac{2\sqrt{\pi} \sigma_{\alpha, k}}{B(\frac{k}{2}, \frac{1}{2})} {}_2F_1(a, b, c, \epsilon; -4\sigma_{\alpha, k}^2 x)$$

708 where $\epsilon = 1/\alpha$ and $b = (k+1)/2$ on the RHS.

△

710 PROOF. Let Q be the scale that we want to solve. (5.11) is rewritten to $F'(-x)$ such that

$$F'(-x) := \frac{\sqrt{Q}}{B} F(-Qx) = \sqrt{Q} \int_0^\infty M(-Qx\nu) \bar{\chi}_{\alpha, k}^2(\nu; \sigma = 1/4) \sqrt{\nu} d\nu.$$

711 Let $s = Q\nu$,

$$\begin{aligned} F'(-x) &= \int_0^\infty M(-xs) \bar{\chi}_{\alpha,k}^2(s/Q; \sigma = 1/4)/Q \sqrt{s} ds \\ &= \int_0^\infty M(-xs) \bar{\chi}_{\alpha,k}^2(s; \sigma = Q/4) \sqrt{s} ds \end{aligned}$$

712 Let $Q = 4\sigma_{\alpha,k}^2$, we obtain the integral form in terms of FCM2,

$$F'(-x) = \int_0^\infty M(-xs) \bar{\chi}_{\alpha,k}^2(s) \sqrt{s} ds$$

713 This is the first line of (5.12). Then apply (7.20) and (7.21) to get the second line. And on the FGHF
714 side, we have

$$F'(-x) = \frac{\sqrt{Q}}{B} F(-Qx) = \frac{2\sqrt{\pi} \sigma_{\alpha,k}}{B(\frac{k}{2}, \frac{1}{2})} F(-4\sigma_{\alpha,k}^2 x)$$

715 \square

716 **5.2.4. Example 1: GSaS.** In Lemma 8.3 of [15], a fractional extension was explored for the
717 CDF of GSaS. We formalized it further here. However, we note that the $M(-x)$ function needed to
718 describe GAS-SN is more complicated than a Kummer function. See (10.2) and (10.3).

719 LEMMA 5.9. Assume $\Phi[L_{\alpha,k}](x)$ is the CDF of a GSaS, which is (12.2) with $\beta = 0$. It can be
720 expressed by the scaled FGHF via

$$(5.14) \quad \Phi[L_{\alpha,k}](x) = \frac{1}{2} + \frac{x}{\sqrt{2\pi}} F'_{\alpha,k} \left(\frac{1}{2}, \frac{3}{2}; -\frac{x^2}{2} \right).$$

721 \triangle

722 PROOF. From Lemma 8.3 of [15],

$$\Phi[L_{\alpha,k}](x) = \frac{1}{2} + \frac{x}{\sqrt{k}} M_{\alpha,k} \left(a, c; -\frac{x^2}{k} \right),$$

723 where $a = \frac{1}{2}, c = \frac{3}{2}$ and

$$M_{\alpha,k}(a, c; x) := \sqrt{\frac{k}{2\pi}} \int_0^\infty s ds M \left(a, c; \frac{xks^2}{2} \right) \bar{\chi}_{\alpha,k}(s).$$

724 This pattern fits right in with the second line of (5.13). It is immediately clear that its $M_{\alpha,k}(a, c; x)$
725 is our $\sqrt{k/2\pi} F'_{\alpha,k}(a, c; kx/2)$. Therefore,

$$\Phi[L_{\alpha,k}](x) = \frac{1}{2} + \frac{x}{\sqrt{2\pi}} F'_{\alpha,k} \left(a, c; -\frac{x^2}{2} \right),$$

726 where $a = \frac{1}{2}, c = \frac{3}{2}$.

727 \square

728 Notice that this formula is much cleaner, without the cluttering of k in the previous attempt in
729 [15].

730 **5.2.5. Example 2: Fractional F.**

731 LEMMA 5.10. From (8.2), the standard CDF of a fractional F distribution $F_{\alpha,d,k}$ is

$$\Phi[F_{\alpha,d,k}](x) = \frac{1}{\Gamma\left(\frac{d}{2}\right)} \int_0^\infty ds \gamma\left(\frac{d}{2}, \frac{dxs}{2}\right) \bar{\chi}_{\alpha,k}^2(s).$$

732 It can be expressed by the scaled FGHF via

$$(5.15) \quad \Phi[F_{\alpha,d,k}](x) = \left[C_{\alpha,d,k} \frac{(dx/2)^{d/2}}{\Gamma\left(\frac{d}{2} + 1\right)} \right] F'_{\alpha,k+d-1}\left(\frac{d}{2}, \frac{d}{2} + 1; -\frac{dx}{2\Sigma}\right).$$

733 where $C_{\alpha,d,k}$ is defined in (5.16) and $\Sigma := \sigma_{\alpha,k+d-1}^2 / \sigma_{\alpha,k}^2$. \triangle

734 PROOF. Note that

$$\frac{1}{\Gamma\left(\frac{d}{2}\right)} \gamma\left(\frac{d}{2}, \frac{x}{2}\right) = \frac{(x/2)^{d/2}}{\Gamma\left(\frac{d}{2} + 1\right)} M\left(\frac{d}{2}, \frac{d}{2} + 1; -\frac{x}{2}\right).$$

735 Then

$$\begin{aligned} \Phi[F_{\alpha,d,k}](x) &= \int_0^\infty \left[\frac{(dxs/2)^{d/2}}{\Gamma\left(\frac{d}{2} + 1\right)} M\left(\frac{d}{2}, \frac{d}{2} + 1; -\frac{dxs}{2}\right) \right] \bar{\chi}_{\alpha,k}^2(s) ds \\ &= \frac{(dx/2)^{d/2}}{\Gamma\left(\frac{d}{2} + 1\right)} \int_0^\infty M\left(\frac{d}{2}, \frac{d}{2} + 1; -\frac{dxs}{2}\right) s^{(d-1)/2} \bar{\chi}_{\alpha,k}^2(s) \sqrt{s} ds. \end{aligned}$$

736 When $d = 1$, it fits right in with FGHF. When $d > 1$, it needs more work.

737 From (7.5), let $m = (d-1)/2$, then $k+2m = k+d-1$ and

$$\Phi[F_{\alpha,d,k}](x) = C_{\alpha,d,k} \frac{(dx/2)^{d/2}}{\Gamma\left(\frac{d}{2} + 1\right)} \int_0^\infty M\left(\frac{d}{2}, \frac{d}{2} + 1; -\frac{dxy}{2\Sigma}\right) \bar{\chi}_{\alpha,k+d-1}^2(y) \sqrt{y} dy,$$

738 where $\Sigma := \sigma_{\alpha,k+d-1}^2 / \sigma_{\alpha,k}^2$ and $y = \Sigma s$, and

$$(5.16) \quad C_{\alpha,d,k} := \frac{\sigma_{\alpha,k}^{d-1}}{\sqrt{\Sigma}} \frac{C_{\alpha,k}}{C_{\alpha,k+d-1}} = \frac{\sigma_{\alpha,k}^d}{\sigma_{\alpha,k+d-1}} \frac{C_{\alpha,k}}{C_{\alpha,k+d-1}}.$$

739 The integral matches the FGHF pattern in Lemma 5.12, and we get (5.15). \square

740

741 REMARK 5.11. One final note. There is a connection between (5.14) and (5.15). When $d = 1$,
742 $\Sigma = 1$ and $C_{\alpha,d,k} = 1$. Then

$$(5.17) \quad \Phi[F_{\alpha,1,k}](x^2) = \frac{2x}{\sqrt{2\pi}} F'_{\alpha,k}\left(\frac{1}{2}, \frac{3}{2}; -\frac{x^2}{2}\right)$$

743 which is $2\Phi[L_{\alpha,k}](x) - 1$ in (5.14).

744 This is a reflection of Lemma 8.3. If the variable X distributes as a GSaS $L_{\alpha,k}$, then X^2 distributes
745 as a one-dimensional F, aka $F_{\alpha,1,k}$. It is particularly easy to see this relation in the FGHF form above.

746

Part 2

747

One-Sided Distributions

CHAPTER 6

FG: Fractional Gamma Distribution

749 FG is the backbone that allows many features in this book. In particular, FCM is a member of
 750 FG. It is a fractional version of the generalized gamma distribution, as would become clear to the
 751 reader in this chapter.

752 In my 2024 work[15], it was called *the generalized stable count distribution*, where the name "stable
 753 count distribution" came from my 2020 work[14]. However, after several years of study, it became
 754 clear that it is better to name it after *the gamma distribution*.

755 6.1. Definition

756 DEFINITION 6.1 (Fractional Gamma distribution (FG)). FG is a four-parameter one-sided distri-
 757 bution family, whose PDF is defined as

$$(6.1) \quad \mathfrak{N}_\alpha(x; \sigma, d, p) := C \left(\frac{x}{\sigma} \right)^{d-1} F_\alpha \left(\left(\frac{x}{\sigma} \right)^p \right) \quad (x \geq 0)$$

758 where $F_\alpha(x) = W_{-\alpha,0}(-x)$ from (3.9) and $\alpha \in [0, 1]$ controls the shape of the Wright function; σ is
 759 the scale parameter; p is also the shape parameter controlling the tail behavior ($p \neq 0, dp \geq 0$); d is
 760 the *degree of freedom* parameter. When $\alpha \rightarrow 1$, the PDF becomes a Dirac delta function: $\delta(x - \sigma)$
 761 assuming σ is finite. When $d \geq 1$, all the moments of the FG exist and have closed forms.

762 6.2. Determination of C

763 The normalization constant C is:

$$(6.2) \quad C = \begin{cases} \frac{|p|}{\sigma} \frac{\Gamma(\alpha d/p)}{\Gamma(d/p)} & , \text{ for } \alpha \neq 0, d \neq 0. \\ \frac{|p|}{\sigma \alpha} & , \text{ for } \alpha \neq 0, d = 0. \end{cases}$$

764 It is important to note that d and p are allowed to be negative, as long as $dp \geq 0$.

765 PROOF. The normalization constant C in (6.1) is obtained from the requirement that the integral
 766 of the PDF must be 1:

$$\int_0^\infty \mathfrak{N}_\alpha(x; \sigma, d, p) dx = \frac{C \sigma}{|p|} \frac{\Gamma(\frac{d}{p})}{\Gamma(\frac{d}{p} \alpha)} = 1$$

768 where the integral is carried out by the moment formula of the Wright function.

769 We typically constrain $dp \geq 0$ and p is typically positive. However, it becomes negative in the
 770 inverse distribution and/or characteristic distribution types. So we need $|p|$ to ensure that C is positive.

771 For the case of $\alpha \neq 0$ and $d \rightarrow 0$, due to (A.3), we have

$$C = \frac{|p|}{\sigma \alpha} \quad (\alpha \neq 0, d = 0)$$

772 These two cases are combined to form (6.2). \square

773 6.3. FG Subsumes Generalized Gamma Distribution

774 Since the Wright function extends an exponential function to the fractional space, FG is the
 775 fractional extension of the generalized gamma (GG) distribution[30], whose PDF is defined as:

$$(6.3) \quad f_{\text{GG}}(x; a, d, p) = \frac{|p|}{a\Gamma(d/p)} \left(\frac{x}{a}\right)^{d-1} e^{-(x/a)^p}.$$

776 The parallel use of parameters is obvious, except that a in GG is replaced by σ in FG to avoid confusion
 777 with α .

778 GG is subsumed to FG in two ways:

$$(6.4) \quad f_{\text{GG}}(x; \sigma, d, p) := \begin{cases} \mathfrak{N}_0(x; \sigma, d = d - p, p) & , \text{ at } \alpha = 0. \\ \mathfrak{N}_{\frac{1}{2}}(x; \sigma = \frac{\sigma}{2^{2/p}}, d = d - \frac{p}{2}, p = \frac{p}{2}) & , \text{ at } \alpha = \frac{1}{2}. \end{cases}$$

779 The first line is treated as the definition of FG at $\alpha = 0$. The proof is given in [15].

780 Although the first line is more obvious, it is the second line that leads to the fractional extension
 781 of the χ distribution.

782 6.4. Mellin Transform

783 From Example 2.4, we add σ and C . The Mellin transform of the PDF of the fractional gamma
 784 distribution is

$$(6.5) \quad \begin{aligned} \mathfrak{N}_\alpha(x; \sigma, d, p) &\xleftrightarrow{\mathcal{M}} \frac{C \sigma^s}{|p|} \frac{\Gamma((s + d - 1)/p)}{\Gamma(\alpha(s + d - 1)/p)} \\ &= \sigma^{s-1} \frac{\Gamma(ad/p)}{\Gamma(d/p)} \frac{\Gamma((s + d - 1)/p)}{\Gamma(\alpha(s + d - 1)/p)}, \end{aligned}$$

785 where C is from Section 6.2. The typical limiting case for the gamma functions shall be taken care in
 786 each scenario.

787 FG is often used in a ratio distribution, such as the role of $g^*(s)$ in (2.6), where $s \rightarrow 2 - s$. The
 788 term $s + d - 1$ becomes $d + 1 - s$. Furthermore, in the FCM case, since $d = k - 1$, it becomes the
 789 elegant $k - s$ term.

790 6.5. CDF and Fractional Incomplete Gamma Function

791 The CDF of FG is

$$(6.6) \quad \Phi(x) := \int_0^x \mathfrak{N}_\alpha(s; \sigma, d, p) ds \quad (x \geq 0).$$

792 This integral leads to fractionalization of the incomplete gamma function in Section 3.4.

793 LEMMA 6.2. The CDF of FG can be represented by γ_α^* in (3.20) or Γ_α^* in (3.21) as

$$(6.7) \quad \Phi(x) = \begin{cases} z^{d+p} \gamma_\alpha^*(d/p + 1, z^p) & , \text{ when } p > 0. \\ z^{d+p} \Gamma_\alpha^*(d/p + 1, z^p) & , \text{ when } p < 0. \end{cases}$$

794 where $z = x/\sigma$ is the standardized variable.

795 This could be viewed as one form of fractional extension to the regularized lower incomplete gamma
 796 function, $\gamma(s, z)/\Gamma(s)$, which is the CDF of GG mentioned above.

797 Due to this result, this distribution is called the *fractional gamma distribution* (FG). △

799 PROOF. The CDF of FG is

$$\begin{aligned}\Phi(x) &= \int_0^x \mathfrak{N}_\alpha(s; \sigma, d, p) ds \\ &= C \int_0^x ds \left(\frac{s}{\sigma}\right)^{d-1} W_{-\alpha,0} \left(-\left(\frac{s}{\sigma}\right)^p\right). \\ &= C \int_0^x ds \left(\frac{s}{\sigma}\right)^{d-1} F_\alpha \left(\left(\frac{s}{\sigma}\right)^p\right).\end{aligned}$$

800 Since $F_\alpha(x) = \alpha x M_\alpha(x)$ from (3.9), and let $u = s/x$, then $u \in [0, 1]$ and

$$\begin{aligned}\Phi(x) &= \alpha C \int_0^x ds \left(\frac{s}{\sigma}\right)^{d+p-1} M_\alpha \left(\left(\frac{s}{\sigma}\right)^p\right) \\ &= \alpha C x \int_0^1 du \left(\frac{xu}{\sigma}\right)^{d+p-1} M_\alpha \left(\left(\frac{xu}{\sigma}\right)^p\right)\end{aligned}$$

801 Recognize that $u^p \in [0, 1]$ when $p > 0$. Let $t = u^p$, and $dt/t = p du/u$,

$$\Phi(x) = \frac{\alpha \sigma C}{p} z^{d+p} \int_0^1 dt t^{d/p} M_\alpha(z^p t)$$

802 Compare the last line with γ_α^* in (3.20), and we get

$$\Phi(x) = \frac{\alpha \sigma C}{p} \frac{\Gamma(\frac{d}{p} + 1)}{\Gamma((1 - \alpha) + \alpha(\frac{d}{p} + 1))} z^{d+p} \gamma_\alpha^*(d/p + 1, z^p)$$

803 Using the case of $\alpha \neq 0, d \neq 0$ for C , it can be shown that the constant part is just 1. Hence,

$$\Phi(x) = z^{d+p} \gamma_\alpha^*(d/p + 1, z^p), \quad \text{for } p > 0.$$

804 On the other hand, $u^p \in [1, \infty]$ when $p < 0$. The range of the integral changes to \int_1^∞ . It leads to
805 the use of the supplementary function (3.21):

$$\Phi(x) = z^{d+p} \Gamma_\alpha^*(d/p + 1, z^p).$$

806 □

807 Numerically, it is better to use γ_α^* when $z^p \leq 1$ and to use Γ_α^* when $z^p > 1$, as long as the identity
808 relation (3.22) is preserved.

6.6. Inverse Expression of Several Fractional Distributions

810 Several known fractional distributions could be expressed in the FG in Table 1. This shows that
811 the FG is the super set of the one-sided fractional distribution system. Its parametrization provides
812 immense flexibility to express other formerly known one-sided distributions.

Distribution (PDF)	Wright Equiv.	FG: $\mathfrak{N}_\alpha(x; \sigma, d, p)$			
		α	σ	d	p
One-sided stable: $L_\alpha(x)$	$x^{-1}W_{-\alpha,0}(-x^{-\alpha})$	α	1	0	$-\alpha$
Stable Count: $\mathfrak{N}_\alpha(x)$		α	1	1	α
Stable Vol: $V_\alpha(x)$		$\frac{\alpha}{2}$	$\frac{1}{\sqrt{2}}$	1	α
M-Wright: $M_\alpha(x)$	$\frac{1}{\alpha x}W_{-\alpha,0}(-x)$	α	1	0	1
M-Wright II: $\Gamma(\alpha)F_\alpha(x)$	$\Gamma(\alpha)W_{-\alpha,0}(-x)$	α	1	1	1

TABLE 1. FG mapping of several known fractional distributions in the literature.
 $\mathfrak{N}_\alpha(x)$ and $V_\alpha(x)$ first appeared in [14], which led to this work.

813

6.7. Alternative Definition

814 DEFINITION 6.3. It is reasonable to argue that the PDF of FG can be defined via the M-Wright
 815 function directly, such that

$$(6.8) \quad \mathfrak{N}'_\alpha(x; \sigma, d', p) := C' \left(\frac{x}{\sigma} \right)^{d'-1} M_\alpha \left(\left(\frac{x}{\sigma} \right)^p \right). \quad (x \geq 0)$$

816

However, since $F_\alpha(z) = \alpha z M_\alpha(z)$, it is easy to see that

$$\mathfrak{N}'_\alpha(x; \sigma, d', p) = \alpha C' \left(\frac{x}{\sigma} \right)^{d'+p-1} F_\alpha \left(\left(\frac{x}{\sigma} \right)^p \right).$$

817 Therefore, this is merely a reparameterization of $d = d' + p$. This definition will encounter some issues
 818 in FCM later due to the assignment of $d \rightarrow k - 1$, $\alpha \rightarrow \alpha/2$ and $p \rightarrow \alpha$ (see (7.4)). We learn from
 819 Figures 12.1 and 12.2 that there is a natural linear relation between k and $\epsilon = 1/\alpha$. Mixing the role
 820 of d with α from p is not a good idea.

CHAPTER 7

821

Fractional Chi Distributions

822

7.1. Introduction to Fractional Chi Distribution

823 In Chapter 4, we've discussed the insight that leads to the fractional χ is to interpret the Mellin
824 transform of the PDF of the α -stable distribution as a ratio distribution of two components:

$$L_\alpha^\theta(x) \xleftrightarrow{\mathcal{M}} \epsilon \left[\frac{\Gamma(s)}{\Gamma(1 - \gamma + \gamma s)} \right] \left[\frac{\Gamma(\epsilon(1 - s))}{\Gamma(\gamma(1 - s))} \right]$$

where $\epsilon = \frac{1}{\alpha}$, $\gamma = \frac{\alpha - \theta}{2\alpha}$.

825 The first bracket is the Mellin transform of the M-Wright function.

826 The second bracket is interpreted as the Mellin transform of the PDF of the fractional χ -mean
827 distribution (FCM) at $k = 1$:

$$\bar{\chi}_{\alpha,1}^\theta(x) \xleftrightarrow{\mathcal{M}} \bar{\chi}_{\alpha,1}^{\theta,*}(s) \propto \frac{\Gamma(\epsilon(s - 1))}{\Gamma(\gamma(s - 1))},$$

828 apart from the normalization constant and scale in the PDF.

829 It becomes obvious after replacing $s \rightarrow 2 - s$ in $\bar{\chi}_{\alpha,1}^{\theta,*}(s)$ in order to comply with the rule of Mellin
830 transform of a ratio distribution.

831 In this chapter, the "degrees of freedom" parameter k is inserted by replacing $s - 1$ with $s + k - 2$,
832 such that

$$(7.1) \quad \bar{\chi}_{\alpha,k}^\theta(x) \xleftrightarrow{\mathcal{M}} \bar{\chi}_{\alpha,k}^{\theta,*}(s) \propto \frac{\Gamma(\epsilon(s + k - 2))}{\Gamma(\gamma(s + k - 2))}.$$

833 This forms the foundation for more rigorous treatment of FCM.

834

7.2. FCM: Fractional Chi-Mean Distribution

835 There are two ways to define FCM. The first approach is to define it via Mellin transform. The
836 second approach is to define the shape of its PDF.

837 DEFINITION 7.1 (Fractional χ -mean distribution (FCM) via Mellin Transform). The Mellin trans-
838 form of FCM's PDF is enriched from (7.1) to

$$(7.2) \quad \begin{aligned} \bar{\chi}_{\alpha,k}^\theta(x) &\xleftrightarrow{\mathcal{M}} \bar{\chi}_{\alpha,k}^{\theta,*}(s) \\ &= (\sigma_{\alpha,k}^\theta)^{s-1} \frac{\Gamma(\gamma(k-1))}{\Gamma(\epsilon(k-1))} \frac{\Gamma(\epsilon(s+k-2))}{\Gamma(\gamma(s+k-2))}, \\ &\text{where } \sigma_{\alpha,k}^\theta := \gamma^\gamma k^{\gamma-\epsilon}. \end{aligned}$$

839 The main differences are (1) to address the normalization of the total density, and (2) to have a
840 proper scale $\sigma_{\alpha,k}^\theta$ such that it is consistent with the classic χ distribution and α -stable distribution.

841 For positive k , the PDF of an FCM is

$$(7.3) \quad \begin{aligned} \bar{\chi}_{\alpha,k}^{\theta}(x) &:= \mathfrak{N}_{\gamma\alpha}(x; \sigma = \sigma_{\alpha,k}^{\theta}, d = k - 1, p = \alpha) \\ &= \frac{\Gamma(\gamma(k - 1))}{\epsilon\Gamma(\epsilon(k - 1))} (\sigma_{\alpha,k}^{\theta})^{1-k} x^{k-2} F_{\gamma\alpha} \left(\left(\frac{x}{\sigma_{\alpha,k}^{\theta}} \right)^{\alpha} \right), \end{aligned} \quad (x \geq 0)$$

842 where $\mathfrak{N}_{\lambda}(x; \sigma, d, p)$ is FG (6.1), and $F_{\lambda}(x) := W_{-\lambda,0}(-x)$ is the Wright function of the second kind
843 (3.9).

844

845 Notice the appearances of γ that replaces all the $1/2$ in Section 7.6 of [15]. That is how θ comes
846 into play in the upgraded FCM. This full representation is used in Chapter 11.

847 However, for GAS-SN in Chapter 12 and beyond, such θ upgrade is unnecessary. The skew-normal
848 framework is based on modulation of normal distributions. It is required to have $\theta = 0$ ($\gamma = 1/2$).

849 Hence, we recite the original definition of FCM PDF ($k > 0$):

$$(7.4) \quad \begin{aligned} \bar{\chi}_{\alpha,k}(x) &= \bar{\chi}_{\alpha,k}^0(x) := \mathfrak{N}_{\alpha/2}(x; \sigma = \sigma_{\alpha,k}, d = k - 1, p = \alpha) \\ &= (C_{\alpha,k}) (\sigma_{\alpha,k})^{1-k} x^{k-2} F_{\frac{\alpha}{2}} \left(\left(\frac{x}{\sigma_{\alpha,k}} \right)^{\alpha} \right), \end{aligned} \quad (x \geq 0)$$

850 where

$$(7.5) \quad C_{\alpha,k} := \frac{\alpha\Gamma((k - 1)/2)}{\Gamma((k - 1)/\alpha)}$$

$$(7.6) \quad \sigma_{\alpha,k} := \frac{|k|^{1/2-1/\alpha}}{\sqrt{2}}.$$

851 Note that the difference between (7.3) and (7.4) is very small: Just replace $\mathfrak{N}_{\gamma\alpha}(\dots)$ to $\mathfrak{N}_{\alpha/2}(\dots)$.

852 **7.2.1. FCM CDF.** Extending directly from Lemma 6.2, we have

853 LEMMA 7.2. The CDF of FCM can be represented by γ_{α}^* in (3.20) as

$$(7.7) \quad \Phi[\bar{\chi}_{\alpha,k}](x) = z^{k-1+\alpha} \gamma_{\alpha/2}^* \left(\frac{k-1+\alpha}{\alpha}, z^{\alpha} \right), \quad (k > 0, \alpha \in [0, 2])$$

854 where $z = x/\sigma_{\alpha,k}$. △

855

856

7.3. FCM Moments

858 By letting $s = n + 1$ and $\theta = 0$ in (7.2), its n -th moment is

$$(7.8) \quad \mathbb{E}(X^n | \bar{\chi}_{\alpha,k}) = (\sigma_{\alpha,k})^n \frac{\Gamma((k - 1)/2)}{\Gamma((k - 1)/\alpha)} \frac{\Gamma((n + k - 1)/\alpha)}{\Gamma((n + k - 1)/2)}, \quad (k > 0, \alpha > 0)$$

859 which requires $k > 1$ and $n + k > 1$ to avoid the singularity of the gamma functions (See Section 7.6
860 of [15]).

861 The explicit form of the first moment is

$$(7.9) \quad \mathbb{E}(X | \bar{\chi}_{\alpha,k}) = \sigma_{\alpha,k} \frac{\Gamma((k - 1)/2)}{\Gamma((k - 1)/\alpha)} \frac{\Gamma(k/\alpha)}{\Gamma(k/2)} = \sigma_{\alpha,k} \frac{C_{\alpha,k}}{C_{\alpha,k+1}}. \quad (k > 0, \alpha > 0)$$

862 Notice that it can be used as a bridge connecting the coefficient C between k and $k + 1$.

863 The moment formula of FCM is fundamental to all the fractional distributions built on top of it.
864 However, ironically, due to the nature of a ratio distribution, it is often evaluated as negative moments
865 $n < 0$. Hence, n is restricted in the range of $1 - k < n < 0$.

866 This results in non-existing moments when k is not "large enough", which happens to be a core
 867 feature of the α -stable distribution and Student's t distribution. Our two-dimensional parameter space
 868 (α, k) adds more complexity to it.

869 **7.3.1. FCM at Infinite Degrees of Freedom.** The choice of $\sigma_{\alpha,k}$ is intentional, such that

$$(7.10) \quad \lim_{k \rightarrow \infty} \mathbb{E}(X^n | \bar{\chi}_{\alpha,k}) = \alpha^{-n/\alpha}. \quad (k > 0, \alpha > 0)$$

870 Under such conditions, its variance is zero. That is, FCM becomes a delta function, $\delta(x - \alpha^{-1/\alpha})$,
 871 as $k \rightarrow \infty$.

872 7.4. FCM Reflection Formula and Negative k

873 **7.4.1. FCM for Negative k.** We quote Definition 3.2 of [15] for FCM in the negative k space.
 874 Its PDF defined by FG is

$$(7.11) \quad \bar{\chi}_{\alpha,-k}(x) := \mathfrak{N}_{\alpha/2}(x; \sigma = (\sigma_{\alpha,k})^{-1}, d = -k, p = -\alpha). \quad (x \geq 0, k > 0)$$

875 It is the *characteristic FCM* discussed in Lemma 9.6, that is, $[\bar{\chi}_{\alpha,k}]_\phi := \bar{\chi}_{\alpha,-k}$ in Lemma 9.6. Hence,

$$(7.12) \quad \bar{\chi}_{\alpha,-k}(x) = \frac{x^{-3}}{\mathbb{E}(X | \bar{\chi}_{\alpha,k})} \bar{\chi}_{\alpha,k} \left(\frac{1}{x} \right). \quad (x \geq 0, k > 0)$$

876 TODO should prove this !?

877 This is used to define the fractional exponential power distribution within the GSaS (and GAS-SN)
 878 nomenclature. See Section 12.7. The readers interested in full detail are referred to the FCM sections
 879 in [15].

880 The negative k case is derived from the properties of the α -stable characteristic function in Chapter
 881 9. It is used to build a generalized two-sided distribution (Section 9 of [15]) that subsumes the
 882 exponential power distribution (Section 3.11.1 of [24]).

883 We quote the FCM reflection formula from Section 7 of [15] to summarize the relation:

$$(7.13) \quad \mathbb{E}(X^n | \bar{\chi}_{\alpha,-k}) = \frac{\mathbb{E}(X^{-n+1} | \bar{\chi}_{\alpha,k})}{\mathbb{E}(X | \bar{\chi}_{\alpha,k})}, \quad k > 0.$$

884 This indicates an elegant relation for the first moment that $\mathbb{E}(X | \bar{\chi}_{\alpha,-k}) = 1 / \mathbb{E}(X | \bar{\chi}_{\alpha,k})$.

885 **7.5. FCM2: Fractional Chi-Squared-Mean Distribution**

886 If $Z \sim \bar{\chi}_{\alpha,k}$, then $X \sim Z^2$ is FCM2, denoted as $X \sim \bar{\chi}_{\alpha,k}^2$. This is the fractional extension of the
887 classic χ_k^2/k , which is subsumed by it at $\alpha = 1$.

888 $\bar{\chi}_{\alpha,k}^2$ is used in the fractional F distribution in the area of the squared variable and the quadratic
889 form in the multivariate elliptical distribution.

890 DEFINITION 7.3. The PDF of FCM2 is

$$(7.14) \quad \bar{\chi}_{\alpha,k}^2(x) = \frac{1}{2\sqrt{x}} \bar{\chi}_{\alpha,k}(\sqrt{x}) \quad (x \geq 0, \alpha \in [0, 2])$$

891 Expressed in FG and (7.4), it is

$$(7.15) \quad \begin{aligned} \bar{\chi}_{\alpha,k}^2(x) &:= \mathfrak{N}_{\alpha/2}(x; \sigma = \sigma_{\alpha,k}^2, d = (k-1)/2, p = \alpha/2) \quad (k > 0) \\ &= \frac{C_{\alpha,k}}{2\sigma_{\alpha,k}^2} \left(\frac{x}{\sigma_{\alpha,k}^2} \right)^{k/2-3/2} F_{\frac{\alpha}{2}} \left(\left(\frac{x}{\sigma_{\alpha,k}^2} \right)^{\alpha/2} \right). \end{aligned}$$

892 Or for $k < 0$,

$$(7.16) \quad \bar{\chi}_{\alpha,k}^2(x) := \mathfrak{N}_{\alpha/2}(x; \sigma = \sigma_{\alpha,k}^{-2}, d = k/2, p = -\alpha/2) \quad (k < 0)$$

893

894 When dealing with the fractional Gauss hypergeometric function (FGHF) in Section 5.2, we need
895 two more variations from FCM2. The first allows an FCM2 to take a different scale:

$$(7.17) \quad \bar{\chi}_{\alpha,k}^2(x; \sigma) := \mathfrak{N}_{\alpha/2}(x; \sigma = \sigma, d = (k-1)/2, p = \alpha/2) \quad (k > 0)$$

896 from which the constant-scale variant is defined by replacing $\sigma_{\alpha,k}$ with $1/2$,

$$(7.18) \quad \hat{\chi}_{\alpha,k}^2(x) := \bar{\chi}_{\alpha,k}^2(x; \sigma = 1/4) = \mathfrak{N}_{\alpha/2}(x; \sigma = 1/4, d = (k-1)/2, p = \alpha/2) \quad (k > 0)$$

897 Notice the hat symbol replaces the bar symbol.

898 **7.5.1. FCM2 CDF.** Extending directly from Lemma 6.2, we have:

899 LEMMA 7.4. The CDF of FCM2 can be represented by γ_{α}^* as

$$(7.19) \quad \Phi[\bar{\chi}_{\alpha,k}^2](x) = z^{(k-1+\alpha)/2} \gamma_{\alpha/2}^* \left(\frac{k-1+\alpha}{\alpha}, z^{\alpha/2} \right) \quad (k > 0, \alpha \in [0, 2])$$

900 where $z = x/\sigma_{\alpha,k}^2$. △

901 **7.5.2. Representing FCM by FCM2.** In (7.14), let $s = \sqrt{x}$, we get the inverse relation:

$$(7.20) \quad \bar{\chi}_{\alpha,k}(s) = 2s \bar{\chi}_{\alpha,k}^2(s^2) \quad (s \geq 0)$$

902 Many ratio distribution integrals involving FCM can be rewritten in terms of FCM2, such that

$$(7.21) \quad \begin{aligned} f(x) &:= \int_0^\infty g(xs) \bar{\chi}_{\alpha,k}(s) s ds \\ &= \int_0^\infty g(x\sqrt{\nu}) \bar{\chi}_{\alpha,k}^2(\nu) \sqrt{\nu} d\nu \end{aligned}$$

903 For the CDF case, the incomplete integral can be transformed as

$$(7.22) \quad \begin{aligned} F(x) &:= \int_0^x f(x) dx = \int_0^\infty G(xs) \bar{\chi}_{\alpha,k}(s) ds \\ &= \int_0^\infty G(x\sqrt{\nu}) \bar{\chi}_{\alpha,k}^2(\nu) d\nu \end{aligned}$$

904 where $G(x) := \int_0^x g(x) dx$. The lower bound of the incomplete integrals can be $-\infty$ such as $\int_{-\infty}^x dx$
 905 too.

906 **7.5.3. Universal Expression.** Assume $x \geq 0$, let $M(x^2) := G(x)/x$ in (7.22) or $g(x)$ in (7.21),
 907 we get the universal expression of

$$(7.23) \quad F(x) = x \int_0^\infty M(x^2\nu) \bar{\chi}_{\alpha,k}^2(\nu) \sqrt{\nu} d\nu$$

$$(7.24) \quad f(x) = \int_0^\infty M(x^2\nu) \bar{\chi}_{\alpha,k}^2(\nu) \sqrt{\nu} d\nu$$

908 Most of the univariate PDFs and CDFs in subsequent chapters can be understood in such framework.
 909 It is just a matter of what $M(x)$ is.

910 When $M(x)$ can be expressed by a Kummer function (apart from a negative sign), these integrals
 911 are members of the FGHF in Section 5.2.

912 7.6. FCM2 Mellin Transform

913 From (6.5), the Mellin transform of FCM2's PDF is

$$(7.25) \quad \begin{aligned} \bar{\chi}_{\alpha,k}^2(x) &\xleftarrow{\mathcal{M}} \bar{\chi}_{\alpha,k}^{2*}(s) \\ &= (\sigma_{\alpha,k})^{2s-2} \frac{\Gamma((k-1)/2)}{\Gamma((k-1)/\alpha)} \frac{\Gamma((s+k/2-3/2) \times 2/\alpha)}{\Gamma(s+k/2-3/2)}. \end{aligned} \quad (k > 0)$$

914 Likewise, for the constant-scale variant, it becomes

$$(7.26) \quad \begin{aligned} \hat{\chi}_{\alpha,k}^2(x) &\xleftarrow{\mathcal{M}} \hat{\chi}_{\alpha,k}^{2*}(s) \\ &= 2^{2-2s} \frac{\Gamma((k-1)/2)}{\Gamma((k-1)/\alpha)} \frac{\Gamma((s+k/2-3/2) \times 2/\alpha)}{\Gamma(s+k/2-3/2)}, \end{aligned} \quad (k > 0)$$

915 whose most important special case is $\alpha = 1$,

$$(7.27) \quad \hat{\chi}_{1,k}^2(x) \xleftarrow{\mathcal{M}} \hat{\chi}_{1,k}^{2*}(s) = \frac{\Gamma(s+k/2-1)}{\Gamma(k/2)}$$

916 $\Gamma(s+k/2-1)$ in $\hat{\chi}_{1,k}^{2*}(s)$ is just an ordinary gamma function without a fractional coefficient in
 917 front of s . This property is the basis that connects the fractional Gauss hypergeometric function to
 918 its classic form in Section 5.2.

919 7.7. FCM2 Moments

920 From the Mellin transform by $s = n + 1$, its n -th moment is

$$(7.28) \quad \begin{aligned} \mathbb{E}(X^n | \bar{\chi}_{\alpha,k}^2) &= \mathbb{E}(X^{2n} | \bar{\chi}_{\alpha,k}) \\ &= (\sigma_{\alpha,k})^{2n} \frac{\Gamma((k-1)/2)}{\Gamma((k-1)/\alpha)} \frac{\Gamma((n+k/2-1/2) \times 2/\alpha)}{\Gamma(n+k/2-1/2)}. \end{aligned} \quad (k > 0)$$

921 As mentioned in Section 7.3, due to the nature of a ratio distribution, it is often evaluated as
 922 negative moments, $n < 0$. Hence, n is confined in the range of $1/2 - k/2 < n < 0$.

923 This puts stricter constraint on non-existing moments than FCM when k is not "large enough".
 924 For instance, in the case of fractional F distribution in Section 8.4, $k \approx 3$ is in the neighborhood where
 925 it second moment barely exists. This makes it rather hard for the statistics of the SPX daily return
 926 data set, since its k is just slightly larger than 3 while α is slightly below 1.

927 **7.8. FCM2 Increment of k**

928 LEMMA 7.5. When x^m is multiplied to $\bar{\chi}_{\alpha,k}^2(x)$, it follows a scaling rule where k is incremented to
929 $k + 2m$ in the parametrization.

$$(7.29) \quad x^m \bar{\chi}_{\alpha,k}^2(x) = \sigma_{\alpha,k}^{2m} Q \frac{C_{\alpha,k}}{C_{\alpha,k+2m}} \bar{\chi}_{\alpha,k+2m}^2(y).$$

930 where $Q := \sigma_{\alpha,k+2m}^2 / \sigma_{\alpha,k}^2$ and $y = Qx$. \triangle

931 PROOF. From (7.15),

$$x^m \bar{\chi}_{\alpha,k}^2(x) = \sigma_{\alpha,k}^{2m} \frac{C_{\alpha,k}}{2 \sigma_{\alpha,k}^2} \left(\frac{x}{\sigma_{\alpha,k}^2} \right)^{(k+2m)/2-3/2} F_{\frac{\alpha}{2}} \left(\left(\frac{x}{\sigma_{\alpha,k}^2} \right)^{\alpha/2} \right).$$

932 We see that $\bar{\chi}_{\alpha,k}^2$ should become $\bar{\chi}_{\alpha,k+2m}^2$ according to the power in the $x^{(k+2m)/2-3/2}$ term, but other
933 parts of the formula need to be adjusted too.

934 Since

$$\bar{\chi}_{\alpha,k+2m}^2(y) = \frac{C_{\alpha,k+2m}}{2 \sigma_{\alpha,k+2m}^2} \left(\frac{y}{\sigma_{\alpha,k+2m}^2} \right)^{(k+2m)/2-3/2} F_{\frac{\alpha}{2}} \left(\left(\frac{y}{\sigma_{\alpha,k+2m}^2} \right)^{\alpha/2} \right),$$

935 we obtain $y = x \sigma_{\alpha,k+2m}^2 / \sigma_{\alpha,k}^2$ in order to match the two structurally.

936 Then take the ratio of $x^m \bar{\chi}_{\alpha,k}^2(x) / \bar{\chi}_{\alpha,k+2m}^2(y)$ to determine the needed constant, we arrive at
937 (7.29). \square

938

939 **7.9. Sum of Two Chi-Squares with Correlation**

940 The sum of bivariate variables is studied here.

941 LEMMA 7.6. Let $Z = Z_1/s_1 + Z_2/s_2$ where Z_1, Z_2 are two independent χ_1^2 variables. The PDF of
942 Z is

$$\begin{aligned} \chi_{11}^2(z, s_1, s_2) &= \frac{\sqrt{s_1 s_2}}{2} e^{-s_2 z/2} {}_1F_1 \left(\frac{1}{2}, 1; \frac{(s_2 - s_1)z}{2} \right) \\ &= \frac{\sqrt{s_1 s_2}}{2} e^{-(s_1 + s_2)z/4} I_0(|s_2 - s_1|z/4) \end{aligned}$$

943 We apply DLMF 12.6.9 to get the second line, where the symmetry of a, b is explicit since $I_0(x)$ is
944 symmetric. For $x \gg 1$, $I_0(x) \approx e^x / \sqrt{2\pi x}$ (DLMF 10.40.5). \triangle

945 When $Z_1 = U_1^2$, $Z_2 = U_2^2$, and U_1, U_2 has correlation ρ , then s_1, s_2 must be modified by the
946 eigenvalue solution of $\bar{\Omega}^{-1} \text{diag}(s)$ such that

$$\begin{aligned} \chi_{11}^2(z, s_1, s_2, \rho) &= \chi_{11}^2(z, s'_1, s'_2) \\ \text{where } (s'_1, s'_2) &= \frac{(s_1 + s_2) \pm \sqrt{(s_1 - s_2)^2 - 4\rho^2 s_1 s_2}}{2(1 - \rho^2)} \end{aligned}$$

CHAPTER 8

Fractional F Distribution

The classic F distribution comes from the ratio of two χ^2 distributions. Assume $U_1 \sim \chi^2_d/d$ and $U_2 \sim \chi^2_k/k$, then $F \sim U_1/U_2$ is an F distribution, $F_{d,k}$.

Two use cases were mentioned in Azzalini (2013)[1]. In Section 4.3 there, the squared variable of a univariate skew-t with k degrees of freedom is distributed as $F_{1,k}$.

In Section 6.2 there, the quadratic form a $d \times d$ multivariate skew-t with k degrees of freedom is distributed as $F_{d,k}$.

954 Thus, the meaning of d and k is quite clear in such a context: d is the dimension of the multivariate
955 skew-normal process; k is the degree of freedom in the denominator of the ratio distribution. This
956 chapter extends it fractionally.

8.1. Definition

DEFINITION 8.1. Assume $U_1 \sim \chi_d^2/d$ and $U_2 \sim \chi_{\alpha,k}^2$, then $F \sim U_1/U_2$ is a fractional F distribution.
 We use the notation $F \sim F_{\alpha,d,k}$.

960 The standard PDF of $F_{\alpha,d,k}$ is

$$(8.1) \quad F_{\alpha,d,k}(x) = \int_0^\infty s \, ds \left[d \chi_d^2(dx s) \right] \overline{\chi}_{\alpha,k}^2(s)$$

⁹⁶¹ and note that the classic term in the integrand, $d\chi_d^2(dz)$, is equivalent to our $\bar{\chi}_{1,d}^2(z)$.

The reader should be aware of the subtlety that "ds" in "s ds" is the calculus notation, while d in $[d \chi_d^2(ds)]$ is the constant from $F_{\alpha,d,k}$.

964 The standard CDF of $F_{\alpha,d,k}$ is

$$\begin{aligned}
 (8.2) \quad \Phi[F_{\alpha,d,k}](x) &= \int_0^x F_{\alpha,d,k}(s) ds \\
 (8.3) \quad &= \int_0^\infty \left[\frac{1}{\Gamma(\frac{d}{2})} \gamma\left(\frac{d}{2}, \frac{ds}{2}\right) \right] \bar{\chi}_{\alpha,k}^2(s) ds
 \end{aligned}$$

965 since the CDF of a χ_d^2 is the regularized lower incomplete gamma function of $\gamma\left(\frac{d}{2}, \frac{x}{2}\right)/\Gamma\left(\frac{d}{2}\right)$.

It can also be represented by a fractional Gauss hypergeometric function. See Section 5.2.5.

8.1.1. The Origin of Fractional F. $F_{\alpha,d,k}$ is connected to the quadratic form of a d -dimensional multivariate GAS-SN distribution, $L_{\alpha,k}(0, \bar{\Omega}, \beta)$. Indeed, its three parameters, α, d, k , are designated such that the symbols convey the same meanings. However, $\bar{\Omega}$ and β doesn't affect the outcome of $F_{\alpha,d,k}$.

To elaborate from Section 15.6, assume Z is a $d \times d$ multivariate skew-normal (SN) distribution $SN(0, \bar{\Omega}, \beta)$, and $\bar{\chi}_{\alpha,k}$ is a standard FCM. Then $X = Z/\bar{\chi}_{\alpha,k}$ is an $L_{\alpha,k}(0, \bar{\Omega}, \beta)$.

The quadratic form of X is $Q = \frac{1}{d} X^\top \bar{\Omega}^{-1} X$. And $Q \sim F_{\alpha, d, k}$ is a fractional F distribution.

8.1.2. Fractional F Subsumes F.

LEMMA 8.2. When $\alpha = 1$, it becomes a classic F. That is, $F_{1,d,k} = F_{d,k}$.

976 **8.1.3. Fractional F Subsumes GSaS-Squared and GAS-SN-Squared.** The following cases
 977 are for $d = 1$:

978 LEMMA 8.3. If $X_1 \sim L_{\alpha,k}$, then $X_1^2 \sim F_{\alpha,1,k}$. △

979 LEMMA 8.4. If $X_2 \sim L_{\alpha,k}(\beta)$, then $X_2^2 \sim F_{\alpha,1,k}$, independent of β . △

980 They will be discussed in Chapter 12.

981 8.2. PDF at Zero

982 The PDF of an F distribution is singular as $x \rightarrow 0$ when $d < 2$. We can see that from

$$(8.4) \quad \begin{aligned} F_{\alpha,d,k}(x) &\approx \frac{(d/2)^{d/2}}{\Gamma(d/2)} x^{d/2-1} \int_0^\infty s^{d/2} ds |\bar{\chi}_{\alpha,k}(s)| \\ &= \frac{(d/2)^{d/2}}{\Gamma(d/2)} \mathbb{E}(X^d | \bar{\chi}_{\alpha,k}) x^{d/2-1} \end{aligned}$$

983 for very small x .

984 When $d = 1$, the peak is divergent as $F_{\alpha,1,k}(x) \approx \frac{1}{\sqrt{2\pi}} \mathbb{E}(X | \bar{\chi}_{\alpha,k}) \sqrt{x}^{-1}$. But its CDF $\propto \sqrt{x}$.

985 When $d = 2$, this peak is finite. $F_{\alpha,2,k}(0) = \mathbb{E}(X^2 | \bar{\chi}_{\alpha,k})$.

986 When $d > 2$, $F_{\alpha,d,k}(x)$ drops to zero at $x = 0$. This strange phenomenon seems to indicate that
 987 the bivariate system is the lowest dimension to have stable quadratic statistics. And a three dimension
 988 system is likely more stable. But we only analyze the bivariate case in this book.

989 8.3. Mellin Transform

990 From (7.25), and note that $\bar{\chi}_d^2 = \bar{\chi}_{1,d}^2$, the Mellin transform of Fractional F's PDF is

$$(8.5) \quad F_{\alpha,d,k}(x) \xleftrightarrow{\mathcal{M}} (\bar{\chi}_{1,d}^2)^*(s) (\bar{\chi}_{\alpha,k}^2)^*(2-s) \quad (d > 0, k > 0)$$

$$(8.6) \quad = \left(\sqrt{2d} \sigma_{\alpha,k} \right)^{2-2s} \left[\frac{\Gamma((d-1)/2)}{\Gamma(d-1)} \frac{\Gamma((k-1)/2)}{\Gamma((k-1)/\alpha)} \right] \left[\frac{\Gamma(2p(s))}{\Gamma(p(s))} \frac{\Gamma(2q(s)/\alpha)}{\Gamma(q(s))} \right],$$

where $p(s) := s + d/2 - 3/2$, $q(s) := 1/2 + k/2 - s$.

991 The number of gamma functions can be reduced via the Legendre duplication formula (A.2).

992 8.4. Moments

993 Its n -th moment is

$$(8.7) \quad \begin{aligned} \mathbb{E}(X^n | F_{\alpha,d,k}) &= d^{-n} \mathbb{E}(X^n | \bar{\chi}_d^2) \mathbb{E}(X^{-n} | \bar{\chi}_{\alpha,k}^2) \\ &= \left(\frac{2}{d} \right)^n (d/2)_n \mathbb{E}(X^{-n} | \bar{\chi}_{\alpha,k}^2). \end{aligned}$$

994 where $(d/2)_n$ is the Pochhammer symbol, $(a)_n := \Gamma(a+n)/\Gamma(a)$.

995 Its first moment is $\mathbb{E}(X^{-1} | \bar{\chi}_{\alpha,k}^2) = \mathbb{E}(X^{-2} | \bar{\chi}_{\alpha,k}^2)$, independent of d . This is due to $\mathbb{E}(X | \bar{\chi}_d^2) = d$.

996 Note that this first moment is also the second moment of an univariate GAS-SN in (12.9), or
 997 simply the variance of the corresponding GSaS.

998 Its second moment is $(1 + 2/d) \mathbb{E}(X^{-2} | \bar{\chi}_{\alpha,k}^2)$. Hence, its variance is

$$(8.8) \quad \begin{aligned} \text{var}\{F_{\alpha,d,k}\} &= (1 + 2/d) \mathbb{E}(X^{-2} | \bar{\chi}_{\alpha,k}^2) - \mathbb{E}(X^{-1} | \bar{\chi}_{\alpha,k}^2)^2 \\ &= (1 + 2/d) \mathbb{E}(X^{-4} | \bar{\chi}_{\alpha,k}^2) - \mathbb{E}(X^{-2} | \bar{\chi}_{\alpha,k}^2)^2. \end{aligned}$$

999 **8.4.1. Stability Issue of the Second Moment.** The moment formula appears to be straight-
1000 forward. But the devil is in the detail.

1001 The stability of moments symbolizes the challenge of stability in the α -stable distribution. Even
1002 the second moment has dramatic behaviors when k is smaller than 4.

1003 First, we shall recognize that the first moment of F is actually the second moment of the underlying
1004 two-sided distribution, because the variable of F is squared. Having a finite and stable first moment
1005 in F is quite meaningful. But it is much harder to make sense of the variance when k is too small.

1006 Notice that, when $d \rightarrow \infty$, the variance is independent of d ,

$$\text{var}\{F_{\alpha,\infty,k}\} = \mathbb{E}(X^{-2}|\bar{\chi}_{\alpha,k}^2) - \mathbb{E}(X^{-1}|\bar{\chi}_{\alpha,k}^2)^2$$

1007 This is the most relevant quantity, if exists, that other variances of finite d are relative to in an inverse
1008 d relation, such as

$$\text{var}\{F_{\alpha,d,k}\} - \text{var}\{F_{\alpha,\infty,k}\} = \frac{2}{d} \mathbb{E}(X^{-2}|\bar{\chi}_{\alpha,k}^2).$$

1009 8.5. Sum of Two Fractional Chi-Square Mixtures with Correlation

1010 This section addresses a complication that arises from the multivariate adaptive distribution.

1011 TODO need to re-write this. but I may not have enough result to write it though. Alas...

1012 Consider $X_1^2 \sim F_{\alpha_1,1,k_1}$ and $X_2^2 \sim F_{\alpha_2,1,k_2}$. Assume that there is a correlation between X_1 and
1013 X_2 as described in Section 7.9. The PDF of the quadratic form $Q = (X_1^2 + X_2^2)/2$ is a convolution
1014 that wraps around $Z \sim \chi_{11}^2(\rho)$ such that

$$\begin{aligned} f_Q(x) &= 2 \int_0^{2x} F_{\alpha_1,1,k_1}(w) \cdot F_{\alpha_2,1,k_2}(2x-w) dw \\ &= 2 \int_0^\infty ds_1 \bar{\chi}_{\alpha_1,k_1}^2(s_1) \int_0^\infty ds_2 \bar{\chi}_{\alpha_2,k_2}^2(s_2) \chi_{11}^2(2x, s_1, s_2, \rho) \end{aligned}$$

1015 This is the PDF of the quadratic form of a standard 2-dimensional adaptive GAS-SN distribution.
1016 TODO When ρ and β mingle together, there are additional complications.

1017 8.6. Fractional Adaptive F Distribution

1018 It should look like this: $\overrightarrow{F}_{\alpha,d,k}$, but it is a bit strange, mixing vectors and numbers together...
1019 TODO Ah, this is much harder than I thought !!!

CHAPTER 9

The Framework of Continuous Gaussian Mixture

1021 The construction of a symmetric two-sided distribution is in the form of a continuous Gaussian
 1022 mixture. Both the ratio and product distribution methods could be used.

1023 In the case of the symmetric α -stable distribution (SaS)[5], the exponential power distribution
 1024 comes from its characteristic function (CF)[24]. In our framework, both distributions will be expanded
 1025 by adding the parameter for the degrees of freedom (k).

1026 In addition, we use positive k for the former and negative k for the latter. Hence, the " $k \in \mathbb{R}$ "
 1027 domain will consolidate both distributions into one.

1028 We would like to present a unified framework and familiarize the reader with the notations, which
 1029 would otherwise be subtle and confusing.

1030 The results of this chapter are the following. First, the symmetric two-sided distribution can be
 1031 enriched using the characteristic function transform.

1032 Second, the features of the two-sided distribution are transferred to the one-sided distribution
 1033 because of the Gaussian mixture.

1034 Third, that one-sided distribution could be transformed to the inverse distribution that represents
 1035 the marginal distribution of a volatility process. This is more meaningful in applications, such as
 1036 quantitative finance.

9.1. The Inverse Chi Distribution

1038 Assume the PDF of a two-sided symmetric distribution is $L(x)$ where $x \in \mathbb{R}$. It has zero mean,
 1039 $\mathbb{E}(X|L) = 0$. Assume the PDF of a one-sided distribution is $\chi(x)$ ($x > 0$) such that

$$(9.1) \quad L(x) := \int_0^\infty s ds \mathcal{N}(xs) \chi(s)$$

1040 This is not new. It is the definition of a ratio distribution with a standard normal variable \mathcal{N} . This
 1041 is the first form of the Gaussian mixture: $L \sim \mathcal{N}/\chi$. A typical example is that L is a Student's t
 1042 distribution when χ is $\sqrt{\chi_k^2}$.

1043 The skewness is added by replacing the normal distribution \mathcal{N} with its skew-normal counterpart
 1044 $\mathcal{N}(\beta)$. See next chapter for more details.

1045 It has the equivalent expression in terms of a product distribution using the *inverse distribution*
 1046 χ^\dagger such that $L \sim \mathcal{N}\chi^\dagger$ [10]. This is the second form of the Gaussian mixture.

1047 The advantage of this expression is that χ^\dagger is closer to our typical understanding of the marginal
 1048 distribution of a volatility process. For example, when the Brownian motion process $dX_t = \sigma_t dW_t$ is
 1049 measured in a particular time interval Δt , we have $\Delta X_t \sim L$ and $\sigma_t \sim \chi^\dagger$.

1050 Since χ in the ratio form is more natural in the expression of the α -stable distribution, we are
 1051 more inclined to use the ratio distribution. The reader should keep this subtlety in mind.

1052 LEMMA 9.1. (Inverse distribution) Let the inverse distribution of χ be χ^\dagger , the relation between
 1053 their density functions is

$$(9.2) \quad \chi^\dagger(s) := s^{-2} \chi\left(\frac{1}{s}\right)$$

1054 such that

$$(9.3) \quad \int_0^\infty s ds \mathcal{N}(xs) \chi(s) = \int_0^\infty \frac{ds}{s} \mathcal{N}\left(\frac{x}{s}\right) \chi^\dagger(s) \quad (x \in \mathbb{R})$$

$$(9.4) \quad \int_0^\infty s ds \mathcal{N}(xs) \chi^\dagger(s) = \int_0^\infty \frac{ds}{s} \mathcal{N}\left(\frac{x}{s}\right) \chi(s)$$

1055 The proof is straightforward by a change of variable $t = 1/s$. You can move between LHS and RHS
1056 easily.

1057 \triangle

1058

9.2. The Characteristic Distributions

1060 The characteristic transform of a symmetric α -stable distribution (SaS) leads to an exponential
1061 power distribution. We would like to generalize this concept in this section.

1062 When the PDF of a distribution is represented by a Gaussian mixture, the features of a charac-
1063 teristic transform are transferred to its χ distribution counterpart.

1064 We use the notation $\text{CF}\{g\}(t) = \mathbb{E}(e^{itX}|g)$ to represent the characteristic function transform of
1065 the PDF $g(x)$. Note that \mathcal{N} has a special property that its CF is still itself: $\text{CF}\{\mathcal{N}\}(t) = \sqrt{2\pi} \mathcal{N}(t)$.

1066 LEMMA 9.2. (Characteristic function transform of L) Let $\phi(t)$ be the CF of L such that $\phi(t) :=$
1067 $\text{CF}\{L\}(t) = \int_{-\infty}^\infty dx \exp(itx) L(x)$. (9.1) is transformed to

$$(9.5) \quad \phi(t) = \sqrt{2\pi} \int_0^\infty ds \mathcal{N}\left(\frac{t}{s}\right) \chi(s) \quad (t \in \mathbb{R})$$

1068 The proof is straightforward from the fact that $\text{CF}\{\mathcal{N}(0, \sigma^2)\}(t) = \sqrt{2\pi} \mathcal{N}(\sigma t)$.

1069 \triangle

1070 (9.5) is quite similar to the RHS of (9.4). It inspires us to define a new distribution pair, L_ϕ and
1071 χ_ϕ^\dagger , in terms of a product distribution, such that

$$(9.6) \quad L_\phi(x) := \int_0^\infty \frac{ds}{s} \mathcal{N}\left(\frac{x}{s}\right) \chi_\phi^\dagger(s) \quad (x \in \mathbb{R})$$

$$(9.7) \quad \chi_\phi^\dagger(s) := \frac{s \chi(s)}{\mathbb{E}(X|\chi)}$$

1072 where $\mathbb{E}(X|\chi)$ is the first moment of χ . Here χ_ϕ^\dagger is the inverse distribution of χ_ϕ , which can be
1073 reverse-engineered according to (9.2),

$$(9.8) \quad \chi_\phi(s) := \frac{s^{-3}}{\mathbb{E}(X|\chi)} \chi\left(\frac{1}{s}\right)$$

1074
1075 We are in an interesting place: We start with a one-sided distribution χ , we derive two variants
from it: χ_ϕ and χ_ϕ^\dagger . We also obtain two two-sided distributions: L and L_ϕ .

1077 We shall call χ_ϕ the *characteristic distribution* of χ as it facilitates $L_\phi \sim \mathcal{N}/\chi_\phi$.

1078 **9.3. Summary of Gaussian Mixture**

1079 In summary, considering the inverse distribution and characteristic transform, we obtain four
 1080 Gaussian mixture relations. The first two parallel relations in terms of ratio distribution:

$$L \sim \mathcal{N}/\chi; \\ L_\phi \sim \mathcal{N}/\chi_\phi, \quad \chi_\phi(s) := \frac{s^{-3}}{\mathbb{E}(X|\chi)} \chi\left(\frac{1}{s}\right).$$

1081 In terms of production distribution, they become

$$L \sim \mathcal{N} \chi^\dagger, \quad \chi^\dagger(s) := s^{-2} \chi\left(\frac{1}{s}\right) = \frac{s}{\mathbb{E}(X|\chi)} \chi_\phi(s); \\ L_\phi \sim \mathcal{N} \chi_\phi^\dagger, \quad \chi_\phi^\dagger(s) := \frac{s}{\mathbb{E}(X|\chi)} \chi(s).$$

1082 Both χ^\dagger and χ_ϕ^\dagger are the volatility processes that generate L and L_ϕ .

1083 Next, the ϕ suffix in $\chi_\phi(s)$ will be replaced by the *negation* (sign change) of the degree of freedom
 1084 ($k \rightarrow -k$).

1085 The multiplication of $\frac{s}{\mathbb{E}(X|f)}$ is closely related to an increase in the degree of freedom ($k \rightarrow k+1$)
 1086 of the underlying FG, which is equivalent to the scaling of χ_ϕ and χ .

$$g(s) = \frac{s}{\mathbb{E}(X|\chi)} f_k(s; \sigma_k) \\ = \frac{1}{\sigma} f_{k+1}\left(\frac{s}{\sigma}; \sigma_{k+1}\right)$$

1087 **9.4. FCM Extensions**

1088 In this section, we explicitly define the three extensions of $\bar{\chi}_{\alpha,k}$ and prove their connections. They
 1089 are sub-families of FG. Hence, their density functions should be expressed by $\mathfrak{N}_{\alpha/2}(x; \dots)$ in (6.1).

1090 First, we quote the PDF of $\bar{\chi}_{\alpha,k}$ from (7.4) below. For $x \geq 0$ and $k > 0$,

$$(9.9) \quad \bar{\chi}_{\alpha,k}(x) := \mathfrak{N}_{\alpha/2}(x; \sigma = \sigma_{\alpha,k}, d = k-1, p = \alpha) \quad (x \geq 0, k > 0) \\ = (C_{\alpha,k}) (\sigma_{\alpha,k})^{1-k} x^{k-2} F_{\frac{\alpha}{2}}\left(\left(\frac{x}{\sigma_{\alpha,k}}\right)^\alpha\right).$$

1091 The characteristic FCM $[\bar{\chi}_\phi]_{\alpha,k}$ uses the $-k$ index of $\bar{\chi}_{\alpha,k}$. Its PDF is

$$(9.10) \quad [\bar{\chi}_\phi]_{\alpha,k}(x) = \bar{\chi}_{\alpha,-k}(x) := \mathfrak{N}_{\alpha/2}(x; \sigma = (\sigma_{\alpha,k})^{-1}, d = -k, p = -\alpha). \\ = (C_{\alpha,k+1}) (\sigma_{\alpha,k})^{-k} x^{-k-1} F_{\frac{\alpha}{2}}\left((\sigma_{\alpha,k} x)^{-\alpha}\right).$$

1092 DEFINITION 9.3. The density functions of the two inverse distributions are as follows.

$$(9.11) \quad \bar{\chi}_{\alpha,k}^\dagger(x) := \mathfrak{N}_{\alpha/2}(x; \sigma = (\sigma_{\alpha,k})^{-1}, d = -k+1, p = -\alpha). \\ = (C_{\alpha,k}) (\sigma_{\alpha,k})^{-k+1} x^{-k} F_{\frac{\alpha}{2}}\left((\sigma_{\alpha,k} x)^{-\alpha}\right).$$

1093 And

$$(9.12) \quad [\bar{\chi}_\phi^\dagger]_{\alpha,k}(x) = \bar{\chi}_{\alpha,-k}^\dagger(x) := \mathfrak{N}_{\alpha/2}(x; \sigma = \sigma_{\alpha,k}, d = k, p = \alpha). \\ = (C_{\alpha,k+1}) (\sigma_{\alpha,k})^{-k} x^{k-1} F_{\frac{\alpha}{2}}\left(\left(\frac{x}{\sigma_{\alpha,k}}\right)^\alpha\right).$$

1094 **9.4.1. Expressed via Alpha-Stable Extremal Distribution.** From (4.2), we have $L_\alpha(x) =$
 1095 $x^{-1}F_\alpha(x^{-\alpha})$. The two density functions, $\bar{\chi}_{\alpha,k}^\dagger(x)$ and $[\bar{\chi}_\phi]_{\alpha,k}(x)$, can be expressed by $L_\alpha(x)$ more
 1096 elegantly since

$$(9.13) \quad F_{\frac{\alpha}{2}}(x^{-\alpha}) = x^2 L_{\frac{\alpha}{2}}(x^2).$$

1097 Therefore, the PDF of the characteristic distribution becomes

$$(9.14) \quad [\bar{\chi}_\phi]_{\alpha,k}(x) = \bar{\chi}_{\alpha,-k}(x) = (C_{\alpha,k+1})(\sigma_{\alpha,k})^{-k+2} x^{-k+1} L_{\frac{\alpha}{2}}((\sigma_{\alpha,k} x)^2).$$

1098 which is a FG-type manipulation on the α -stable extremal distribution.

1099 Likewise, the PDF of the inverse distribution becomes

$$(9.15) \quad \bar{\chi}_{\alpha,k}^\dagger(x) = (C_{\alpha,k})(\sigma_{\alpha,k})^{-k+3} x^{-k+2} L_{\frac{\alpha}{2}}((\sigma_{\alpha,k} x)^2).$$

1100 LEMMA 9.4. Show that

$$(9.16) \quad \bar{\chi}_{\alpha,k}^\dagger(x) = \frac{x}{\mathbb{E}(X | [\bar{\chi}_\phi]_{\alpha,k})} [\bar{\chi}_\phi]_{\alpha,k}(x)$$

1102 \triangle

1103 PROOF. Divide (9.15) by (9.14). The result is $\bar{\chi}_{\alpha,k}^\dagger(x) / [\bar{\chi}_\phi]_{\alpha,k}(x) = x \sigma_{\alpha,k} C_{\alpha,k} / C_{\alpha,k+1}$, which is
 1104 $x \mathbb{E}(X | \bar{\chi}_{\alpha,k})$ according to (7.9). And $\mathbb{E}(X | \bar{\chi}_{\alpha,k}) = 1 / \mathbb{E}(X | [\bar{\chi}_\phi]_{\alpha,k})$. We arrive at the desired result. \square

1105 Furthermore, this indicates the following.

1106 LEMMA 9.5. $\bar{\chi}_{\alpha,k}^\dagger(x)$ is a rescaled $[\bar{\chi}_\phi]_{\alpha,k-1}(x)$, which is $\bar{\chi}_{\alpha,-k+1}(x)$. That is,

$$(9.17) \quad \bar{\chi}_{\alpha,k}^\dagger(x) = \frac{1}{\sigma} [\bar{\chi}_\phi]_{\alpha,k+1}\left(\frac{x}{\sigma}\right), \quad \text{where } \sigma = \frac{\sigma_{\alpha,k-1}}{\sigma_{\alpha,k}}.$$

1107 \triangle

1108 PROOF. From (9.14), we have

$$[\bar{\chi}_\phi]_{\alpha,k-1}(x) = (C_{\alpha,k})(\sigma_{\alpha,k-1})^{-k+3} x^{-k+2} L_{\frac{\alpha}{2}}((\sigma_{\alpha,k-1} x)^2).$$

1109 Compare the argument in $L_{\frac{\alpha}{2}}()$ to (9.15) after the substitution x/σ . We obtain $\sigma_{\alpha,k-1}^2/\sigma^2 = \sigma_{\alpha,k}^2$ and
 1110 arrive at the desired result for σ . \square

1111 9.4.2. Proofs of Other Relations.

1112 LEMMA 9.6. Show that (9.8) is true in the FCM implementation.

$$(9.18) \quad [\bar{\chi}_\phi]_{\alpha,k}(x) = \frac{x^{-3}}{\mathbb{E}(X | \bar{\chi}_{\alpha,k})} \bar{\chi}_{\alpha,k}\left(\frac{1}{x}\right)$$

1113 \triangle

1114 PROOF. The proof is straightforward. First, replace x with $1/x$ in (9.9). Second, divide it by
 1115 (9.10). The result is $[\bar{\chi}_\phi]_{\alpha,k}(x) / [\bar{\chi}_\phi]_{\alpha,k}(x) = \sigma_{\alpha,k} x^3 C_{\alpha,k} / C_{\alpha,k+1}$, which is $x^3 \mathbb{E}(X | \bar{\chi}_{\alpha,k})$ according
 1116 to (7.9). We arrive at the desired result. \square

1117 LEMMA 9.7. Show that

$$(9.19) \quad [\bar{\chi}_\phi]_{\alpha,k}^\dagger(x) = \frac{x}{\mathbb{E}(X | \bar{\chi}_{\alpha,k})} \bar{\chi}_{\alpha,k}(x)$$

1118 This indicates that $[\bar{\chi}_\phi]_{\alpha,k}^\dagger(x)$ is a rescaled $\bar{\chi}_{\alpha,k+1}(x)$. This makes it a trivial case. \triangle

1119 PROOF. Divide (9.9) by (9.12). The result is $\bar{\chi}_{\alpha,k}(x) / \left[\bar{\chi}_\phi^\dagger \right]_{\alpha,k}(x) = \sigma_{\alpha,k} x^{-1} C_{\alpha,k} / C_{\alpha,k+1}$, which
1120 is $x^{-1} \mathbb{E}(X | \bar{\chi}_{\alpha,k})$ according to (7.9). We arrive at the desired result. \square

1121 These relations from different angles ensure that all the formulas are consistent with each other.

1122 **9.4.3. Rescaling and Simplification.** TODO

1123

Part 3

1124

Two-Sided Univariate Distributions

CHAPTER 10

SN: The Skew-Normal Distribution - Review

10.1. Definition

The skew-normal distribution family is well documented in A. Azzalini's 2013 monograph[1]. We recap the results and clarify the symbology. My contribution is to incorporate the skew-normal methodology into the fractional distributions wherever suitable. The enhanced distributions are flexible and can adapt to many different shapes and tails with high skewness and kurtosis.

10.1.1. The Selective Sampling. The *selective sampling* method is used to inject skewness into the stochastic system, which is otherwise symmetric. This mechanism is fairly common in an applied context, for example, in social sciences, where a variable X_0 is observed only when a correlated variable X_1 , which is usually unobserved, satisfies a certain condition (p.128 of [1]).

In quantitative finance, the condition could be market regimes. In a two-regime model, a market index such as the S&P 500 index (SPX) is classified into the growth regime or the crash regime at a given time. It is well known that the volatility of the market behaves differently in each regime. In the growth regime, volatility tends to be low, and the market is trending upward. In the crash regime, volatility tends to be high, and the market is trending downward.

A univariate random variable $Z \sim SN(0, 1, \beta)$ is a standard skew-normal variable with skew parameter $\beta \in \mathbb{R}$ (Section 2.1 of [1]). The sign of β determines the sign of its skewness (10.14).

One of its stochastic representations is

$$(10.1) \quad Z = \begin{cases} X_0 & \text{if } X_1 < \beta X_0, \\ -X_0 & \text{otherwise.} \end{cases}$$

where X_0, X_1 are independent $\mathcal{N}(0, 1)$ variables.

An alternative representation uses filtering, or rejection, such that $Z = (X_0 | X_1 < \beta X_0)$. That is, X_0 is accepted as Z only when the condition $X_1 < \beta X_0$ is satisfied. Otherwise, it is discarded.

10.1.2. The PDF and CDF. The standard PDF is

$$(10.2) \quad \mathcal{N}(x; \beta) := 2 \mathcal{N}(x) \Phi_{\mathcal{N}}(\beta x), \quad (x \in \mathbb{R})$$

where $\mathcal{N}(x)$ and $\Phi_{\mathcal{N}}(x)$ are the PDF and CDF of $\mathcal{N}(0, 1)$.

Its extremal distribution occurs at $\beta \rightarrow \infty$, where $\Phi_{\mathcal{N}}(\beta x)$ becomes a step function. The PDF becomes that of a half-normal distribution.

The standard CDF is

$$(10.3) \quad \Phi_{SN}(x; \beta) := \Phi_{\mathcal{N}}(x) - 2 T(x, \beta)$$

where $T(h, a)$ is called the Owen's T function[25]. Its numerical methods are widely implemented in modern software packages.

Several important properties are quoted from Proposition 2.1 of [1]:

- $\mathcal{N}(0; 0) = 1/\sqrt{2\pi}$. Universal anchor at $x = 0, \beta = 0$.
- $\mathcal{N}(x; 0) = \mathcal{N}(x)$. Continuity at $\beta = 0$.
- $\mathcal{N}(-x; \beta) = \mathcal{N}(x; -\beta)$. This is the reflection rule.

- 1157 • $Z^2 \sim \chi_1^2$, irrespective of β .

1158 Notice that Z^2 is independent of β . This is an important property, but may not be intuitive for
 1159 new students. This is due to the fact that the squares of X_0 and $-X_0$ are the same in (10.1). This
 1160 property is carried into the quadratic form of the multivariate elliptical distribution.

1161 10.2. The Location-Scale Family

1162 Its location-scale family is $Y = \xi + \omega Z \sim SN(\xi, \omega^2, \beta)$, where $\xi \in \mathbb{R}$ and $\omega > 0$. Its PDF becomes

$$(10.4) \quad \frac{1}{\omega} \mathcal{N}\left(\frac{x - \xi}{\omega}; \beta\right).$$

1163 10.3. Invariant Quantities

1164 The following quantity plays an important role in the selective sampling concept of SN:

$$(10.5) \quad \delta = \frac{\beta}{\sqrt{1 + \beta^2}}, \quad \delta \in (-1, 1).$$

1165 It can be thought of as some kind of correlation in the following. Inversely, β can be calculated from

$$(10.6) \quad \beta = \frac{\delta}{\sqrt{1 - \delta^2}}.$$

1166 These two quantities will appear in many places in the ensuing chapters. They are invariants in the
 1167 context of the multivariate elliptical distribution, called the Canonical Form.

1168 In a trigonometry representation, one can think of δ as $\sin(\theta)$ of a right triangle, where one leg is
 1169 1, the other leg is β , and θ is the angle facing β .

Three representations use δ as the correlation coefficient to generate SN. (Section 2.1.3 of [1])
 First, designate the correlation matrix as

$$\bar{\Omega} = \begin{pmatrix} 1 & \delta \\ \delta & 1 \end{pmatrix}.$$

The Cholesky factor of $\bar{\Omega}$ is

$$L = \begin{pmatrix} 1 & 0 \\ \delta & \sqrt{1 - \delta^2} \end{pmatrix},$$

1170 so that $L L^T = \bar{\Omega}$.

1171 Assume U_0 and U_1 are two independent $\mathcal{N}(0, 1)$ variates. The first representation of $Z \sim SN(0, 1, \beta)$
 1172 is

$$(10.7) \quad Z = \begin{cases} X_0 & \text{if } X_1 > 0, \\ -X_0 & \text{otherwise.} \end{cases}$$

where X_0, X_1 are marginals of a standard correlated normal bivariate with $\text{cor}\{X_0, X_1\} = \delta$ such that

$$\begin{pmatrix} X_0 \\ X_1 \end{pmatrix} = L \begin{pmatrix} U_0 \\ U_1 \end{pmatrix}.$$

The second representation is from

$$\begin{pmatrix} - \\ Z \end{pmatrix} = L \begin{pmatrix} U_0 \\ |U_1| \end{pmatrix}$$

1173 such that $Z = \sqrt{1 - \rho^2} U_0 + \delta |U_1| \sim SN(0, 1, \beta)$.

The third representation is $Z = \max\{X_0, X_1\} \sim SN(0, 1, \beta)$, where X_0, X_1 are marginals of a standard correlated bivariate such that

$$\begin{pmatrix} X_0 \\ X_1 \end{pmatrix} = \begin{pmatrix} 1 & 0 \\ \rho & \sqrt{1-\rho^2} \end{pmatrix} \begin{pmatrix} U_0 \\ U_1 \end{pmatrix}.$$

1174 and $\text{cor}\{X_0, X_1\} = \rho = 1 - 2\delta^2$.

1175 10.4. Mellin Transform

1176 The following result is elegant, but also peculiar. It is discovered by the author.

1177 LEMMA 10.1. The Mellin transform of the SN PDF is

$$(10.8) \quad \mathcal{N}(x; \beta) \xrightarrow{\mathcal{M}} \mathcal{N}^*(s; \beta) := 2 \mathcal{N}^*(s) \Phi[t_s](\beta\sqrt{s}),$$

where $\mathcal{N}^*(s) = \frac{1}{2} \frac{2^{s/2}}{\sqrt{2\pi}} \Gamma\left(\frac{s}{2}\right)$

1178 is the Mellin transform of the PDF of $\mathcal{N}(0, 1)$ in (2.9). And $\Phi[t_k](x)$ is the CDF of a Student's t
1179 distribution with k degrees of freedom. But it is used in a strange way, where s substitutes k and goes
1180 into x at the same time.

1181 \triangle

1182 PROOF. We prove (10.8) via the CDF of GSaS with $\alpha = 1$. By definition,

$$\mathcal{N}^*(s; \beta) = \int_0^\infty x^{s-1} [2\mathcal{N}(x)\Phi_{\mathcal{N}}(\beta x)] dx.$$

1183 We use the known result from $\bar{\chi}_{1,k}$ where

$$x^{k-1} \mathcal{N}(x) = \frac{2^{k/2-1} \Gamma(k/2)}{\sqrt{2\pi k}} \bar{\chi}_{1,k}(x/\sqrt{k}) = \frac{1}{\sqrt{k}} \mathcal{N}^*(k) \bar{\chi}_{1,k}(x/\sqrt{k}).$$

1184 Then

$$\begin{aligned} \mathcal{N}^*(s; \beta) &= \frac{2 \mathcal{N}^*(s)}{\sqrt{s}} \int_0^\infty \Phi_{\mathcal{N}}(\beta x) \bar{\chi}_{1,s}(x/\sqrt{s}) dx \\ &= 2 \mathcal{N}^*(s) \int_0^\infty \Phi_{\mathcal{N}}(\beta\sqrt{st}) \bar{\chi}_{1,s}(t) dt \quad \text{via } t = x/\sqrt{s}. \end{aligned}$$

1185 The integral is exactly the CDF of a GSaS, $L_{1,s}$, with the argument $\beta\sqrt{s}$. That is, $\mathcal{N}^*(s; \beta) =$
1186 $2 \mathcal{N}^*(s) \Phi[L_{1,s}](\beta\sqrt{s})$.

1187 When $\alpha = 1$, $L_{1,s}$ becomes t_s . Therefore, $\mathcal{N}^*(s; \beta) = 2 \mathcal{N}^*(s) \Phi[t_s](\beta\sqrt{s})$.

1188 \square

1189 The beauty of this lemma is that $\mathcal{N}^*(s; \beta)$ is the multiplication of a symmetric component and a
1190 skew component, just like its PDF counterpart.

1191 From (2.14), we also obtain that

$$(10.9) \quad \Phi_{SN}(0; \beta) = 1 - \mathcal{N}^*(1; \beta) = \frac{1}{2} - \frac{1}{\pi} \arctan(\beta).$$

1192 This is due to $\mathcal{N}^*(1) = \frac{1}{2}$ and $\Phi[t_1](\beta) = \frac{1}{2} + \frac{1}{\pi} \arctan(\beta)$. This result is stated in Proposition 2.7 of
1193 [1], and is proved here via the Mellin transform.

1194 **10.4.1. Mellin Transform of Owen's T Function.** Another peculiar result from the Mellin
 1195 transform is

LEMMA 10.2.

$$(10.10) \quad T(x, \beta) \xleftrightarrow{\mathcal{M}} s^{-1} \mathcal{N}^*(s+1) \left[\Phi[t_{s+1}] (\beta \sqrt{s+1}) - \frac{1}{2} \right]$$

1196 △

1197 PROOF. Define the upper incomplete integral as

$$\begin{aligned} \Gamma_f(x) &:= \int_x^\infty \mathcal{N}(x; \beta) dx = 1 - \Phi_{SN}(x; \beta) \\ &= 1 - \Phi_N(x) + 2T(x, \beta) \end{aligned}$$

1198 According to Lemma 2.6, its Mellin transform is

$$\begin{aligned} \Gamma_f(x) &\xleftrightarrow{\mathcal{M}} s^{-1} \mathcal{N}^*(s+1; \beta) \\ &= 2s^{-1} \mathcal{N}^*(s+1) \Phi[t_{s+1}] (\beta \sqrt{s+1}) \end{aligned}$$

1199 Combining the two results above, we obtain

$$T(x, \beta) = \frac{\Gamma_f(x) - (1 - \Phi_N(x))}{2} \xleftrightarrow{\mathcal{M}} s^{-1} \mathcal{N}^*(s+1) \left[\Phi[t_{s+1}] (\beta \sqrt{s+1}) - \frac{1}{2} \right]$$

1200 where $1 - \Phi_N(x) \xleftrightarrow{\mathcal{M}} s^{-1} \mathcal{N}^*(s+1)$.

1201 □

1202 10.5. Moments

1203 LEMMA 10.3. According to Section 2.2.2, by assigning $s = n+1$, the Mellin transform is converted
 1204 to the moment formula. It is easy to show that the n -th moment of Z is

$$\begin{aligned} (10.11) \quad \mathbb{E}(Z^n) &= \mathbb{E}(X^n | \mathcal{N}(\beta)) = \mathcal{N}^*(n+1; \beta) + (-1)^n \mathcal{N}^*(n+1; -\beta) \\ &= 2\mathcal{N}^*(n+1) \times \begin{cases} 1, & \text{when } n \text{ is even,} \\ 1 - 2\Phi[t_{n+1}](-\beta \sqrt{n+1}), & \text{when } n \text{ is odd.} \end{cases} \end{aligned}$$

1205 The even moments are identical to those of $\mathcal{N}(0, 1)$. It is the odd moments that make the difference
 1206 when $\beta \neq 0$.

1207 △

1208 The first four moments of Z' have simple analytic forms. Its first moment is

$$(10.12) \quad \mu_z = b\delta, \quad \text{where } b = \sqrt{2/\pi}.$$

1209 The second moment is simply 1. Its variance is

$$(10.13) \quad \sigma_z^2 = 1 - (b\delta)^2.$$

1210 The third moment is $b\delta(3 - \delta^2)$. Its skewness is

$$(10.14) \quad \gamma_1\{Z\} = \frac{4 - \pi}{2} \frac{\mu_z^3}{\sigma_z^3}.$$

1211 The fourth moment is 3. Its kurtosis is

$$(10.15) \quad \gamma_2\{Z\} = 2(\pi - 3) \frac{\mu_z^4}{\sigma_z^4}.$$

1212 The maximum skewness of SN is approximately 0.9953 and the maximum kurtosis is 0.8692. They
 1213 are not very interesting, since the extremal distribution is just a half-normal distribution.

1214 However, these analytical forms are useful when SN is extended to GAS-SN. Both skewness and
1215 kurtosis are extended to much wider ranges, or even infinity!

CHAPTER 11

GAS: Generalized Alpha-Stable Distribution (Experimental)

In this chapter, we show how the *degrees of freedom* k is added to the α -stable distribution L_α^θ using the Mellin transform approach. This experiment is an early attempt and one of the cleanest approaches to understanding how k interacts with skewness. It is a valuable lesson on the mathematical structure of the α -stable distribution. Therefore, it is documented in this chapter.

With this note, the readers not interested in this mathematical exploration can skip this chapter.

A new distribution results, which is called the generalized α -stable distribution (GAS), with the notation $L_{\alpha,k}^\theta$. The distribution is structurally elegant and capable of properly generating skewness. However, there are discontinuity issues with the reflection rule.

The discontinuity is a major flaw that prevents the distribution from being useful in real-world application. A method to remedy it is proposed, which is documented in this chapter. The value of this chapter is to understand the origin of the fractional χ distribution and GSaS.

After learning this hard lesson, I turned to the skew-normal approach, which can generate skewness without any problem with the continuity of the PDF. And it is also theoretically elegant. After this chapter, all subsequent chapters are based on the skew-normal approach.

11.1. Definition

First, we recap the Mellin transform (4.4) of the PDF of the α -stable distribution from Section 4.3,

$$L_\alpha^\theta(x) \xleftrightarrow{\mathcal{M}} \epsilon \left[\frac{\Gamma(s)}{\Gamma(1-\gamma+\gamma s)} \right] \left[\frac{\Gamma(\epsilon(1-s))}{\Gamma(\gamma(1-s))} \right].$$

It is interpreted in Lemma 4.2 as a multiplication of two components,

$$L_\alpha^\theta(x) \xleftrightarrow{\mathcal{M}} \tilde{M}_\gamma^*(s) \bar{\chi}_{\alpha,1}^\theta(s)^*(2-s).$$

The PDF of the second term $\bar{\chi}_{\alpha,1}$ is defined as

$$\bar{\chi}_{\alpha,1}^\theta(x) \xleftrightarrow{\mathcal{M}} \bar{\chi}_{\alpha,1}^\theta(s)^* \propto \frac{\Gamma(\epsilon(s-1))}{\Gamma(\gamma(s-1))},$$

apart from the normalization constant and scale in the PDF. It is interpreted as the FCM of "one degree of freedom" in Section 7.1.

In (7.1) it is shown that the "degrees of freedom" parameter k is added to the FCM by replacing $s-1$ with $s+k-2$ such that

$$\bar{\chi}_{\alpha,k}^\theta(x) \xleftrightarrow{\mathcal{M}} \bar{\chi}_{\alpha,k}^\theta(s)^* \propto \frac{\Gamma(\epsilon(s+k-1))}{\Gamma(\gamma(s+k-1))}.$$

Next, it is natural to use $\bar{\chi}_{\alpha,k}^\theta(s)$ in the Mellin space to extend L_α^θ as follows.

DEFINITION 11.1 (The ratio-distribution representation of (unadjusted) GAS). The Mellin transform of the PDF of (unadjusted) GAS is defined as

$$(11.1) \quad \tilde{L}_{\alpha,k}^\theta(x) \xleftrightarrow{\mathcal{M}} \tilde{M}_\gamma^*(s) \bar{\chi}_{\alpha,k}^\theta(s)^*(2-s)$$

1243 Based on the Mellin transform, its PDF can be written in a ratio distribution form,

$$(11.2) \quad \tilde{L}_{\alpha,k}^{\theta}(x) := \int_0^{\infty} \tilde{M}_{\gamma}(xs) \bar{\chi}_{\alpha,k}^{\theta}(s) s ds \quad (x \geq 0)$$

1244 Since the Mellin integral is only valid for $x \geq 0$, it is supplemented with *the reflection rule*:

$$(11.3) \quad \tilde{L}_{\alpha}^{\theta}(-x) := \tilde{L}_{\alpha}^{-\theta}(x)$$

1245 Thus, we have constructed a version of GAS for $x \in \mathbb{R}$, which produces fat tails and skewness -

1246 (1) $\tilde{L}_{\alpha,k}^{\theta}$ subsumes the α -stable distribution L_{α}^{θ} .

1247 (2) $\tilde{L}_{\alpha,k}^{\theta}$ subsumes Student's t distribution t_k .

1248 (3) $\tilde{L}_{\alpha,k}^{\theta}$ subsumes the power-exponential distribution, with the proper definition of negative k
1249 in FCM.

1250 **What is wrong with it?** The problem is that the PDF and its derivatives are discontinuous at
1251 $x = \pm 0$ when $k \neq 1$ and $\theta \neq 0$.

1252

1253 The remaining sections of this chapter will explain this problem and provide a remediation. The
1254 reader who just wants to explore the skew-normal implementation can safely skip the rest of this
1255 chapter. The conclusion is that such discontinuity makes the PDF far from mathematical elegance,
1256 which motivates the author to explore other alternatives. The answer is to abandon the M-Wright
1257 kernel for skewness ($\tilde{M}_{\gamma}(xs)$ in (11.2)), and integrate with the skew-normal distribution, outlined in
1258 the next chapter.

1259

11.2. Limitation

1260 The issue of discontinuity of the PDF $\tilde{L}_{\alpha,k}^{\theta}(x)$ at $x = 0$ is encountered when $k \neq 1$. We lay out a
1261 generic framework to understand and address it.

1262 Assume that the unadjusted two-sided density function is $\tilde{f}(x) := \tilde{L}_{\alpha,k}^{\theta}(x)$, which is discontinuous
1263 at $x = 0$. It also must satisfy the reflection rule, where, for $x > 0$, $\tilde{f}(x) := \tilde{f}^+(x)$ and $\tilde{f}(-x) := \tilde{f}^-(x)$.

1264 $\tilde{f}(x)$ can be expanded at $x = 0$ in terms of x by

$$(11.4) \quad \tilde{f}^{\pm}(x) := \tilde{L}_{\alpha,k}^{\pm\theta}(x) = \tilde{f}_0^{\pm} + \tilde{f}_1^{\pm} x + \dots$$

1265 where \tilde{f}_0^{\pm} are the densities at $x = 0$, and \tilde{f}_1^{\pm} are the respective slopes (aka the first derivatives).

1266 The series expansion can be achieved via either (11.2), or (11.1) in conjunction with Ramanujan's
1267 master theorem in Section 2.3, such that

$$(11.5) \quad \tilde{f}_0^+ = \frac{\gamma^{1-\gamma}}{\Gamma(1-\gamma)} E(X|\bar{\chi}_{\alpha,k}^{\theta}),$$

$$(11.6) \quad \tilde{f}_1^+ = \frac{-\gamma^{1-2\gamma}}{\Gamma(1-2\gamma)} E(X^2|\bar{\chi}_{\alpha,k}^{\theta}).$$

1268 Notice that they are based on the first and second moments of $\bar{\chi}_{\alpha,k}^{\theta}$. $(\tilde{f}_0^-, \tilde{f}_1^-)$ are obtained by applying
1269 the reflection rule from $(\tilde{f}_0^+, \tilde{f}_1^+)$. That is, θ is replaced with $-\theta$, and γ with $1 - \gamma$ in every occurrence
1270 of the formula.

1271 Furthermore, it is known that

$$(11.7) \quad \int_0^{\infty} \tilde{f}^+(x) dx = \gamma, \quad \int_0^{\infty} \tilde{f}^-(x) dx = 1 - \gamma.$$

1272 These two are the only conditions required for $\tilde{f}^{\pm}(x)$.

1273 *The discontinuity occurs* because $\tilde{f}_0^+ \neq \tilde{f}_0^-$ and $\tilde{f}_1^+ \neq \tilde{f}_1^-$ when $k \neq 1$ and $\theta \neq 0$. In fact, this is
1274 true for all orders of derivatives $\tilde{f}_n^+ \neq \tilde{f}_n^-$ in the n -th term, $\tilde{f}_n^{\pm} x^n$.

1275 Obviously, when $\theta = 0$, the density function is symmetric by definition: $\tilde{f}^+(x) = \tilde{f}^-(x)$. There is
1276 no issue here. So the issue is specific to the injection of skewness from $\theta \neq 0$.

1277 On the other hand, when $k = 1$, the density function is continuous under the reflection rule,
1278 regardless the value of θ . This is the original α -stable distribution. It is perfectly fine. So the issue is
1279 specific to our attempt of adding degrees of freedom $k \neq 1$.

1280 Either one of θ or k are fine, but when we try to do both, the distribution is broken, so to speak.
1281 That is the limitation. The dilemma is that adding θ and k is exactly what we try to achieve.

1282 11.3. Workaround

1283 An adjustment algorithm is proposed such that the PDF and its first derivative are continuous.

1284 DEFINITION 11.2 (The adjusted GAS). The PDF of the adjusted GAS is defined as

$$(11.8) \quad L_{\alpha,k}^{\pm\theta}(x) := \frac{1}{A^\pm\sigma^\pm} \tilde{f}^\pm(x) \left(\frac{x}{\sigma^\pm} \right) \quad (x \geq 0)$$

1285 It is required that (a) the new density function satisfies the reflection rule of $L_{\alpha,k}^\theta(-x) := L_{\alpha,k}^{-\theta}(x)$;
1286 (b) A^\pm, σ^\pm are constrained by the continuity conditions that, at $x = 0$, both its density is continuous:
1287 $L_{\alpha,k}^\theta(0) = L_{\alpha,k}^{-\theta}(0)$; and its slope is continuous: $\frac{d}{dx} L_{\alpha,k}^\theta(0) = -\frac{d}{dx} L_{\alpha,k}^{-\theta}(0)$.
1288

1289 With such definition, we proceed to find the solutions of A^\pm, σ^\pm . The solutions form a distribution
1290 family. There is a canonical solution, simple and elegant, from which all other solutions are derived as
1291 a member of the location-scale family.

1292 A member in the location-scale family shares the same "shapes" such as the skewness and kurtosis.
1293 Apart from the location and scale, it brings nothing new to the table. Hence, we can focus on analyzing
1294 the canonical distribution.

1295 DEFINITION 11.3 (Two essential quantities for the canonical distribution). We define two essential
1296 quantities:

$$(11.9) \quad \Sigma := -\frac{\tilde{f}_0^+}{\tilde{f}_0^-} \frac{\tilde{f}_1^-}{\tilde{f}_1^+}$$

$$(11.10) \quad \Psi := \Sigma \frac{\tilde{f}_0^+}{\tilde{f}_0^-} = - \left(\frac{\tilde{f}_0^+}{\tilde{f}_0^-} \right)^2 \frac{\tilde{f}_1^-}{\tilde{f}_1^+}$$

1297 Notice that $\tilde{f}_0^+/\tilde{f}_0^-$ is the ratio of the original densities from two sides of $x = 0$. And $\tilde{f}_1^-/\tilde{f}_1^+$ is the ratio
1298 of the slopes of the two sides. Since $\tilde{f}_1^-, \tilde{f}_1^+$ always have the opposite signs, Σ is a positive quantity.
1299

1300 Note that Σ is singular when $\gamma = 1/2$. Both $\tilde{f}_1^-, \tilde{f}_1^+$ approach zero at the same speed. Hence,
1301 $\Sigma \rightarrow 1$ and $\Psi \rightarrow 1$.

1302 The most important contribution is the discovery of the canonical distribution.

1303 DEFINITION 11.4 (The canonical GAS). The canonical GAS distribution is defined according to
1304 $\sigma^+ = 1$ and $\sigma^- = \Sigma$. Hence, its PDF for $x \geq 0$ is (with the hat symbol)

$$(11.11) \quad \hat{L}_{\alpha,k}^\theta(x) := \frac{1}{A^+} \tilde{f}^+(x)$$

$$(11.12) \quad \hat{L}_{\alpha,k}^{-\theta}(x) := \frac{1}{A^- \Sigma} \tilde{f}^-\left(\frac{x}{\Sigma}\right)$$

1305 where $A^+ = \gamma + \Psi(1 - \gamma)$ and $A^- = A^+/\Psi$ from Lemma 11.7.

1306 The reflection rule applies: $\hat{L}_{\alpha,k}^\theta(-x) := \hat{L}_{\alpha,k}^{-\theta}(x)$.
1307

1308 **11.3.1. The Location-scale Family.** The following lemmas show that all other solutions must
 1309 obey $\sigma^-/\sigma^+ = \Sigma$. They are just the location-scale family of the canonical distribution.

1310 Briefly, all other solutions are defined by a choice of scale $\sigma^+ > 0$, such that

$$(11.13) \quad L_{\alpha,k}^\theta(x) := \frac{1}{\sigma^+} \widehat{L}_{\alpha,k}^\theta\left(\frac{x}{\sigma^+}\right)$$

1311 For instance, we found that $\sigma^+ = \Sigma^\gamma$ to be a very good alternative. In the remark of Definition 11.9,
 1312 we show that the n -th moment of $L_{\alpha,k}^\theta$ is just that of $\widehat{L}_{\alpha,k}$ multiplied by its scale $(\sigma^+)^n$.

1313 LEMMA 11.5. The requirement that the density and slope of the *adjusted* density function should
 1314 be smooth at $x = 0$ leads to

$$(11.14) \quad \frac{1}{A^+\sigma^+} \tilde{f}_0^+ = \frac{1}{A^-\sigma^-} \tilde{f}_0^-$$

$$(11.15) \quad \frac{1}{A^+(\sigma^+)^2} \tilde{f}_1^+ = -\frac{1}{A^-(\sigma^-)^2} \tilde{f}_1^-$$

△

1315 PROOF. To solve A^\pm and σ^\pm , take (11.8) and carry out the series expansions from (11.4):

$$(11.16) \quad L_{\alpha,k}^{\pm\theta}(x) = \frac{\tilde{f}_0^\pm}{A^\pm\sigma^\pm} + \frac{\tilde{f}_1^\pm}{A^\pm(\sigma^\pm)^2} x + \dots$$

1317 (11.14) is straightforward from requiring $L_{\alpha,k}^\theta(0) = L_{\alpha,k}^{-\theta}(0)$ in (11.16). Likewise, (11.15) is the
 1318 result of $\frac{d}{dx} L_{\alpha,k}^\theta(0) = \frac{d}{dx} L_{\alpha,k}^{-\theta}(0)$ from (11.16). □

1319 LEMMA 11.6. The equations in Lemma 11.5 lead to the following invariant:

$$(11.17) \quad \frac{\sigma^-}{\sigma^+} = \Sigma$$

△

1320 PROOF. Divide the LHS and RHS of (11.14) by those of (11.15) respectively,

$$\sigma^+ \frac{\tilde{f}_0^+}{\tilde{f}_1^+} = -\sigma^- \frac{\tilde{f}_0^-}{\tilde{f}_1^-}$$

1322 Rearrange the items and we obtain (11.17). □

1323 LEMMA 11.7. The solution for A^\pm are

$$(11.18) \quad A^+ = \gamma + \Psi(1 - \gamma)$$

$$(11.19) \quad A^+/A^- = \Psi$$

△

1324 PROOF. (11.19) is derived by rearranging the items in (11.14) and following the definition of Ψ .

1325 (11.18) is derived from the fact that the total density of the adjusted distribution should be equal
 1326 to 1, that is, $\int_{-\infty}^{\infty} f(x)dx = 1$. Hence,

$$\int_0^{\infty} f^+(x)dx + \int_0^{\infty} f^-(x)dx = \frac{1}{A^+} \int_0^{\infty} \tilde{f}^+(x)dx + \frac{1}{A^-} \int_0^{\infty} \tilde{f}^-(x)dx = 1$$

1328 Apply (11.7), we get $\frac{\gamma}{A^+} + \frac{1-\gamma}{A^-} = 1$. Multiply it by A^+ on both sides, we obtain (11.18). □

1329 We've shown that A^\pm are well-defined constants based on (α, k, θ) , while σ^\pm is a choice of
 1330 parametrization, constrained by (11.17).

1331

11.4. Moments

1332 The structure of the *moments* reveals critical information about the adjusted distribution. We
 1333 show the moment formula of the canonical distribution, and how the location-scale family relates to
 1334 it.

1335 To simplify the notations below, let

- 1336 • $f^\pm = L_{\alpha,k}^{\pm\theta}$ be the adjusted distribution family,
- 1337 • $\tilde{f}^\pm = \tilde{L}_{\alpha,k}^{\pm\theta}$ be the canonical distribution,
- 1338 • $\tilde{f}^\pm = \tilde{L}_{\alpha,k}^{\pm\theta}$ be the original (unadjusted) distribution.

1339 First, the n -th one-sided moments of the adjusted distribution are ($x > 0$)

$$(11.20) \quad E(X^n|f^\pm) = \frac{1}{A^\pm\sigma^\pm} \int_0^\infty x^n \tilde{f}^\pm(x/\sigma^\pm) dx = \frac{(\sigma^\pm)^n}{A^\pm} E(X^n|\tilde{f}^\pm)$$

1340 where $E(X^n|\tilde{f}^\pm)$ are the original n -th one-sided moments. They can be obtained from the Mellin
 1341 transform (11.1).

1342 The n -th total moment, given the notation of m_n , is the sum of $E(X^n|f^+)$ and $(-1)^n E(X^n|f^-)$.
 1343 We show the following.

1344 LEMMA 11.8. The n -th total moment of the adjusted distribution is based on the original one-sided
 1345 moments such as

$$(11.21) \quad m_n := E(X^n|f) = \frac{(\sigma^+)^n}{A^+} \left[E(X^n|\tilde{f}^+) + \Psi(-\Sigma)^n E(X^n|\tilde{f}^-) \right]$$

1346

△

1347 PROOF. By definition, we have

$$\begin{aligned} m_n := E(X^n|f) &= \int_{-\infty}^\infty x^n f(x) dx = \int_0^\infty x^n f^+(x) dx + (-1)^n \int_0^\infty x^n f^-(x) dx \\ &= E(X^n|f^+) + (-1)^n E(X^n|f^-) \end{aligned}$$

1348 Apply (11.20), we get

$$m_n = \frac{(\sigma^+)^n}{A^+} E(X^n|\tilde{f}^+) + \frac{(-\sigma^-)^n}{A^-} E(X^n|\tilde{f}^-)$$

1349 Factor out $\frac{(\sigma^+)^n}{A^+}$, apply $\sigma^-/\sigma^+ = \Sigma$ from Lemma 11.6, and $A^+/A^- = \Psi$ from 11.7, we obtain (11.21).
 1350 □

1351 LEMMA 11.9 (The moments of the canonical distribution). The n -th moment of the canonical
 1352 distribution is

$$(11.22) \quad \hat{m}_n := E(X^n|\hat{f}) = \frac{1}{A^+} \left[E(X^n|\tilde{f}^+) + \Psi(-\Sigma)^n E(X^n|\tilde{f}^-) \right]$$

1353

△

1354 PROOF. Lemma 11.8 shows that the canonical distribution \hat{f} is obtained by letting $\sigma^+ = 1$ and
 1355 $\sigma^- = \Sigma$. Put them to (11.21), we obtain (11.22). □

1356 Lastly, compare (11.21) with (11.22). We reach $m_n = (\sigma^+)^n \hat{m}_n$. That is, all other members in
 1357 the adjusted distribution family are rescaled canonical distributions.

CHAPTER 12

GAS-SN: Generalized Alpha-Stable Distribution with Skew-Normal

This fractional univariate distribution combines the features from a classic skew-normal distribution that provides skewness and a fractional distribution that provides fatter tails. The resulting distribution is analytically tractable. The PDF and all of its derivatives are continuous everywhere in \mathbb{R} .

12.1. Definition

DEFINITION 12.1. Assume $Z_0 \sim SN(0, 1, \beta)$ is a skew-normal variable and $V \sim \bar{\chi}_{\alpha, k}$ is an FCM variable.

Then $Z \sim Z_0/V$ is a variable with a GAS-SN distribution. We use the notation $Z \sim L_{\alpha, k}(\beta)$ for this standard distribution.

Assume $\mathcal{N}(x)$ and $\Phi_{\mathcal{N}}(x)$ are the PDF and CDF of $N(0, 1)$. The PDF of Z is

$$(12.1) \quad L_{\alpha, k}(x; \beta) = 2 \int_0^\infty \mathcal{N}(xs) \Phi_{\mathcal{N}}(\beta xs) \bar{\chi}_{\alpha, k}(s) s ds.$$

This is the fractional extension of (10.2).

Its CDF is

$$(12.2) \quad \begin{aligned} \Phi[L_{\alpha, k}(\beta)](x) &:= \int_0^\infty \Phi_{SN}(xs; \beta) \bar{\chi}_{\alpha, k}(s) ds. \\ &= \int_0^\infty [\Phi_{\mathcal{N}}(xs) - 2T(xs, \beta)] \bar{\chi}_{\alpha, k}(s) ds. \end{aligned}$$

where $\Phi_{SN}(xs; \beta)$ is the CDF of $SN(0, 1, \beta)$ in (10.3), and $T(h, a)$ is the Owen's T function.

We can clearly see that the CDF has two components: One from the symmetric part, and the other skew. The second component vanishes due to $T(h, 0) = 0$.

12.1.1. GAS-SN Subsumes GSaS.

LEMMA 12.2. When $\beta = 0$, it becomes a symmetric distribution, previously called GSaS. The notation of $L_{\alpha, k}$ is given in [15].

The PDF of a GSaS is

$$(12.3) \quad L_{\alpha, k}(x) = \int_0^\infty \mathcal{N}(xs) \bar{\chi}_{\alpha, k}(s) s ds.$$

When $\alpha \rightarrow 2$ or $k \rightarrow \infty$, the symmetric distribution approaches a normal distribution $N(0, \alpha^{2/\alpha})$ (Section 8.2 of [15]). \triangle

This integral is a normal mixture (9.1) that enjoys several nice properties outlined in Chapter 9.

In particular, the generalized exponential power distribution can be obtained via the characteristic function transform in Lemma 9.2 (Section 9 of [15]). We point out that the skew extension is straightforward, but leave the detailed description to future research.

1386 **12.1.2. GAS-SN Subsumes Skew-t Distribution.** An important bridge between SN and
 1387 GAS-SN is the skew-t (ST) distribution. It is documented in Section 4.3 of [1].
 1388 ST is fully consistent with GAS-SN by setting $\alpha = 1$. That is, in his notation, $T(\beta, k) = L_{1,k}(\beta)$.

1389 12.2. The Location-Scale Family

1390 Its location scale family is $Y = \xi + \omega Z \sim L_{\alpha,k}(\xi, \omega^2, \beta)$. Its PDF becomes

$$(12.4) \quad \phi(x) = \frac{1}{\omega} L_{\alpha,k} \left(\frac{x - \xi}{\omega}; \beta \right). \quad (x \in \mathbb{R})$$

1391 In real-world applications, this PDF is used for optimization, e.g. in the maximum likelihood
 1392 estimation (MLE). See Section 12.9.

1393 12.3. Mellin Transform

1394 The Mellin transform of the PDF follows the rule of the ratio distribution. From (10.8) and (7.2),
 1395 we have

$$(12.5) \quad \begin{aligned} L_{\alpha,k}(x; \beta) &\xrightarrow{\mathcal{M}} L_{\alpha,k}^*(s; \beta) \\ &= \mathcal{N}^*(s; \beta) \bar{\chi}_{\alpha,k}^*(2 - s) \\ (12.6) \quad &= [2 \Phi[t_s](\beta \sqrt{s})] \times [\mathcal{N}^*(s) \bar{\chi}_{\alpha,k}^*(2 - s)] \end{aligned}$$

1396 Notice that the contribution for the skewness is $2 \Phi[t_s](\beta \sqrt{s})$ in the first bracket, which becomes one
 1397 if $\beta = 0$.

1398 The second bracket is the Mellin transform of the GSaS PDF. From (2.9) and (7.2), it is

$$(12.7) \quad \begin{aligned} L_{\alpha,k}(x) &\xrightarrow{\mathcal{M}} L_{\alpha,k}^*(s) = \mathcal{N}^*(s) \bar{\chi}_{\alpha,k}^*(2 - s) \\ &= \frac{1}{2\sqrt{\pi}} \left(\frac{2}{\sigma} \right)^{s-1} \Gamma \left(\frac{s}{2} \right) \frac{\Gamma((k-1)/2)}{\Gamma((k-1)/\alpha)} \frac{\Gamma((k-s)/\alpha)}{\Gamma((k-s)/2)}, \end{aligned}$$

1399 where $\sigma := k^{1/2-1/\alpha}$ and $k > 0$ is assumed.

1400 12.4. Moments

1401 Based on $\mathbb{E}(X^n | \mathcal{N}(\beta))$ from (10.11), the n -th moment of Z is

$$(12.8) \quad \begin{aligned} \mathbb{E}(X^n | L_{\alpha,k}(\beta)) &:= \mathbb{E}(X^n | \mathcal{N}(\beta)) \mathbb{E}(X^{-n} | \bar{\chi}_{\alpha,k}) \\ &= 2 \mathcal{N}^*(n+1) \mathbb{E}(X^{-n} | \bar{\chi}_{\alpha,k}) \\ &\quad \times \begin{cases} 1, & \text{when } n \text{ is even,} \\ 1 - 2\Phi[t_{n+1}](-\beta \sqrt{n+1}), & \text{when } n \text{ is odd.} \end{cases} \end{aligned}$$

1402 Its first moment is $\mu_z = b \delta$, where $b = \sqrt{2/\pi} \mathbb{E}(X^{-1} | \bar{\chi}_{\alpha,k})$.

1403 The second moment is $\mathbb{E}(X^{-2} | \bar{\chi}_{\alpha,k})$. Its variance is

$$(12.9) \quad \sigma_z^2 = \mathbb{E}(X^{-2} | \bar{\chi}_{\alpha,k}) - (b \delta)^2.$$

1404 To simplify the symbology, let $q_n := \mathbb{E}(X^{-n} | \bar{\chi}_{\alpha,k})$. The third moment is $\delta_3 q_3$, where $\delta_3 =$
 1405 $\sqrt{\frac{2}{\pi}} \delta(3 - \delta^2)$. The fourth moment is $3 q_4$. To carry out the skewness γ_1 and excess kurtosis γ_2 ,

$$\begin{aligned} \gamma_1 \times \sigma_z^{3/2} &= \delta_3 q_3 - 3\mu_z q_2 + 2\mu_z^3, \\ \gamma_2 \times \sigma_z^4 &= 3(q_4 - q_2^2) - 4\mu_z(\gamma_1 \times \sigma_z^{3/2}) + 2\mu_z^4. \end{aligned}$$

1406 The maximum skewness and kurtosis can be infinite. Since $\delta = \sin \theta$, where $\beta = \tan \theta$, we have
 1407 $\delta \in [-1, 1]$. Infinity has to come from q_3 and q_4 .

1408 A typical example is the skew-t distribution at $\alpha = 1$. It is well known that kurtosis approaches
 1409 infinity when k approaches 4 from above, and the skewness approaches infinity when k approaches 3
 1410 from above.

1411 **12.4.1. Excess Kurtosis of GSaS.** It is important to understand the behavior of excess kurtosis
 1412 γ_2 . However, the presence of skewness adds more complexity to γ_2 . Consider the symmetric case where
 1413 $\beta = 0$, and we quote the result from [15] below.

1414 The excess kurtosis of GSaS is plotted in Figure 12.1 in the (k, α) coordinate. Notice that a major
 1415 division occurs along the line of $k = 5 - \alpha$. In the region where $0 < k \leq 5 - \alpha$, there are complicated
 1416 patterns caused by the infinities of the gamma function. Only small pockets of valid kurtosis exist.

1417 LEMMA 12.3. In the region where $k > 5 - \alpha$, the excess kurtosis of GSaS is a continuous function
 1418 with positive values. At large k 's, the closed form of the moments can be expanded by Sterling's
 1419 formula. The excess kurtosis γ_2 becomes part of a linear equation:

$$(12.10) \quad \left(\epsilon - \frac{1}{2} \right) = \left(\frac{k-3}{4} \right) \log \left(1 + \frac{\gamma_2}{3} \right), \quad \text{where } \epsilon = 1/\alpha$$

1420 This equation shows how GSaS works under the **Central Limit Theorem**. GSaS approaches
 1421 a normal distribution when γ_2 becomes zero. This can happen from two directions: when $\alpha \rightarrow 2$ or
 1422 when $k \rightarrow \infty$.

△

1423 The contour plot of excess kurtosis is shown in the (k, ϵ) coordinate in Figure 12.2. It is visually
 1424 amusing. Notice the singular point at $\epsilon = 1/2, k = 3$.

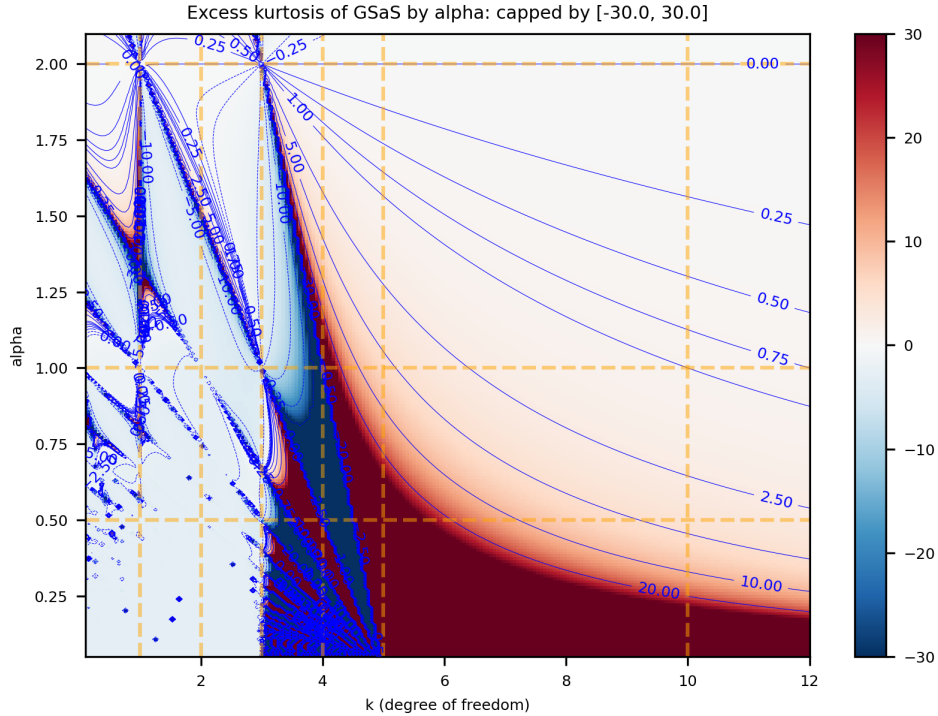


FIGURE 12.1. The contour plot of excess kurtosis in GSaS by (k, α) .

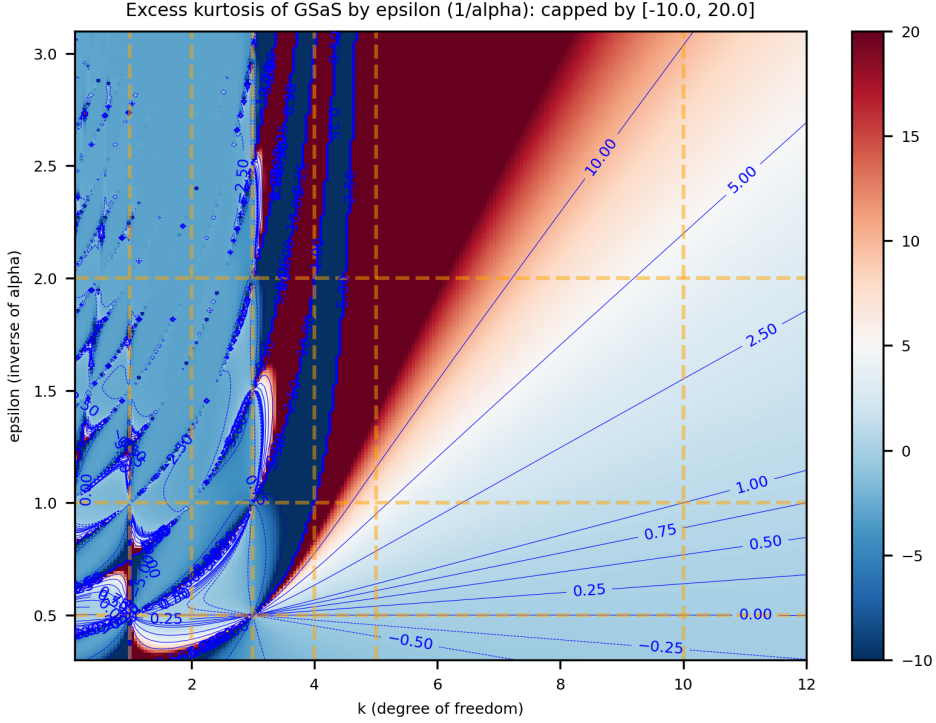


FIGURE 12.2. The contour plot of excess kurtosis in GSaS by (k, ϵ) where $\epsilon = 1/\alpha$. This best describes the linearity in (12.10) for large k 's.

12.5. Tail Behavior

The tail behavior of GAS-SN is a "modified GSaS" type. Hence, it is well within what was known. Without losing generality, assume $\beta > 0$, that the decay of the left tail is more pronounced than that of the right tail. But it still follows the same power law of x^{-k} as in a $L_{\alpha,k}$.

It takes a small tweak to GSaS to capture that behavior.

DEFINITION 12.4. The shifted GSaS is defined as

$$(12.11) \quad L_{\alpha,k}(x||\mu) = \int_0^\infty \mathcal{N}(xs - \mu) \bar{\chi}_{\alpha,k}(s) s ds$$

Note that the shift μ is not a location parameter that shifts x . It is a shift inside the argument of $\mathcal{N}()$. When $\mu = 0$, it is restored to the PDF of GSaS, $L_{\alpha,k}(x)$.

We use the following approximation of the erf function in (12.1)[11]

$$(12.12) \quad 1 - \text{erf}(x) \approx \frac{1}{B\sqrt{\pi}x} (1 - e^{-Ax}) e^{-x^2} \quad (x \geq 0)$$

where $A = 1.98$ and $B = 1.135$. It is much better than the first-order expansion of $e^{-x^2}/(\sqrt{\pi}x)$ for the entire range of $x \in [0, \infty)$.

LEMMA 12.5. The left tail ($x < 0$) of the PDF in (12.1) can be approximated by

$$(12.13) \quad \hat{L}_{\alpha,k}(x; \beta) = \frac{G}{\beta x} \left[e^{\mu^2/2} L_{\alpha,k-1}(qx||\mu) - L_{\alpha,k-1}(qx) \right]$$

1438 where

$$\begin{aligned}\mu &= \frac{A\delta}{\sqrt{2}} \\ q &= \sqrt{1 + \beta^2} \frac{\sigma_{\alpha,k}}{\sigma_{\alpha,k-1}} \\ G &= \sqrt{\frac{2}{\pi}} \frac{B C_{\alpha,k}}{\sigma_{\alpha,k-1} C_{\alpha,k-1}}\end{aligned}$$

1439 and both $C_{\alpha,k} = \frac{\alpha\Gamma((k-1)/2)}{\Gamma((k-1)/\alpha)}$ and $\sigma_{\alpha,k}$ are according to FCM in (7.4).

1440 The right tail ($x > 0$) is simply

$$(12.14) \quad L_{\alpha,k}(x) - \hat{L}_{\alpha,k}(-x; \beta)$$

1441 where the second term $\hat{L}_{\alpha,k}(-x; \beta)$ becomes much smaller than the first term as $x \rightarrow \infty$. \triangle

1442 PROOF. TODO add more content here.

1443 \square

1444 12.6. Maximum Skewness and Half GSaS

1445 When $\beta \rightarrow \pm\infty$, a GAS-SN becomes a half-GSaS, which is a one-sided distribution with the
1446 notation of $L_{\alpha,k}^\pm := L_{\alpha,k}(\beta = \pm\infty)$. Its PDF is

$$(12.15) \quad L_{\alpha,k}^+(x) = \begin{cases} 2L_{\alpha,k}(x) & \text{if } x \geq 0, \\ 0 & \text{otherwise.} \end{cases}$$

1447 It follows the reflection rule of $L_{\alpha,k}^-(x) = L_{\alpha,k}^+(-x)$. Hence, we only need to study the $+\infty$ case.

1448 A half-GSaS possesses the maximum skewness that a GAS-SN family can achieve for a given pair
1449 of (α, k) . In Section 10.5, it was mentioned that the maximum skewness of the SN family is only
1450 0.9953. GAS-SN allows the skewness to reach infinity potentially.

1451 From (12.7), the n -th moment is

$$\begin{aligned}(12.16) \quad \mathbb{E}(X^n | L_{\alpha,k}^+) &= 2L_{\alpha,k}^*(n+1) \\ \mathbb{E}(X^n | L_{\alpha,k}^-) &= 2L_{\alpha,k}^*(n+1)(-1)^n\end{aligned}$$

1452 Therefore, it is straightforward to calculate the skewness.

1453 The skewness of half-GSaS $L_{\alpha,k}^+$ is shown in Figure 12.3 in the (k, α) coordinate. There is a clear
1454 division of infinity by the line from $(2, 2)$ to $(4, 0)$.

1455 The contour plot of the skewness is shown in the (k, ϵ) coordinate in Figure 12.4. Each contour
1456 line approaches a straight line as k increases.

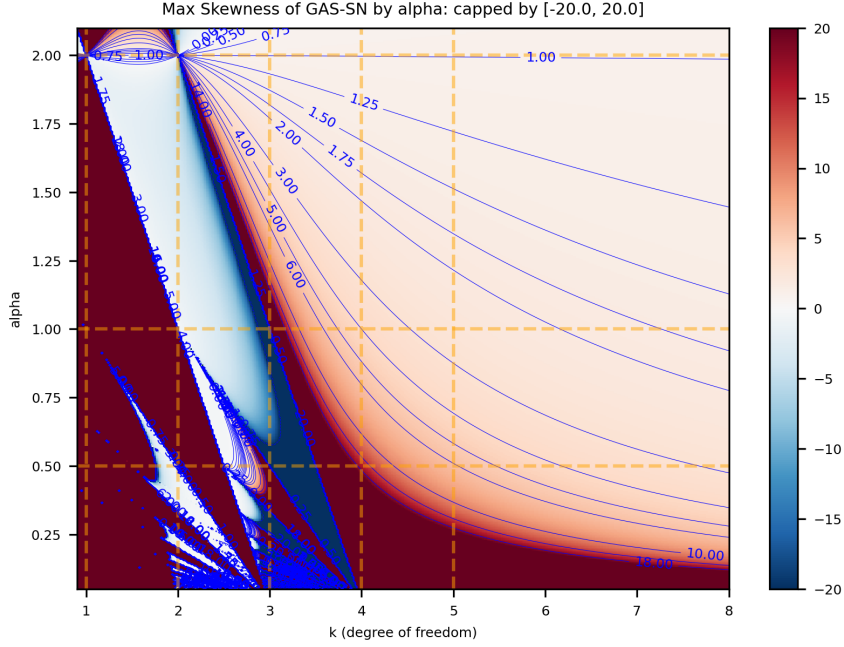


FIGURE 12.3. The contour plot of skewness of the half-GSaS $L_{\alpha,k}^+$ by (k, α) . This represents the maximum skewness that the GAS-SN family can achieve.

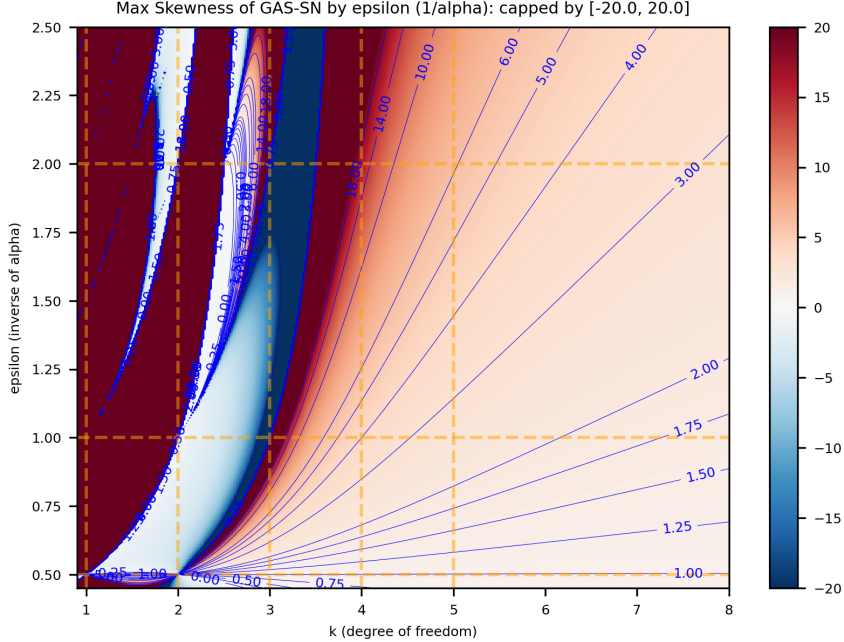


FIGURE 12.4. The contour plot of skewness of the half-GSaS $L_{\alpha,k}^+$ by (k, ϵ) where $\epsilon = 1/\alpha$. Each contour line approaches a straight line as k increases.

1457 12.7. Fractional Skew Exponential Power Distribution

1458 As shown in Definition 3.6 and Section 9 of [15], the negative k space is reserved for the fractional
 1459 exponential power distribution, whose PDF is $\mathcal{E}_{\alpha,k}(x) := L_{\alpha,-k}(x)$. All it takes is to have $\bar{\chi}_{\alpha,k}(s)$ in
 1460 (12.1) properly defined for negative k , which is done in (7.11).

1461 It is natural to extend it with the skew-normal family such that its PDF becomes

$$(12.17) \quad \mathcal{E}_{\alpha,k}(x; \beta) = L_{\alpha,-k}(x; \beta).$$

1462 Then we obtain another flexible skew distribution with a different type of tail behavior. Detailed
 1463 analysis of this distribution is left for future research.

1464 12.8. Quadratic Form

1465 A squared GAS-SN variable Q is distributed as a fractional F distribution with $d = 1$. That is,

$$(12.18) \quad Q := \left(\frac{Y - \xi}{\omega} \right)^2 = Z^2 \sim F_{\alpha,1,k}, \quad \text{for all } \beta.$$

1466 Notice that Q is based on the standard variable Z , which is invariant to the location and scale. See
 1467 Chapter 8 for more detail.

1468 12.9. Univariate MLE

1469 In this section, we document how we fit the one-dimensional data with univariate GAS-SN. The
 1470 main algorithm is *maximum likelihood estimation* (MLE), supplemented with several components of
 1471 regularization.

1472 We applied the MLE fitting on the daily returns of VIX and SPX from 1990 to mid-2025, each
 1473 about 8900 samples. The MLE program is implemented in `python` and `scipy` on github at https://github.com/slihn/gas-impl/blob/main/gas_impl/mle_gas_sn.py.

1474 In the univariate case, the hyperparameter space is $\Theta = \{\alpha, k, \beta, \omega, \xi\}$, where $\alpha \in (0, 2)$, $k \in (2, \infty)$,
 1475 $\omega > 0$, and $\beta, \xi \in \mathbb{R}$. Assume there are N samples in the data set, $Y = \{y_i, i \in 1, 2, \dots, N\}$, the main
 1477 component of the objective function is the minus log-likelihood (MLLK):

$$(12.19) \quad \text{MLLK}(\Theta) = -\frac{1}{N} \sum_{i=1}^N \log(\phi(y_i; \Theta))$$

1478 where $\phi(y; \Theta)$ is the PDF of the univariate location scale family (12.4).

1479 Additional components of regularization are added to the objective function $\ell(\Theta)$. Specifically, the
 1480 L2 distances between the empirical and theoretical statistics are added as follows:

- 1481 • Skewness: $|\Delta\gamma_1|^2 := |\Delta\text{skewness}(Y)|^2$. Section 12.4.
- 1482 • Kurtosis: $|\Delta\gamma_2|^2 := |\Delta\text{kurtosis}(Y)|^2$. Section 12.4.
- 1483 • The mean of the quadratic form: $\Delta\mu_Q^2 := |\Delta\text{mean}(Q)|^2$. Section 15.6.

1484 The MLE seeks the optimal Θ that minimizes the objective function:

$$(12.20) \quad \hat{\Theta} = \operatorname{argmin} \ell(\Theta)$$

$$(12.21) \quad \text{where } \ell(\Theta) = \text{MLLK}(\Theta) + |\Delta\gamma_1|^2 + |\Delta\gamma_2|^2 + \Delta\mu_Q^2$$

1485 A custom version of the stochastic descent (SD) algorithm is developed. Our experience shows
 1486 that it is better to standardize the data set to one standard deviation, so that all parameters in Θ are
 1487 approximately on the same scale.

1488 It is also important to control the learning rate so that it does not take a too large step on α ,
 1489 empirically, no more than 0.01 per step. This ensures that the SD does not wander into the *undefined*
 1490 regions for $\ell(\Theta)$. This is particularly important for the SPX fit below.

1491 The SD algorithm calculates the gradients for each hyperparameter. And make a small move along
 1492 the direction that is most likely to minimize $\ell(\Theta)$. The scale of the move is based on the learning rate,
 1493 which can be dynamically adjusted. Some randomness is added to the small move. This allows the
 1494 algorithm to explore the nearby region and increases its choices.

1495 12.10. Examples of Univariate MLE Fits

1496 **12.10.1. VIX fit.** Figure 12.5 shows the result of the MLE fit to the daily VIX returns from
 1497 1990 to mid-2025. Data are standardized to one standard deviation. This helps the SD algorithm to
 1498 move correctly in all dimensions of Θ .

1499 The VIX data are right-skewed. The sample skewness of 2.0 is quite high. The right tail is very
 1500 stretched due to several high-profile *panic selling* events where the VIX tends to jump a lot in a day.
 1501 This tail creates a very high kurtosis of ~ 17 .

1502 The top two graphs compare the histogram with the theoretical PDF. The right graph shows the
 1503 density on logarithmic scale so that we can examine how the tails are fitted (down to the 10^{-3} level).
 1504 Obviously, the right tail larger than 7 is not properly captured by the theoretical PDF.

1505 The parameters of the theoretical distribution are: α is slightly below 0.8, k is in the neighborhood
 1506 of 5, and β is near 1. The reader is encouraged to locate this point of (α, k) in Figure 12.1.

1507 The PP-plot in the bottom left graph shows that the overall fit is satisfactory. The 45-degree line
 1508 is very clear. This plot is less sensitive to the tails.

1509 The QQ-plot of the quadratic form (or called the squared variable) is shown in the bottom right
 1510 graph. It is a powerful tool for studying how the combined tail (in absolute terms) is doing. The 45-
 1511 degree line is OK below 20, but as the quantiles get larger, the observed quantiles start to tilt upward.
 1512 This means the top 0.5 percent of the combined tail is not properly captured by the distribution.

1513 **12.10.2. SPX fit.** Figure 12.6 shows the result of the MLE fit to the daily SPX returns from
 1514 1990 to mid-2025. The data is also standardized to one standard deviation.

1515 The SPX data are left skewed. The sample skewness of less than -0.1 is mild. The tails are
 1516 stretched due to several high-profile one-day panic selling events. The tails create a very high kurtosis
 1517 of ~ 11 (but not a lot of skewness).

1518 The top two graphs compare the histogram with the theoretical PDF. The graph on the right
 1519 shows the density on a logarithmic scale so that we can examine how the tails are fitted (down to the
 1520 10^{-3} level). Obviously, tails larger than 7 are not captured well by the theoretical PDF.

1521 The parameters of the theoretical distribution are: α is near 0.9, k is in the neighborhood of 3.1,
 1522 and β is near 0. This region is close to t_3 , which is quite peculiar, since theoretical skewness and
 1523 kurtosis barely exist and are very sensitive to α, k, β . It is not easy to find this point visually in Figure
 1524 12.1. This strange result remains a topic for future research.

1525 The PP-plot in the bottom left graph shows that the overall fit is satisfactory. The 45-degree line
 1526 is OK. But there is a small bump between 0 and 0.2. It is well known from the market regime models,
 1527 for example [29], that the crash regime has a negative mean return. This causes the effect of this
 1528 bump on the left side of the distribution.

1529 In the QQ-plot of the quadratic form, the 45-degree line is OK below 100, but as the quantiles get
 1530 larger, the observed quantiles start to tilt downward. The far most 10 data points of the combined
 1531 tail are not properly captured by the distribution.

1532 Notice how far the quantiles have stretched. The theoretical mean is 2.8, while the largest point
 1533 is near 700 (26^2). It spans almost 3 orders of magnitude.

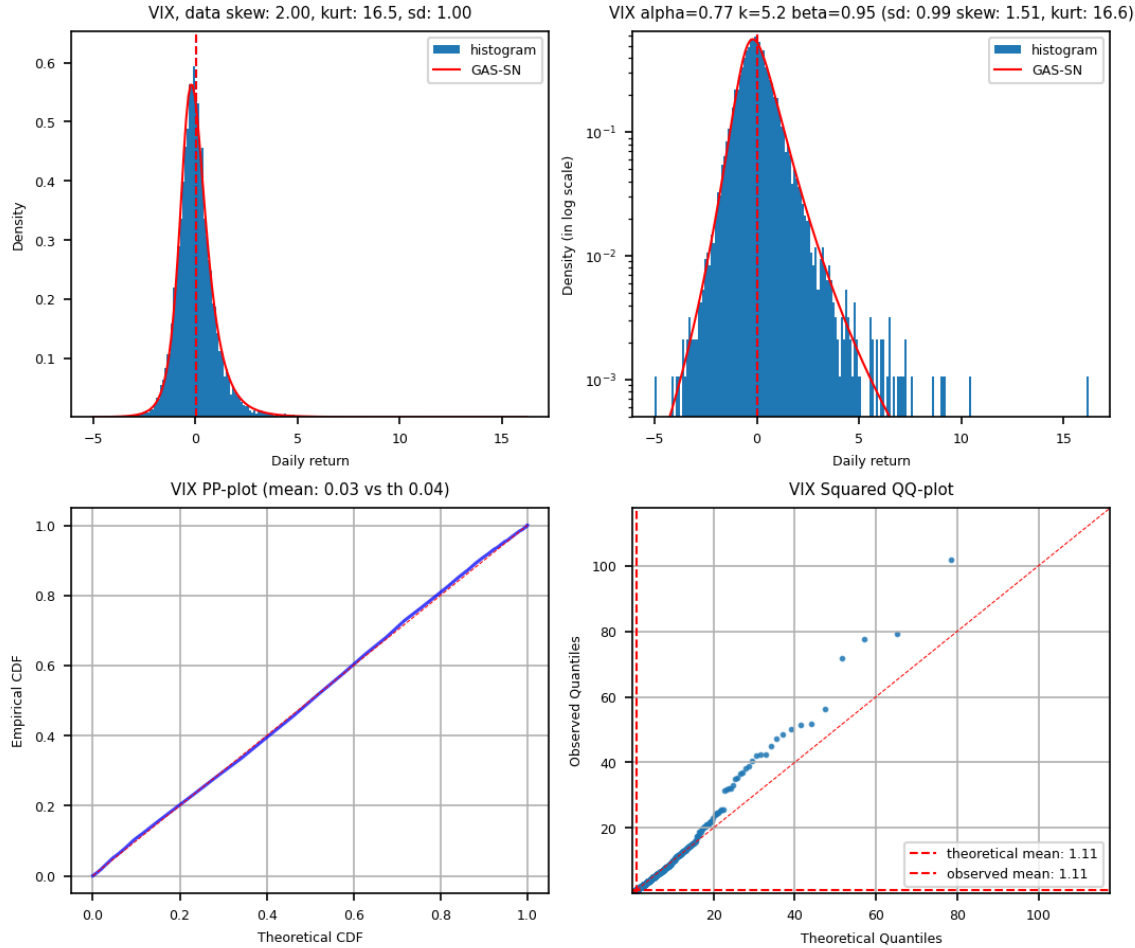


FIGURE 12.5. The MLE fit of VIX daily returns from 1990 to mid-2025. Data is standardized to one standard deviation. Sample skewness is 2.0, sample kurtosis is 16.5. $\hat{\Theta} = \{\alpha = 0.77, k = 5.2, \beta = 0.95\}$. Top left: the PDF vs histogram. Top right: the log-density vs histogram. Bottom left: the PP-plot. Bottom right: the QQ-plot of the quadratic form.

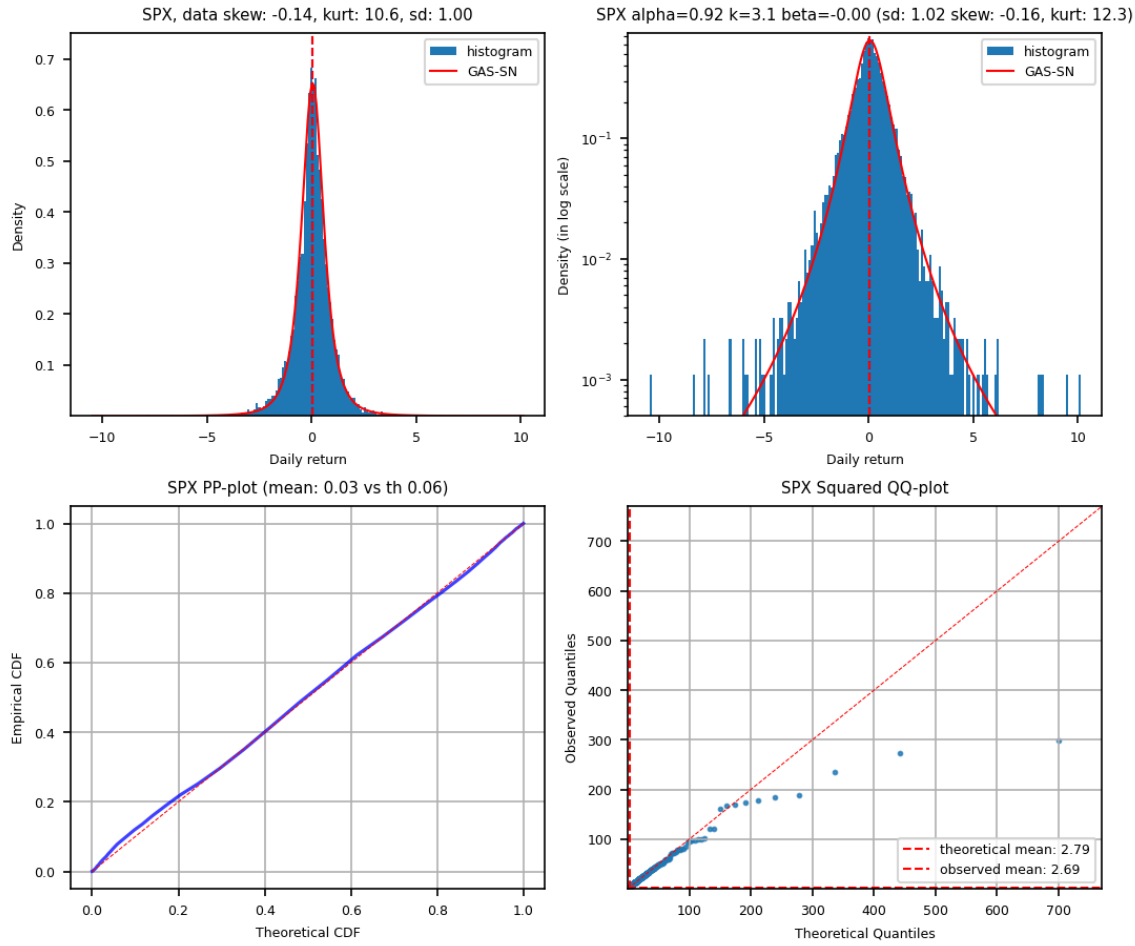


FIGURE 12.6. MLE fit of SPX daily log returns from 1990 to mid-2025. Data is standardized to one standard deviation. Sample skewness is -0.14, sample kurtosis is 10.6. $\hat{\Theta} = \{\alpha = 0.92, k = 3.1, \beta = 0.0\}$. Top left: the PDF vs histogram. Top right: the log-density vs histogram. Bottom left: the PP-plot. Bottom right: the QQ-plot of the quadratic form.

CHAPTER 13

Fractional Feller Square-Root Process

1534 This chapter is copied from Section 11 of [15] for the generation of random variables for FG, FCM,
 1535 and FCM2. Combining this with an SN variable provides a path to generate the random variable for
 1536 GAS-SN and beyond.

1537 For example, assuming that a sequence of random numbers $\{S_t > 0\}$ can be generated for FCM,
 1538 it is straightforward to simulate random numbers $\{X_t\}$ for GAS-SN using the ratio of $X_t = Y_t/S_t$,
 1539 where Y_t is a standard skew-normal variable $Y_t \sim SN(0, 1, \beta)$ in Chapter 12.

1540 Instead of randomly generating $\{S_t\}$, we propose an innovative method based on *Feller square-root*
 1541 process[7]. Given a user-specific volatility $\sigma_u > 0$ that describes how fast S_t should change, a scalar
 1542 function $\mu(x)$, and a scale parameter $\theta_u > 0$ (default to 1), we assume that the random variable S_t
 1543 should evolve according to the following generalized process:

$$(13.1) \quad dS_t = \sigma_u^2 \mu \left(\frac{S_t}{\theta_u} \right) dt + \sigma_u \sqrt{S_t} dW_t$$

1544 As $t \rightarrow \infty$, $\{S_t\}$ will be distributed as the equilibrium distribution for which $\mu(x)$ is designated.

1545 **13.0.1. The Fokker-Planck Equation.** The $\mu(x)$ solution can be derived from the Fokker-
 1546 Planck equation. We obtain the following beautiful relation:

1547 LEMMA 13.1. $\mu(x)$ is one half of the elasticity of the terminal density function $p(x)$ of S_t at $t \rightarrow \infty$
 1548 plus one half:

$$(13.2) \quad \mu(x) = \frac{1}{2} \mathcal{L} p(x) + \frac{1}{2}$$

1549 where $\mathcal{L}(\cdot) := x \frac{d}{dx} \log(\cdot)$ is the elasticity operator defined in Section 3.6.

△

PROOF. Assume $p(x, t)$ is the density function of (13.1) for S_t . It should satisfy the Fokker-Planck
 equation ($\theta_u = 1$):

$$\frac{\partial}{\partial t} p(x, t) = -\frac{\partial}{\partial x} [\sigma_u^2 \mu(x) p(x, t)] + \frac{\partial^2}{\partial x^2} \left[\frac{1}{2} (\sigma_u \sqrt{x})^2 p(x, t) \right]$$

As $t \rightarrow \infty$, $p(x, t)$ approaches the terminal density function $p(x)$. The time dependency is removed.
 σ_u^2 cancels out from both sides and is irrelevant to the solution. The ODE of $p(x)$ becomes

$$\frac{\partial}{\partial x} (\mu(x) p(x)) = \frac{1}{2} \frac{\partial^2}{\partial x^2} (x p(x))$$

1552 Apply $\int_x^\infty dx$ to both sides. Assuming that $\mu(x)p(x)$ at $x = \infty$ should be zero, we get

$$\mu(x)p(x) = \frac{1}{2} \frac{d}{dx} (x p(x)) = \frac{1}{2} \left(x \frac{d}{dx} p(x) + p(x) \right)$$

1553 Moving $p(x)$ from LHS to RHS, we obtain (13.2).

□

1555 **13.0.2. Generation of Random Variables for FG.**

1556 LEMMA 13.2. The $\mu(x)$ solution for FG is obviously

$$\mu(x) = \frac{1}{2} \mathcal{L} \mathfrak{N}_\alpha(x; \sigma, d, p) + \frac{1}{2}$$

1557 With Lemma 3.6, $\mu(x)$ is reduced to a function of $\mathcal{L} M_\alpha(x)$:

$$(13.3) \quad \mu(x) = \frac{p}{2} [\mathcal{L} M_\alpha] \left(\left(\frac{x}{\sigma} \right)^p \right) + \frac{d+p}{2}.$$

1558 \triangle

1559 As an application, since $\mathcal{L} M_{1/2}(x) = -x^2/2$ from Section 3.6, we obtain a simple power-law
1560 solution at $\alpha = 1/2$:

$$(13.4) \quad \mu(x)|_{\mathfrak{N}_{1/2}} = -\frac{p}{4} \left(\frac{x}{\sigma} \right)^{2p} + \frac{d+p}{2}$$

1561 Note that (13.4) at $p = 1/2$ subsumes the renown Cox–Ingersoll–Ross (CIR) model[4] since the
1562 $\mu(x)$ of the model is a linear $a(b - x)$ type, according to its stochastic process of $dS_t = a(b - S_t) dt +$
1563 $\sigma_u \sqrt{S_t} dW_t$.¹

1564 To prepare for the solution of FCM, we prefer to use $Q_\alpha(x)$ defined in (3.33):

$$Q_\alpha(x) := -\frac{W_{-\alpha,-1}(-x)}{W_{-\alpha,0}(-x)}$$

1565 LEMMA 13.3. From (3.35), the $\mu(x)$ solution of a FG in terms of $Q_\alpha(x)$ is

$$(13.5) \quad \mu(x) = \frac{p}{2\alpha} Q_\alpha \left(\left(\frac{x}{\sigma} \right)^p \right) + \left(\frac{d}{2} - \frac{p}{2\alpha} \right)$$

1566 Notice that p/α and d are just constant terms, and σ only affects the scale of x . Neither of them has
1567 any effect on the shape of $\mu(x)$.

1568 \triangle

1569 **13.1. Generation of Random Variables for FCM**

1570 Obviously, what really matters for GAS-SN and GSaS is the solution of FCM, The $\mu(x)$ solution
1571 for $\bar{\chi}_{\alpha,k}$ is denoted as $\mu_{\alpha,k}(x)$. Note that from this point on, $\alpha \in (0, 2)$.

1572 To further simplify the symbology for FCM, define

$$Q_\alpha^{(\chi)}(z) := Q_{\frac{\alpha}{2}}(z^\alpha), \text{ where } \alpha \in (0, 2).$$

1573 Assuming $k > 0$, we set $\sigma = \sigma_{\alpha,k}, d = k - 1, p/\alpha = 2$ and α replaced by $\alpha/2$ in (13.5). We get

$$(13.6) \quad \mu_{\alpha,k}(x) = Q_\alpha^{(\chi)} \left(\frac{x}{\sigma_{\alpha,k}} \right) + \left(\frac{k-3}{2} \right)$$

1574 For validation, $\mu_{1,k}(x) = k(1 - x^2)/2$ can be used to simulate Student's t. And $\mu_{\alpha,1}(x)$ provides a
1575 method to simulate an SaS $L_{\alpha,1}(x)$:

$$\mu_{\alpha,1}(x) = Q_\alpha^{(\chi)}(\sqrt{2}x) - 1$$

1576 Fig. 13.1 shows a simulation of random variables based on the (α, k) parameter obtained from the
1577 fit of the S&P 500 daily log returns. The rest of the parameters are in the caption of the figure. First,
1578 as outlined above, $\mu_{\alpha,k}(s)$ is calculated analytically as shown in the right graph. Second, it enables

1579 ¹It can also be subsumed by the FG at $\alpha = 0, p = 1$. But $\alpha = 0$ is a singular point and we prefer to avoid using it when
possible.

1580 the FG simulation $\{S_t\}$ as shown in the left graph. Third, GSaS $\{X_t\}$ is simulated via $X_t = \mathcal{N}/S_t$,
 1581 where \mathcal{N} is drawn from a standard normal variable.

1582 The simulation is performed daily. The duration of the sampling is 200,000 years. The red areas
 1583 are histograms of the simulated data. The blue lines are from the theoretical density functions. They
 1584 match well.

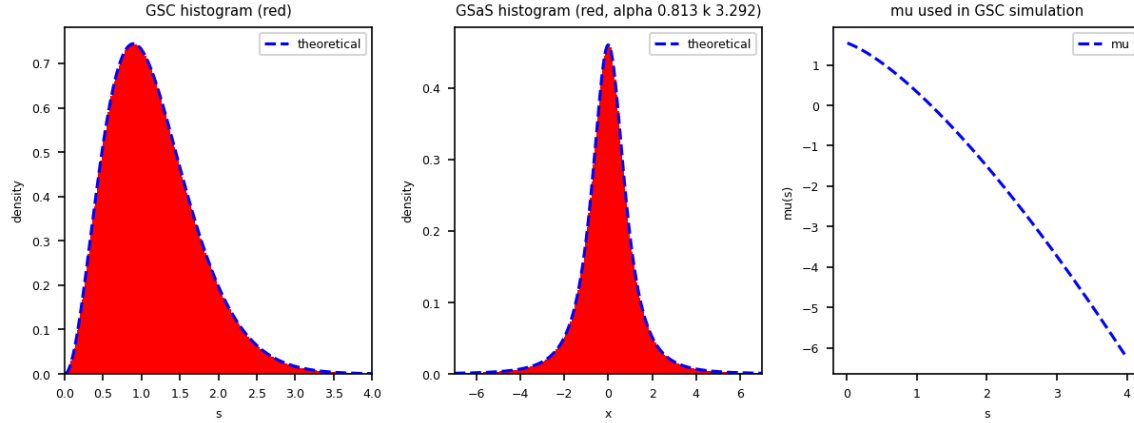


FIGURE 13.1. Simulation of random variables based on the (α, k) parameters obtained from the fit of the S&P 500 daily log returns. The red areas are the histograms from simulated data. The blue lines are from theoretical formulas. The settings of the simulation are $\alpha = 0.813, k = 3.292, dt = 1/365, \sigma_u = 0.85$. Sampling duration is 200,000 years. The simulation takes 11 minutes in python. $\mu_{\alpha,k}(s)$ is discretized to 0.01 and cached to increase performance.

1585 **13.2. Generation of Random Variables for FCM2**

1586 LEMMA 13.4. The $\mu(x)$ solution for $\bar{\chi}_{\alpha,k}^2$ is

$$(13.7) \quad \mu_{\alpha,k}^{(2)}(x) = \frac{1}{2}\mu_{\alpha,k}(\sqrt{x})$$

1587 \triangle

1588 PROOF. From (7.15), we have

$$\bar{\chi}_{\alpha,k}^2(x) := \mathfrak{N}_{\alpha/2}(x; \sigma = \sigma_{\alpha,k}^2, d = (k-1)/2, p = \alpha/2) \quad (k > 0)$$

1589 Combined with (13.5), we obtain the solution for $\bar{\chi}_{\alpha,k}^2$ as

$$\begin{aligned} \mu_{\alpha,k}^{(2)}(x) &= \frac{1}{2}Q_{\alpha/2}\left(\left(\frac{\sqrt{x}}{\sigma_{\alpha,k}}\right)^{\alpha}\right) + \left(\frac{k-1}{4} - \frac{1}{2}\right) \\ &= \frac{1}{2}Q_{\alpha}^{(\chi)}\left(\frac{\sqrt{x}}{\sigma_{\alpha,k}}\right) + \frac{k-3}{4}, \end{aligned}$$

1590 which is just

$$\mu_{\alpha,k}^{(2)}(x) = \frac{1}{2}\mu_{\alpha,k}(\sqrt{x}).$$

1591 \square

1592 This solution can be used to simulate the F distribution in Chapter 8. Let $U_1 \sim \chi_d^2/d = \bar{\chi}_{1,d}^2$ and
1593 $U_2 \sim \bar{\chi}_{\alpha,k}^2$, then $F_{\alpha,d,k} \sim U_1/U_2$ is a fractional F distribution.

1594

Part 4

1595

Multivariate Distributions

CHAPTER 14

Multivariate SN Distribution - Review

1597 In this chapter, we start to explore the multivariate distributions. Data sets from the real world
 1598 are often multidimensional. A flexible multivariate distribution framework with skewness and kurtosis
 1599 can be very useful. That is what we aim to achieve in the next few chapters.

1600 The foundation is the standard multivariate normal distribution $\mathcal{N}_d(0, \bar{\Omega})$, where d is the dimension
 1601 of the random variable, and $\bar{\Omega}$ is a $d \times d$ correlation matrix[32].

1602 In Chapter 5 of Azzalini, the skew normal distribution $SN_d(0, \bar{\Omega}, \beta)$ adds skewness to it from the
 1603 skew parameter β [1]. In its Chapter 6, the skew-elliptical distribution is discussed. The multivariate
 1604 skew-t distribution $ST_d(0, \bar{\Omega}, \beta, k)$ is constructed by combining $SN_d(0, \bar{\Omega}, \beta)$ with χ_k/\sqrt{k} in a ratio
 1605 distribution.

1606 Our work builds on top of this concept of the skew-elliptical distribution. By expanding the
 1607 denominator of χ_k/\sqrt{k} to the FCM $\chi_{\alpha,k}$, the fractional dimension α is added to the shape parameters.
 1608 This forms a super-distribution family called *multivariate GAS-SN elliptical distribution* with the
 1609 notation $L_{\alpha,k}(0, \bar{\Omega}, \beta)$ for its standard distribution.

1610 The multivariate skew-elliptical distribution has beautiful properties inherited from the multivariate
 1611 elliptical distribution framework. However, its deficiency is obvious in real-world applications: The
 1612 structure is multivariate, but the shape parameters α and k are scalars. All dimensions share the same
 1613 (α, k) . This restricts the kurtoses of 1D marginal distributions to a similar range. It even creates some
 1614 strange phenomena that are hard to interpret in the SPX-VIX 2D fit (see Section 17.1.1).

1615 To overcome such a restriction, we propose a more flexible framework called *multivariate adaptive*
 1616 *distribution*, in which the shape parameters (α, k) are d dimensional vectors, just like their skew
 1617 counterpart β .

1618 The flexibility in shapes comes with an expensive computational cost. It is analogous to the *curse*
 1619 *of dimensionality* problem. It becomes much harder to verify the results beyond the bivariate case for
 1620 the adaptive distribution.

1621 The study of quadratic form $Z^\top \bar{\Omega}^{-1} Z$ from the skew-elliptical distribution results in the fractional
 1622 extension of the F distribution $F_{\alpha,d,k}$. The QQ-plot based on the quadratic form and the fractional F
 1623 distribution is a powerful validation of the goodness of the fit.

14.1. Definition

1625 We summarize the results of Chapter 5 of Azzalini[1]. On the one hand, we need to clarify the
 1626 symbology here that is slightly different from that in his book. On the other hand, our multivariate
 1627 distributions rely on many results from there, which are collected in this chapter.

1628 DEFINITION 14.1. The PDF of a standard multivariate normal distribution $\mathcal{N}_d(0, \bar{\Omega})$ is defined as

$$(14.1) \quad \mathcal{N}_d(\mathbf{x}; \bar{\Omega}) := \frac{1}{(2\pi)^{d/2} \det(\bar{\Omega})^{1/2}} \exp\left(-\frac{1}{2}\mathbf{x}^\top \bar{\Omega}^{-1} \mathbf{x}\right), \quad \mathbf{x} \in \mathbb{R}^d.$$

1629 where $\bar{\Omega}$ is a $d \times d$ correlation matrix[32]. That is, $\bar{\Omega}$ is positive definite and all its diagonal elements
 1630 are equal to 1.

DEFINITION 14.2. A standard multivariate skew-normal variable is denoted as $Z \sim SN_d(0, \bar{\Omega}, \beta)$, where $\beta \in \mathbb{R}^d$ is the skew parameter (or the slant parameter). Its PDF is

$$(14.2) \quad \mathcal{N}_d(\mathbf{x}; \bar{\Omega}, \beta) := \mathcal{N}_d(\mathbf{x}; \bar{\Omega}) \Phi_{\mathcal{N}}(\beta^\top \mathbf{x}),$$

where $\Phi_{\mathcal{N}}(x)$ is the CDF of a standard normal distribution $\mathcal{N}(0, 1)$.

Notice that this is a multivariate expansion of SN in Section 10.1. When $d = 1$, (14.2) becomes (10.2).

1637

14.2. The Location-Scale Family

Its location-scale family is $Y = \xi + \omega Z \sim SN_d(\xi, \Omega, \beta)$, where $\xi \in \mathbb{R}^d$ is the location parameter, $\omega = \text{diag}(\omega_1, \dots, \omega_d)$ is a $d \times d$ diagonal scale matrix ($\omega_i > 0, \forall i$) and $\Omega = \omega \bar{\Omega} \omega$.

The PDF of Y becomes

$$(14.3) \quad f_Y(\mathbf{z}) = \det(\omega)^{-1} \mathcal{N}_d(\mathbf{z}; \bar{\Omega}, \beta),$$

where $\mathbf{z} = \omega^{-1}(\mathbf{x} - \xi)$.

The location-scale distribution is used for real-world applications. Internally, it has to be calculated via the standard distribution. The main reason is that β has to work with \mathbf{z} and $\bar{\Omega}$, instead of \mathbf{x} and ω .

14.3. Quadratic Form

DEFINITION 14.3. The quadratic form of a multivariate SN distribution (MSN) is defined as

$$(14.4) \quad Q := \frac{1}{d} (\mathbf{Y} - \xi)^\top \Omega^{-1} (\mathbf{Y} - \xi) = \frac{1}{d} \mathbf{Z}^\top \bar{\Omega}^{-1} \mathbf{Z}.$$

1648

Q distributes as $\chi_d^2/d = \bar{\chi}_{1,d}^2$ for all β . The distribution of Q is independent of β . This is an important property due to the rotational invariance of the elliptical distribution.

Notice that our definition of Q is slightly different from that of Azzalini. We prefer to have the distribution of Q tied to the FCM and the fractional F distribution directly without any constant adjustment. This will make things much simpler in Section 15.6.

To prove $Q \sim \chi_d^2/d$, we quote Corollary 5.9 from [1] below for a skew-normal distribution with 0 location:

LEMMA 14.4. If $\mathbf{Y} \sim SN_d(0, \Omega, \beta)$ and A is a $d \times d$ symmetric matrix, then

$$\mathbf{Y}^\top A \mathbf{Y} = \mathbf{X}^\top A \mathbf{X}$$

where $\mathbf{X} \sim \mathcal{N}_d(0, \Omega)$. △

This lemma allows β to be removed from the statistics of Q . Hence, $Q \sim X^\top \Omega^{-1} X / d \sim \chi_d^2/d$.

14.4. Stochastic Representation

Assuming $X_0 \sim \mathcal{N}_d(0, \bar{\Omega})$ and $X_1 \sim \mathcal{N}(0, 1)$, then the first representation of $Z \sim SN_d(0, \bar{\Omega}, \beta)$ is

$$(14.5) \quad Z = \begin{cases} X_0 & \text{if } X_1 > \beta^\top X_0, \\ -X_0 & \text{otherwise.} \end{cases}$$

This form of selective sampling is quite useful in generating random numbers for Z . It is essentially an extension of (10.1).

1663 This scheme can be rephrased in a more interesting representation. First, define the multivariate
 1664 version of δ as

$$(14.6) \quad \boldsymbol{\delta} = (1 + \boldsymbol{\beta}^\top \bar{\Omega} \boldsymbol{\beta})^{-1/2} \bar{\Omega} \boldsymbol{\beta}, \quad (\boldsymbol{\delta} \in \mathbb{R}^d)$$

which is used to construct a $(d+1) \times (d+1)$ correlation matrix

$$\Omega^* = \begin{pmatrix} \bar{\Omega} & \boldsymbol{\delta} \\ \boldsymbol{\delta}^\top & 1 \end{pmatrix}.$$

Ω^* is used to generate two marginals, $X_0 \in \mathbb{R}^d$ and $X_1 \in \mathbb{R}$, such that

$$\begin{pmatrix} X_0 \\ X_1 \end{pmatrix} \sim \mathcal{N}_{d+1}(0, \Omega^*),$$

1665 which leads to the second representation

$$(14.7) \quad Z = \begin{cases} X_0 & \text{if } X_1 > 0, \\ -X_0 & \text{otherwise.} \end{cases}$$

1666 This form resembles (10.7). It shows that the function of $\boldsymbol{\delta}$ is to add the correlation between X_0
 1667 and X_1 through Ω^* in the selective sampling. This makes (14.7) slightly different from (14.5).

14.5. Moments

1668 The first two moments of Z have simple analytic forms. Its first moment is

$$(14.8) \quad \mu_z = \mathbb{E}(Z) = b \boldsymbol{\delta}, \quad \text{where } b = \sqrt{2/\pi}.$$

1670 The second moment is simply $\bar{\Omega}$. Its variance is

$$(14.9) \quad \Sigma_z = \text{var}\{Z\} = \bar{\Omega} - b^2 \boldsymbol{\delta} \boldsymbol{\delta}^\top.$$

1671 It is easy to obtain $\mathbb{E}\{YY^\top\} = \Omega$ for the location-scale variable Y .

1672 Define the important invariant quantity for the skewness.

$$(14.10) \quad \beta_* = (\boldsymbol{\beta}^\top \bar{\Omega} \boldsymbol{\beta})^{1/2} \geq 0,$$

1673 which is a nonnegative scalar quantity. It encapsulates the departure from normality for the distribution.
 1674

1675 The quadratic form $\mu_z^\top \Sigma_z^{-1} \mu_z$ can be simplified to

$$(14.11) \quad \mu_z^\top \Sigma_z^{-1} \mu_z = \frac{b^2 \beta_*^2}{1 + (1 - b^2) \beta_*^2}.$$

1676 A related quantity is

$$(14.12) \quad \delta_* = (\boldsymbol{\delta}^\top \bar{\Omega}^{-1} \boldsymbol{\delta})^{1/2}$$

1677 where $\delta_* \in [0, 1]$ has the scale of a positive correlation coefficient.

1678 The two are connected by

$$\delta_*^2 = \frac{\beta_*^2}{1 + \beta_*^2}, \quad \beta_*^2 = \frac{\delta_*^2}{1 - \delta_*^2}.$$

1679 Or in a trigonometric form, there exists an angle $\theta \in [0, \frac{\pi}{2})$ such that $\tan \theta = \beta_*$ and $\sin \theta = \delta_*$. In
 1680 such an expression, $\theta > 0$ captures the "degree" of departure from normality.

1681

14.6. Canonical Form

1682 The concept of a canonical form in SN is very important and fascinating. Due to the rotational
 1683 symmetry, an MSN can be rotated and rescaled to an "identity" MSN with a scalar skew parameter.

1684 By Proposition 5.12 of [1], there exists an affine transformation $Z^* = A_*(Y - \xi)$ such that $Z^* \sim$
 1685 $SN_d(0, I_d, \beta_{Z^*})$, where I_d is a $d \times d$ identity matrix, and $\beta_{Z^*} = (\beta_*, 0, \dots, 0)^\top$. β_* is defined by (14.10),
 1686 which is an invariant under transformation.

1687 The variable Z^* is called *the canonical variable*. It is d -dimensional. But only one dimension is
 1688 skew-normal, which is designated as the first dimension. All other dimensions are standard normal
 1689 distributions. That is, the PDF of Z^* is

$$\begin{aligned}\mathcal{N}_*(\mathbf{x}; \beta_*) &= 2\Phi_{\mathcal{N}}(\beta_* x_1) \prod_{i=1}^d \mathcal{N}(x_i) \\ &= \mathcal{N}(x_1; \beta_*) \prod_{i=2}^d \mathcal{N}(x_i).\end{aligned}$$

1690 This structure helps tremendously for the subsequent development of the elliptical distribution and
 1691 adaptive distribution.

1692 Proposition 5.13 in [1] describes how to find such A_* . Due to rotational symmetry, there are many
 1693 choices of A_* . This is not a problem as long as we always look at the system in quadratic form.

1694 LEMMA 14.5 (Affine Transformation). Let $C = \Omega^{1/2}$ be the unique positive definite symmetric
 1695 square root of Ω . Define $M = C^{-1}\Sigma C^{-1}$, where $\Sigma = \text{var}\{Y\}$. Let $Q\Lambda Q^\top$ denote a spectral decomposi-
 1696 tion of M , where we assume that the diagonal elements in the eigenvalue matrix Λ are arranged in
 1697 increasing order.

1698 Let $H = C^{-1}Q$. Then H is the matrix operator to convert Y to Z^* ,

$$Z^* = H^\top(Y - \xi).$$

1699 Since $\delta_{Z^*} = H^\top \omega \delta$ and $\beta_{Z^*} = \delta_{Z^*}/(1 - \delta_*^2)$, the choice of H must make the first element of δ_{Z^*}
 1700 a nonnegative number, that is, $\delta_* \geq 0$. All other elements, except the first ones in δ_{Z^*} and β_{Z^*} , must
 1701 be zero. \triangle

1702 REMARK 14.6. The significance of this lemma is that the skew-elliptical distributions derived from
 1703 the SN framework can only have a single source of skewness. It might be mixed up and not easy to
 1704 observe in real-world data. But there is only one source from the theoretical perspective. Everything
 1705 else comes from the multivariate normal distribution.

1706 If we want a more "sophisticated" distribution that provides multiple sources of skewness, we have
 1707 to go beyond the skew-elliptical distributions.

1708

14.7. 1D Marginal Distribution

1709 We are particularly interested in the 1D marginal distribution, since this is what is actually
 1710 observed in a data set. When we optimize a data fit, we can add the log-likelihood of the 1D marginal
 1711 distributions to the objective function, so that the fitting of each dimension is properly addressed.

1712 In fact, for the adaptive distribution, the full 2D likelihood is so compute-intensive that it is too
 1713 slow to perform MLE on a desktop. The alternative is to compute the sum of the log-likelihoods of
 1714 each 1D marginal distribution, in addition to the regularization on other statistical quantities, such as
 1715 the correlation coefficient between each data pair.

1716 We quote the results from Section 5.1.4 of [1] and adapt them to the 1D case.

LEMMA 14.7. (The marginal β) Assume that the marginal is on the first dimension. The correlation matrix is decomposed as

$$\bar{\Omega} = \begin{pmatrix} \bar{\Omega}_{11} & \bar{\Omega}_{12} \\ \bar{\Omega}_{21} & \bar{\Omega}_{22} \end{pmatrix}.$$

The formula can be simplified due to $\bar{\Omega}_{11} = 1$ in the 1D case.

The marginal distribution is $Y_1 \sim SN(\xi_1, \Omega_{11}, \beta_{1(2)})$. Its $\beta_{1(2)}$ is derived as

$$(14.13) \quad \beta_{1(2)} = (1 + \beta_2^\top \bar{\Omega}_{22,1} \beta_2)^{-1/2} (\beta_1 + \bar{\Omega}_{12} \beta_2)$$

where $\bar{\Omega}_{22,1} = \bar{\Omega}_{22} - \bar{\Omega}_{21} \bar{\Omega}_{12}$.

△

LEMMA 14.8. (The marginals of a bivariate distribution) The bivariate case is quite simple:

$$(14.14) \quad \bar{\Omega} = \begin{pmatrix} 1 & \rho \\ \rho & 1 \end{pmatrix}.$$

Assume that we want to get the marginal β of the i -th dimension, $\beta_{i(j)}$, where j is the other dimension. Then

$$(14.15) \quad \beta_{i(j)} = \frac{\beta_i + \rho \beta_j}{\sqrt{1 + \beta_j^2 |\bar{\Omega}|}}$$

where $|\bar{\Omega}| = 1 - \rho^2$. Since Ω_{ii} is ω_i^2 , the i -th marginal distribution is $Y_i \sim SN(\xi_i, \omega_i^2, \beta_{i(j)})$. The ξ_i and ω_i are the location and scale parameters in the i -th dimension that can be calculated directly from the data.

△

We observe that ρ in the numerator describes how much β_j is mixed with β_i , while $|\bar{\Omega}|$ in the denominator describes how much β_j reduces the scale.

When $\rho = 0$, there is no mixing from the other dimension, only a reduction in total scale. That

is, $\beta_{i(j)}|_{\rho=0} = \beta_i / \sqrt{1 + \beta_j^2}$.

CHAPTER 15

Multivariate GAS-SN Elliptical Distribution

1731 15.1. Definition

1732 This chapter follows the structure laid out in Chapter 6 of Azzalini (2013)[1]. We implemented
 1733 the skew-elliptical distribution by our $\bar{\chi}_{\alpha,k}$, which fully extends his multivariate skew-t distribution.

1734 DEFINITION 15.1. Assume $Z_0 \sim SN_d(0, \bar{\Omega}, \beta)$ is a $d \times d$ standard multivariate skew-normal (SN)
 1735 distribution, and $V \sim \bar{\chi}_{\alpha,k}$ is a standard FCM. $\bar{\Omega}$ is a correlation matrix.

1736 Then $Z \sim Z_0/V$ is a $d \times d$ standard multivariate GAS-SN elliptical distribution. It is given the
 1737 notation of $Z \sim L_{\alpha,k}(0, \bar{\Omega}, \beta)$.

1738 Equivalently, using the location-scale notation, $Z \sim SN_d(0, \Sigma, \beta)$ where $\Sigma = \bar{\Omega}/V^2$.

1740 Assume $\mathcal{N}_d(\mathbf{x}; \bar{\Omega}, \beta)$ is the PDF of a standard multivariate normal distribution $\mathcal{N}_d(0, \bar{\Omega})$ [32].
 1741 $\Phi_{\mathcal{N}}(x)$ is the CDF of a standard normal distribution.

1742 We expand on the construction of multivariate SN distribution in (14.1) and (14.2). And the PDF
 1743 of $Z \sim L_{\alpha,k}(0, \bar{\Omega}, \beta)$ is

$$(15.1) \quad \begin{aligned} L_{\alpha,k}(\mathbf{x}; \bar{\Omega}, \beta) &= \int_0^\infty ds \bar{\chi}_{\alpha,k}(s) s^d \mathcal{N}_d(\mathbf{x}s; \bar{\Omega}, \beta) \\ &= 2 \int_0^\infty ds \bar{\chi}_{\alpha,k}(s) s^d \mathcal{N}_d(\mathbf{x}s; \bar{\Omega}) \Phi_{\mathcal{N}}(\beta^\top \mathbf{x} s). \end{aligned}$$

1744 The s^d term comes from $\det(s\mathbf{I}_d)$ where \mathbf{I}_d is the $d \times d$ identity matrix. It is easy to see how it is
 1745 reduced to a univariate GAS-SN distribution when $d = 1$.

1746 **15.1.1. Multivariate Skew-t Distribution.** An important bridge between multivariate SN and
 1747 GAS-SN is the multivariate skew-t distribution. It is documented in Section 6.2 of [1].

1748 It is fully consistent with multivariate GAS-SN by setting $\alpha = 1$. That is, in his notation of skew-t:
 1749 $ST_d(\Omega, \beta, k) \sim L_{1,k}(\Omega, \beta)$.

1750 15.2. Location-Scale Family

1751 The location-scale family follows the standard procedure: $Y = \xi + \omega Z$, which is denoted as
 1752 $Y \sim L_{\alpha,k}(\xi, \Omega, \beta)$, where $\Omega := \omega^\top \bar{\Omega} \omega$ is the covariance matrix, and ω is a $d \times d$ diagonal scale matrix.
 1753 The PDF of Y is

$$(15.2) \quad L_{\alpha,k}(\mathbf{x}; \xi, \Omega, \beta) := \det(\omega)^{-1} L_{\alpha,k}(\mathbf{z}; \bar{\Omega}, \beta)$$

1754 where $\mathbf{z} := \omega^{-1}(\mathbf{x} - \xi)$. Notice that it has to be computed via the standard PDF.

1755 15.3. Moments

1756 The first moment of Z is $\mu_z := b\delta$, where $b := \sqrt{2/\pi} \mathbb{E}(X^{-1}|\bar{\chi}_{\alpha,k})$.

1757 The second moment of Z is $m_2 \bar{\Omega}$, where $m_2 = \mathbb{E}(X^{-2}|\bar{\chi}_{\alpha,k})$. Hence, the covariance is

$$\text{var}\{Z\} := \Sigma_z := m_2 \bar{\Omega} - b^2 \delta \delta^\top$$

1758 The moments of Y follow the rule of the location-scale family. The first moment of Y is $\boldsymbol{\xi} + \boldsymbol{\omega} \mu_z$.
 1759 The covariance of Y is $\boldsymbol{\omega} \Sigma_z \boldsymbol{\omega}$.

1760 15.4. Canonical Form

1761 The concept of canonical form in GAS-SN is extended from the multivariate SN in Section 14.6.
 1762 There exists an affine transformation $Z^* = A_*(Y - \boldsymbol{\xi})$ such that $Z^* \sim L_{\alpha,k}(0, \mathbf{I}_d, \boldsymbol{\beta}_{Z^*})$, where $\boldsymbol{\beta}_{Z^*} =$
 1763 $(\beta_*, 0, \dots, 0)^\top$ and β_* is defined by (14.10). And the algorithm of finding A_* is exactly the same as in
 1764 Section 14.6.

1765 The variable Z^* , which is called *canonical variable*, comprises d independent components. Only
 1766 one of them contains the skew component. That is, the PDF of Z^* is

$$(15.3) \quad L_{\alpha,k_*}(\mathbf{x}; \beta_*) = 2 \int_0^\infty ds \bar{\chi}_{\alpha,k}(s) s^d \prod_{i=1}^d \mathcal{N}(x_i s) \Phi_N(\beta_* x_1 s).$$

1767 It can be further simplified to an elegant univariate-style integral. When $|\mathbf{x}| \neq 0$, let $\beta_*(\mathbf{x}) :=$
 1768 $\beta_* x_1 / |\mathbf{x}| \in \mathbb{R}$, and

$$(15.4) \quad L_{\alpha,k_*}(\mathbf{x}; \beta_*) = (2\pi)^{-(d-1)/2} \int_0^\infty ds \bar{\chi}_{\alpha,k}(s) s^d \mathcal{N}(|\mathbf{x}|s; \beta_*(\mathbf{x})).$$

1769 When $|\mathbf{x}| = 0$, It is simply

$$(15.5) \quad L_{\alpha,k_*}(0; \beta_*) = (2\pi)^{-d/2} \mathbb{E}(X^d | \bar{\chi}_{\alpha,k}),$$

1770 independent of β_* .

1771 15.5. Marginal 1D Distribution

1772 The construction of the 1D marginal distribution from Y extends directly from Section 14.7, where
 1773 $\beta_{1(2)}$ is calculated.
 1774 Then the marginal distribution is an univariate GAS-SN: $Y_1 \sim L_{\alpha,k}(\xi_1, \Omega_{11}, \beta_{1(2)})$.

1775 15.6. Quadratic Form

1776 The quadratic form is

$$(15.6) \quad Q := \frac{1}{d} (\mathbf{Y} - \boldsymbol{\xi})^\top \Omega^{-1} (\mathbf{Y} - \boldsymbol{\xi}) = \frac{1}{d} \mathbf{Z}^\top \bar{\Omega}^{-1} \mathbf{Z}.$$

1777 This leads to the fractional extension of the classic F distribution.

1778 Q distributes like a fractional F distribution, $Q \sim F_{\alpha,d,k}$ for all β . The QQ-plot between the
 1779 empirical data and theoretical values is used to evaluate the goodness of a fit. A perfect fit should
 1780 produce a 45-degree line.

1781 To prove, from Section 15.1, we have $Z \sim Z_0/V$, $Z_0 \sim SN_d(0, \bar{\Omega}, \boldsymbol{\beta})$, and $V \sim \bar{\chi}_{\alpha,k}$. Put them
 1782 together,

$$Q = \frac{1}{d} \mathbf{Z}^\top \bar{\Omega}^{-1} \mathbf{Z} = \frac{\mathbf{Z}_0^\top \bar{\Omega}^{-1} \mathbf{Z}_0}{d V^2} \sim \left(\frac{X^2}{d} \right) / V^2$$

1783 where $X \sim \mathcal{N}_d(0, \bar{\Omega})$, according to Lemma 14.4.

1784 Since $X^2 \sim \chi_d^2$ and $V^2 \sim \bar{\chi}_{\alpha,k}^2$, this leads to $Q \sim F_{\alpha,d,k}$, according to Section 8.1.

1785 Azzalini (2013) provided a point of validation from his multivariate skew-t distribution. From
 1786 Section 6.2 of [1], Q of a skew-t variable distributes like the classic $F(d, k)$. This is a special case of
 1787 our fractional F distribution at $\alpha = 1$. That is, $Q \sim F_{1,d,k}$.

1788

15.7. Multivariate MLE

1789

TODO write better

1790

A stochastic gradient decent (SGD) method on the maximum likelihood estimation (MLE) can be implemented efficiently. First, we calculate the sum of the minus-log of the PDF evaluated at every data point. This sum is called MLLK. Then we calculate the gradients for each hyperparameter. And make a small move along the direction that is most likely to minimize the MLLK. The scale of the move is based on a learning rate, which can be adjusted dynamically. Some randomness can be added to the small move. This allows the algorithm to explore the nearby regions, and maybe get "unstuck" over unexpected edges.

1797

Use the bivariate optimization as an example. The hyperparameter space is

$$\Theta = \{\rho, \alpha, k, \beta_1, \beta_2, w_1, w_2, \xi_1, \xi_2\}$$

1798

where $\alpha \in (0, 2)$, $k \in (2, \infty)$, $w_1 > 0$, $w_2 > 0$, and $\beta_1, \beta_2, \xi_1, \xi_2 \in \mathbb{R}$. Since $\rho \in (-1, 1)$, it is preferred to use a transformed parameter $\rho_\theta = \arctan(\rho/\pi) \in \mathbb{R}$.

1800

It is also found that each dimension in the data set should be normalized to one standard deviation. This allows all the gradients to have similar scales. This helps the SGD algorithm.

1802

Let Y represent the data set of size N , and $L(Y_i; \Theta)$ is the PDF, then

$$\begin{aligned} \text{MLLK}(\Theta; Y) &:= -\sum_{i=1}^N \log L(Y_i; \Theta) \\ \text{Gradient}(\Theta) &:= \left\{ \frac{\partial \text{MLLK}(\Theta; Y)}{\partial \Theta_j}, \forall \Theta_j \in \Theta \right\} \end{aligned}$$

1803

When N is large, it may not be computationally feasible to evaluate every $L(Y_i; \Theta)$. One may use histogram to compress the data into smaller numbers of bins.

1805

Regularization can be added to the MLLK. For instance, we find it makes a lot of sense to add the L2 distances of the skewness and kurtosis on the marginal 1D distributions.

CHAPTER 16

Multivariate GAS-SN Adaptive Distribution (Experimental)

16.1. Definition

The goal of an adaptive distribution is to allow each dimension to have its own shape parameter in α, k . This is the departure from the the elliptical distribution.

Therefore, $\boldsymbol{\alpha} = \{\alpha_i\}$ is a d -dimensional vector, so is $\mathbf{k} = \{k_i\}$. We now have a list of standard FCM to work with: $\{\bar{\chi}_{\alpha_i, k_i}, i \in 1, 2, \dots, d\}$.

DEFINITION 16.1. Assume Z_0 is a d -dimensional random variable from a standard $d \times d$ multivariate skew-normal (SN) distribution, $SN_d(0, \bar{\Omega}, \boldsymbol{\beta})$, where $\bar{\Omega}$ is a correlation matrix.

Let Z be a d -dimensional random variable. Each element is a ratio distribution such as $Z_i \sim (Z_0)_i / \bar{\chi}_{\alpha_i, k_i}$. Then $Z \sim \vec{L}_{\boldsymbol{\alpha}, \mathbf{k}}(0, \bar{\Omega}, \boldsymbol{\beta})$ is a standard multivariate GAS-SN adaptive distribution. The arrow-over sign is to emphasize the vector nature of $(\boldsymbol{\alpha}, \mathbf{k})$.

Assume $\mathcal{N}(x; \bar{\Omega})$ is the PDF of a standard multivariate normal distribution $N(0, \bar{\Omega})$ [32]. $\Phi_{\mathcal{N}}(x)$ is the CDF of a standard normal distribution.

The PDF of $Z \sim \vec{L}_{\boldsymbol{\alpha}, \mathbf{k}}(0, \bar{\Omega}, \boldsymbol{\beta})$ is

$$(16.1) \quad \vec{L}_{\boldsymbol{\alpha}, \mathbf{k}}(\mathbf{x}; \bar{\Omega}, \boldsymbol{\beta}) = 2 \int \cdots \int_0^\infty \mathcal{N}(\mathbf{s} \mathbf{x}; \bar{\Omega}) \Phi_{\mathcal{N}}(\boldsymbol{\beta}^\top(\mathbf{s} \mathbf{x})) \prod_{i=1}^d s_i ds_i \bar{\chi}_{\alpha_i, k_i}(s_i).$$

where $\mathbf{s} := \text{diag}(s_1, \dots, s_d)$ is the $d \times d$ diagonal matrix from the vector $\{s_i\}$. It is easy to see how it is reduced to a univariate GAS-SN distribution when $d = 1$.

Compared to the elliptical PDF (15.1), the major difference is that (16.1) is a d -dimensional integral. This is much more computationally demanding.

16.2. Location-Scale Family

The location-scale family follows the standard procedure: $Y = \boldsymbol{\xi} + \boldsymbol{\omega}Z$, which is denoted as $Y \sim \vec{L}_{\boldsymbol{\alpha}, \mathbf{k}}(\boldsymbol{\xi}, \Omega, \boldsymbol{\beta})$. The covariance matrix is $\Omega = \boldsymbol{\omega}^\top \bar{\Omega} \boldsymbol{\omega}$, and $\boldsymbol{\omega}$ is the $d \times d$ diagonal scale matrix.

The PDF of Y is

$$(16.2) \quad \vec{L}_{\boldsymbol{\alpha}, \mathbf{k}}(\mathbf{x}; \boldsymbol{\xi}, \Omega, \boldsymbol{\beta}) := \det(\boldsymbol{\omega})^{-1} \vec{L}_{\boldsymbol{\alpha}, \mathbf{k}}(\mathbf{z}; \bar{\Omega}, \boldsymbol{\beta}).$$

where $\mathbf{z} := \boldsymbol{\omega}^{-1}(\mathbf{x} - \boldsymbol{\xi})$. Notice that it has to be computed via the standard PDF because the mixtures $\{s_i\}$ must work with the standardized variable Z , not the location-scale variable Y .

16.3. Moments

The first moment of Z is $\mu_z := \mathbf{b} \odot \boldsymbol{\delta}$, where $b_i := \sqrt{2/\pi} \mathbb{E}(X^{-1} | \bar{\chi}_{\alpha_i, k_i})$ and \odot is the Hadamard product.

The (i, j) element of the second moment of Z is

$$\mathbf{m}_2(i, j) := \begin{cases} \mathbb{E}(X^{-2} | \bar{\chi}_{\alpha_i, k_i}) & \text{if } i = j, \\ \bar{\Omega}_{i,j} \mathbb{E}(X^{-1} | \bar{\chi}_{\alpha_i, k_i}) \mathbb{E}(X^{-1} | \bar{\chi}_{\alpha_j, k_j}) & \text{if } i \neq j. \end{cases}$$

1836 where $\bar{\Omega}_{i,i} = 1$ is ignored in the first line. Hence, the covariance is

$$\text{var}\{Z\} := \Sigma_z := \mathbf{m}_2 - \mu_z \mu_z^\top$$

1837 The moments of Y follow the rule of the location-scale family. The first moment of Y is $\xi + \omega \mu_z$.
 1838 The covariance of Y is $\omega \text{var}\{Z\} \omega$.

1839 16.4. Canonical Form

1840 The adaptive distribution *doesn't* enjoy the rotational symmetry that an elliptical distribution has.
 1841 Its canonical form is *not* particularly useful, since it has no connection to other distributions in the
 1842 family through an affine transformation.

1843 Assume the variable Z^* is a *canonical variable*. Then $Z^* \sim \vec{L}_{\alpha, k}(0, \mathbf{I}_d, \beta_{Z^*})$, where $\beta_{Z^*} =$
 1844 $(\beta_*, 0, \dots, 0)^\top$ and β_* is defined by (14.10).

1845 The PDF of Z^* is

$$(16.3) \quad \vec{L}_{\alpha, k_*}(\mathbf{x}; \beta_*) = L_{\alpha_1, k_1}(x_1; \beta_*) \prod_{j=2}^d L_{\alpha_j, k_j}(x_j).$$

1846 We can clearly see that only the first component is GAS-SN, all other components are GSaS, each
 1847 with its own (α, k) shape.

1848 Only the first component of its μ_z is non-zero, which is $\sqrt{2/\pi} \delta_* \mathbb{E}(X^{-1} | \bar{\chi}_{\alpha_1, k_1})$. Its \mathbf{m}_2 is a
 1849 diagonal matrix where $\mathbf{m}_2(i, i) = \mathbb{E}(X^{-2} | \bar{\chi}_{\alpha_i, k_i})$.

1850 16.5. Marginal 1D Distribution

1851 The construction of the 1D marginal distribution from Y extends directly from Section 14.7, where
 1852 $\beta_{1(2)}$ is calculated.

1853 Then the marginal distribution is an univariate GAS-SN: $Y_1 \sim L_{\alpha_1, k_1}(\xi_1, \Omega_{11}, \beta_{1(2)})$.

1854 16.6. Quadratic Form

1855 TODO The corresponding F distribution is very hard. I have not figured this out yet.

1856 16.7. 2D Adaptive MLE

1857 TODO this needs more refinement since a normal 2D MLE doesn't work here.

1858 TODO I am still working on the numerical method.

1859 A stochastic gradient decent (SGD) method on the maximum likelihood estimation (MLE) can be
 1860 implemented, but some adjustments are needed. Use the bivariate optimization as an example. The
 1861 hyperparameter space is

$$\Theta = \{\rho, \alpha_1, \alpha_2, k_1, k_2, \beta_1, \beta_2, w_1, w_2, \xi_1, \xi_2\}$$

1862 where $\alpha_1, \alpha_2 \in (0, 2)$, $k_1, k_2 \in (2, \infty)$, $w_1 > 0$, $w_2 > 0$, and $\beta_1, \beta_2, \xi_1, \xi_2 \in \mathbb{R}$. Since $\rho \in (-1, 1)$, it is
 1863 preferred to use a transformed parameter $\rho_\theta = \arctan(\rho/\pi) \in \mathbb{R}$.

1864 The computation of the adaptive PDF is very slow on a desktop, even for two dimensions. The
 1865 MLLK is modified to perform on the two marginal 1D distributions. We supplement it with a regu-
 1866 larization on the L2 distance of the correlation coefficient.

1867 It is also found that each dimension in the data set should be normalized to one standard deviation.
 1868 This allows all the gradients to have similar scales. This helps the SGD algorithm.

1869 Let Y represent the data set of size N , and $L_m(Y_i; \Theta)$ is the marginal 1D PDF at dimension m
 1870 ($m = 1 \dots d$), then

$$\text{MLLK}(\Theta; Y) := - \sum_{i=1}^N \sum_{m=1}^d \log L_m(Y_i; \Theta)$$

$$\text{Gradient}(\Theta) := \left\{ \frac{\partial \text{MLLK}(\Theta; Y)}{\partial \Theta_j}, \forall \Theta_j \in \Theta \right\}$$

1871 Once the MLLK and gradients are calculated. The program makes a small move along the direction
 1872 that is most likely to minimize the MLLK. The scale of the move is based on a learning rate, which
 1873 can be adjusted dynamically. Some randomness can be added to the small move. This allows the
 1874 algorithm to explore the nearby regions, and maybe get "unstuck" over unexpected edges.

1875 When N is large, it may not be computationally feasible to evaluate every $L(Y_i; \Theta)$. One may use
 1876 histogram to compress the data into smaller numbers of bins.

1877 More regularization can be added to the MLLK. For instance, we find it makes a lot of sense to
 1878 add the L2 distances of the skewness and kurtosis on the marginal 1D distributions.

1879 We also regulate the mean of the quadratic form. But the exact distribution of the quadratic form
 1880 is still under research.

CHAPTER 17

1881 Fitting SPX-VIX Daily Returns with Bivariate Distributions

1882 Two MLE fits are performed for the VIX/SPX daily log returns from 1990 to 2025. The first fit
 1883 uses the bivariate elliptical GAS-SN distribution. The second fit uses the bivariate adaptive GAS-SN
 1884 distribution.

1885 The major difference is that the adaptive distribution allows each dimension to have its own (α, k)
 1886 shape. However, it is much more compute-intensive, it requires alternative methods to work around.
 1887 And it breaks the rotational symmetry that the elliptical distribution has. This requires a different
 1888 approach to evaluate the quadratic form.

1889 17.1. Elliptical Fit

1890 The bivariate elliptical MLE program is similar to the univariate MLE program. But the hyper-
 1891 parameter space is much larger:

$$\Theta = \{\rho, \alpha, k, \beta_1, \beta_2, w_1, w_2, \xi_1, \xi_2\}$$

1892 where $\alpha \in (0, 2)$, $k \in (2, \infty)$, $w_1 > 0$, $w_2 > 0$, and $\beta_1, \beta_2, \xi_1, \xi_2 \in \mathbb{R}$. ρ is the correlation coefficient.
 1893 Since $\rho \in (-1, 1)$, it is preferred to use a transformed parameter $\rho_\theta = \arctan(\rho/\pi) \in \mathbb{R}$. In the
 1894 program, ρ is converted to $\bar{\Omega}$ according to (14.14).

1895 The bivariate MLE program is implemented in **python** and **scipy** on github at https://github.com/slihn/gas-impl/blob/main/gas_impl/mle_gas_sn_2d.py.

1896 We run the MLE fitting on the daily returns of VIX and SPX from 1990 to mid-2025, about 8900
 1897 two-column samples. Each column in the data set is normalized to one standard deviation. This allows
 1898 all gradients to have similar scales and helps the MLE to operate smoothly.

1899 Assume there are N samples in the data set, $Y = \{\mathbf{y}_i, i \in 1, 2, \dots, N\}$, the minus log-likelihood
 1900 (MLLK) is

$$(17.1) \quad \text{MLLK}(\Theta) = -\frac{1}{N} \sum_{i=1}^N \log(L_{\alpha,k}(\mathbf{y}_i; \boldsymbol{\xi}, \Omega, \boldsymbol{\beta}))$$

1902 where $L_{\alpha,k}(\mathbf{x}; \boldsymbol{\xi}, \Omega, \boldsymbol{\beta})$ is the multivariate PDF of the location scale family (15.2).

1903 When N is large, it may not be computationally feasible to compute the PDF on every \mathbf{y}_i . A
 1904 histogram may be used to compress the data into a grid of bins.

1905 Two components of regularization are added to the objective function $\ell(\Theta)$. The L2 distances
 1906 between the empirical and theoretical statistics are added as follows:

- 1907 • Correlation: $|\Delta\rho(Y)|^2$.
- 1908 • The mean of the quadratic form: $\Delta\mu_Q^2 := |\Delta\text{mean}(Q)|^2$. Section 15.6.

1909 MLE seeks the optimal Θ that minimizes the objective function:

$$(17.2) \quad \hat{\Theta} = \operatorname{argmin} \ell(\Theta)$$

$$(17.3) \quad \text{where } \ell(\Theta) = \text{MLLK}(\Theta) + |\Delta\rho(Y)|^2 + \Delta\mu_Q^2$$

1910 **17.1.1. The VIX-SPX Bivariate Elliptical Fit.** Figure 17.1 shows the results of the bivariate
 1911 elliptical MLE fit on the VIX/SPX daily log returns. The top two graphs show the 2D scatter plot
 1912 (left) and the contour plot (right) of the samples. Two overlapping lines are drawn to indicate the
 1913 angles of the correlation, theoretical vs. empirical. The main accomplishment of this fit is that the
 1914 correlation coefficient matches nicely at about -0.7.

1915 The contour plot is compared to the theoretical elliptical contour plot in the middle left graph.
 1916 We note that the sample contours look rectangular instead of elliptical. This is an important research
 1917 topic left for the future.

1918 The remaining three graphs are for the quadratic form Q in (15.6). The PP-plot in the middle
 1919 right graph and the QQ-plot in log scale in the bottom right graph show very good match with a clear
 1920 45-degree line.

1921 However, the QQ-plot in the bottom left graph is less ideal. The tail is tilted upward after 20.
 1922 This indicates a poor fit on the outside of the contours. This is probably due to the fact that an
 1923 elliptical distribution could not capture the rectangular nature of the contours.

1924 **17.1.2. The Issue in Marginal Distributions.** One major issue with the fit is related to
 1925 the 1-dimensional marginals. The bivariate MLE finds the best fit at $\alpha = 0.75, k = 4.5$. This is a
 1926 strange place when we examine it in Figure 12.1. When the bivariate distribution is projected to the
 1927 1-dimensional marginal distributions according to Section 15.5, the univariate GAS-SN distributions
 1928 are near the border of infinite kurtosis.

1929 (The reader is reminded that the degrees of freedom need to be higher than 4 to have valid kurtosis
 1930 in the Student's t distribution. $k = 4.5$ is in the neighborhood of that threshold.)

1931 Despite the fact that the kurtoses are very off, the graphs in Figures 17.2 and 17.3 generally
 1932 look good except for one area: We notice a problem in the top right graphs. On the one hand, the
 1933 theoretical peak in the VIX marginal PDF is higher than the observed peak. On the other hand, the
 1934 theoretical peak in the SPX marginal PDF is lower than the observed peak.

1935 The guess is that this problem in peak densities has something to do with the different shape
 1936 parameters (α, k) required for VIX and SPX. However, this is impossible with the current structure of
 1937 the elliptical distribution. It is an open question how to inject different α 's and k 's for each dimension.

1938 In summary, it is obviously too naive to think that a single bivariate distribution can describe 35
 1939 years of history in the SPX and VIX data. More research remains to be done. A major step forward
 1940 is to apply this distribution in regime-switching models, such as the Hidden Markov Model (HMM),
 1941 statistical jump model[29], and mixture-VAE model[23].

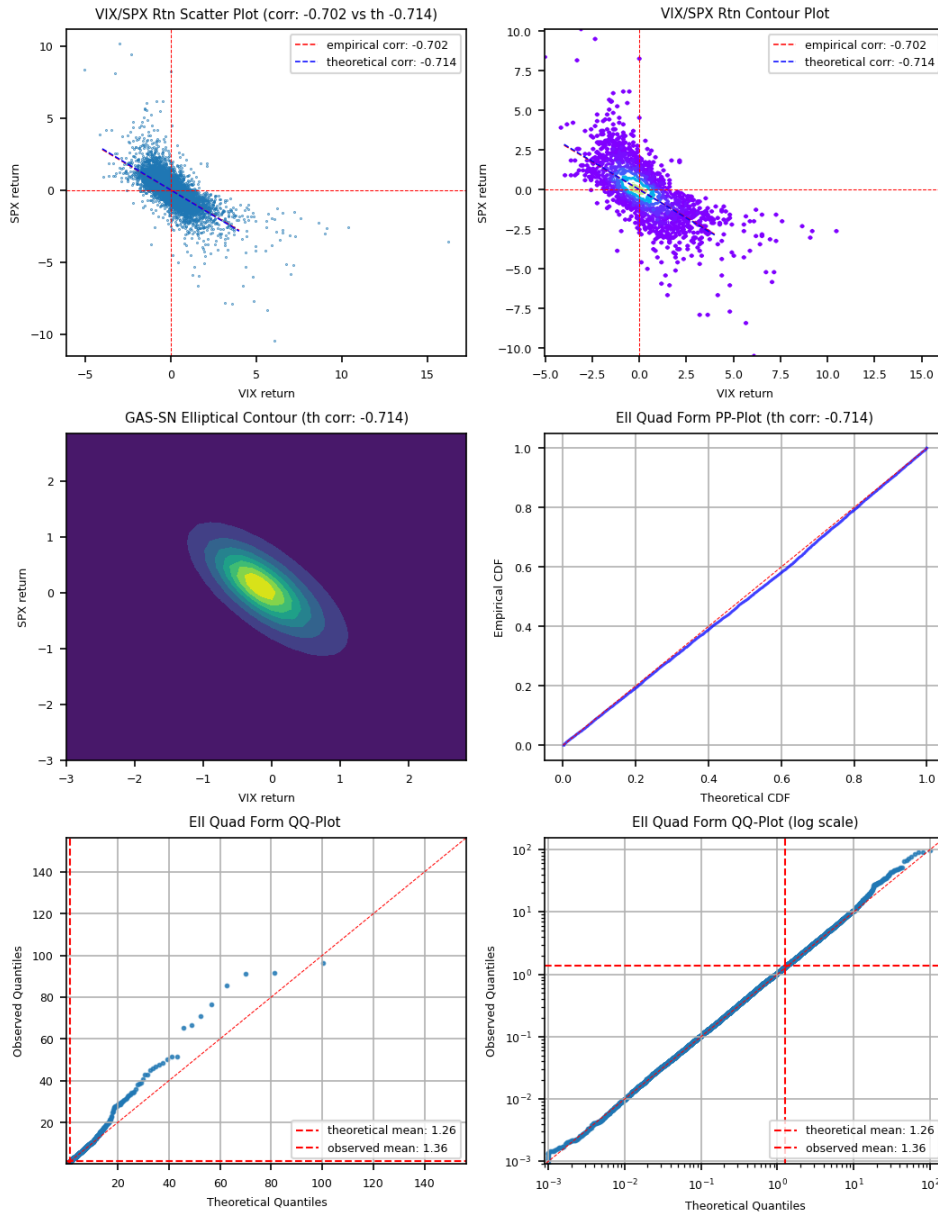


FIGURE 17.1. Elliptical MLE fit of VIX/SPX daily log returns from 1990 to 2025 with the bivariate elliptical GAS-SN distribution. Data is standardized to one standard deviation on each axis. The optimal parameters are: $\hat{\Theta} = \{\rho_\theta = -2.12, \alpha = 0.75, k = 4.5, \beta_0 = 0.78, \beta_1 = 0.27, \omega_0 = 0.92, \omega_1 = 0.88, \xi_0 = -0.35, \xi_1 = 0.19\}$.

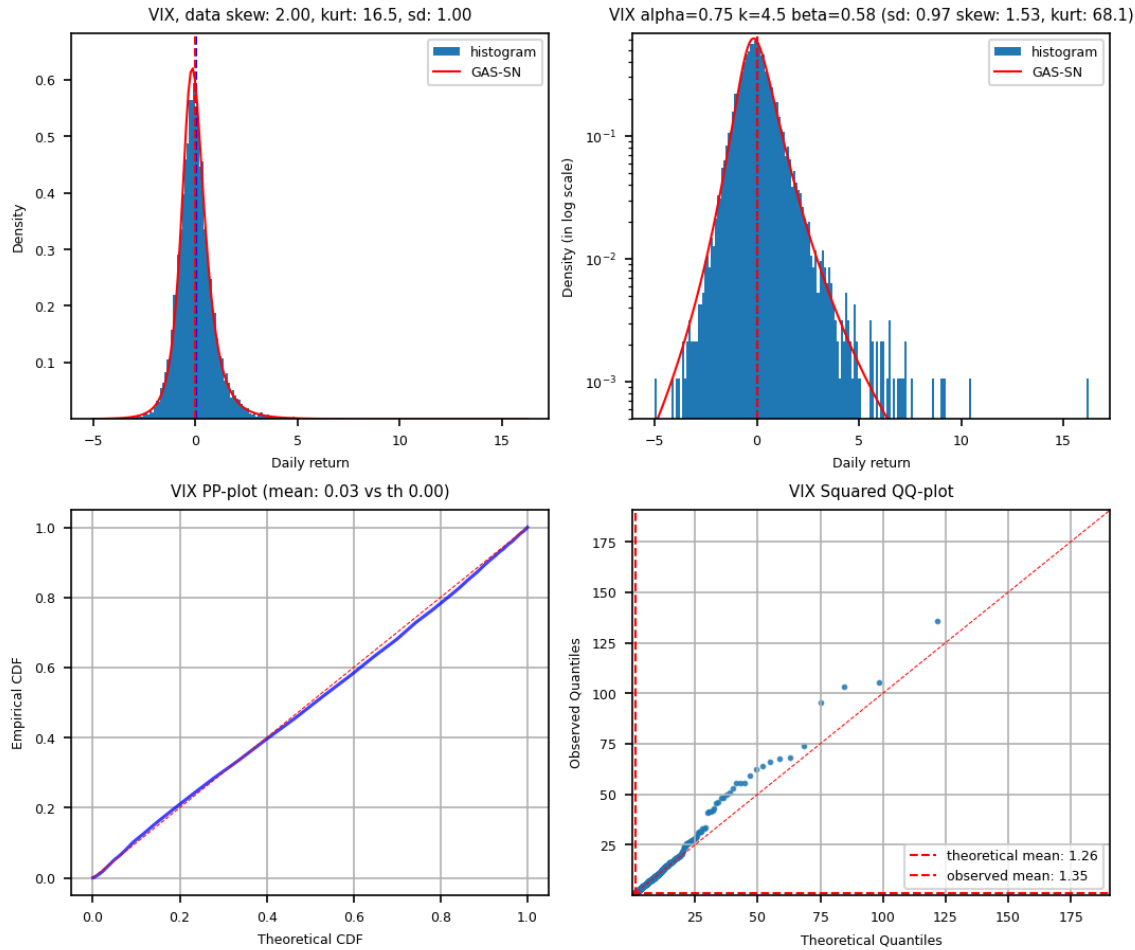


FIGURE 17.2. VIX Marginal from Elliptical MLE fit of VIX/SPX daily log returns from 1990 to 2025 with the bivariate elliptical GAS-SN distribution. Data is standardized to one standard deviation on each axis.

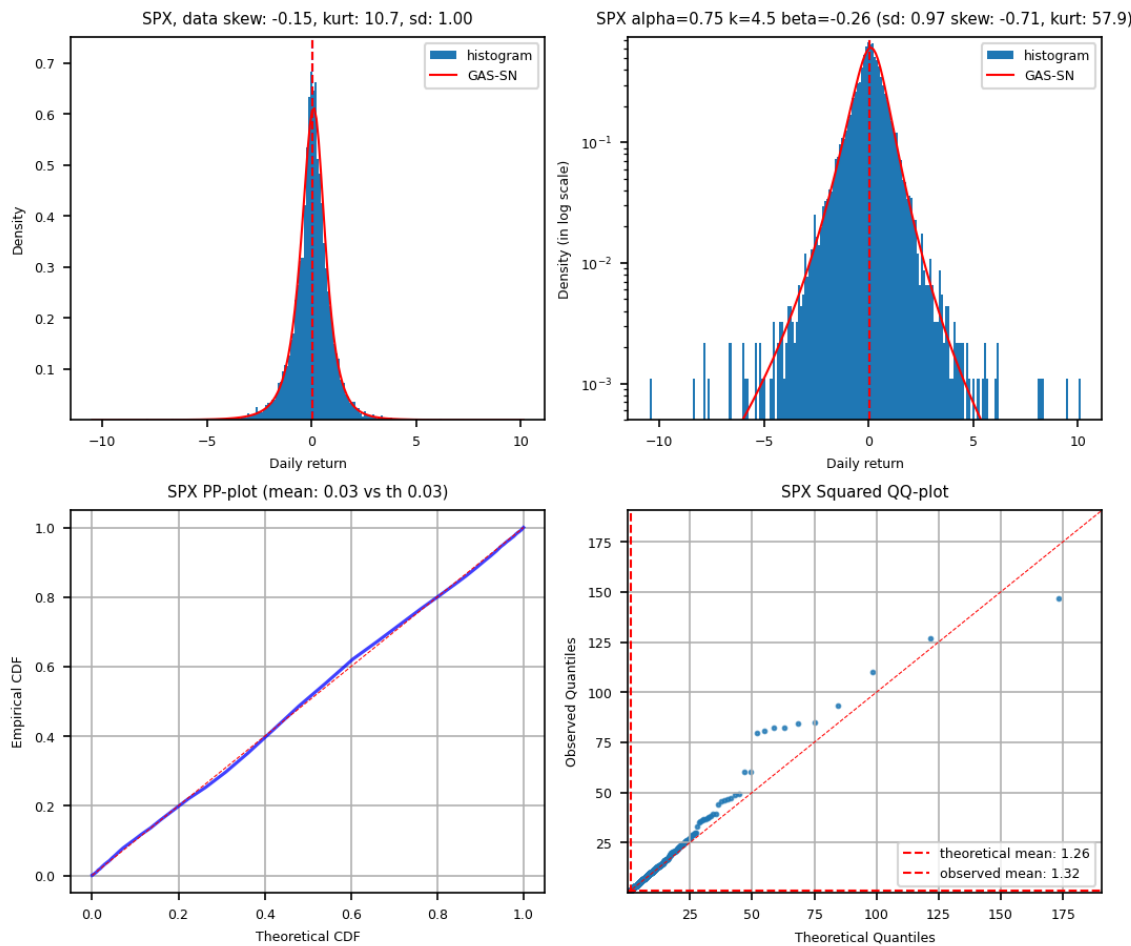


FIGURE 17.3. SPX Marginal from Elliptical MLE fit of VIX/SPX daily log returns from 1990 to 2025 with the bivariate elliptical GAS-SN distribution. Data is standardized to one standard deviation on each axis.

1942

17.2. Adaptive Fit

1943 The adaptive fit is done by MLE on the two marginal distributions with regularization, e.g. the
1944 L2 distance between the empirical and theoretical correlations. This is a hack since a direct bivariate
1945 MLE is computationally infeasible on my workstation.

1946 The adaptive fit produces the contour plot with somewhat rectangular shapes. That is quite
1947 impressive.

1948 The theoretical correlation gets to -0.5, but unable to be closer to the empirical correlation of -0.7.

1949 One would think the adaptive distribution allows each dimension to express its own shape. It
1950 should be much easier to produce a good fit. But the interaction between the correlation parameter
1951 and the skew parameters is quite complicated.

1952 It is difficult to get the skewness and kurtosis to match in the SPX marginal. It is very complex
1953 to navigate the region near $\alpha \approx 1, k \approx 3$. In the Student's t distribution, the skewness and kurtosis
1954 are not defined.

1955 The quadratic form needs a multiplier (scale adjustment) to produce a good fit. The origin of this
1956 multiplier requires further study.

1957 In the squared QQ plots of the marginals, the fits don't capture the tails as good as the elliptical
1958 fits. This is somewhat disappointing.

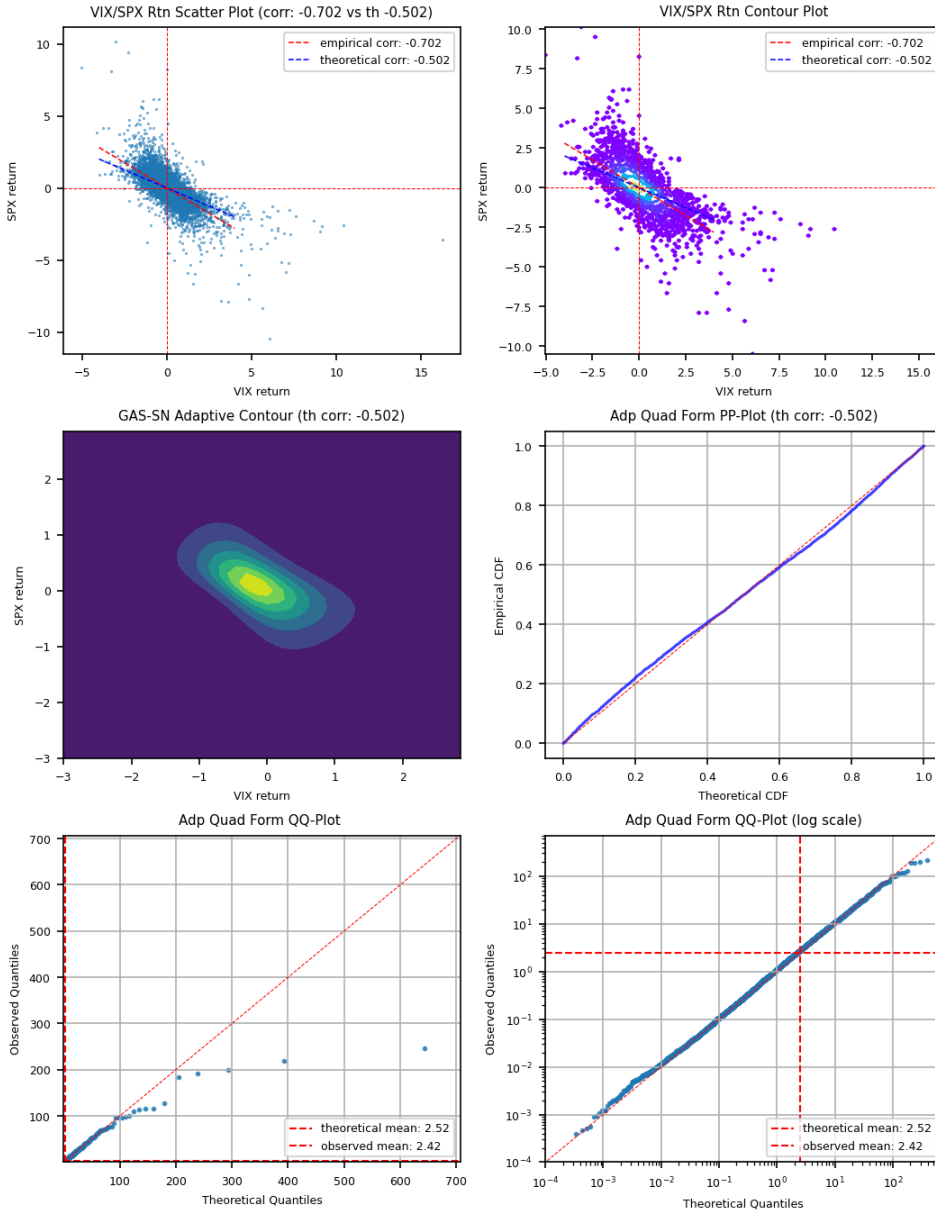


FIGURE 17.4. MLE fit of VIX/SPX daily log returns from 1990 to 2025 with the bivariate adaptive distribution. Data is standardized to one standard deviation on each axis.

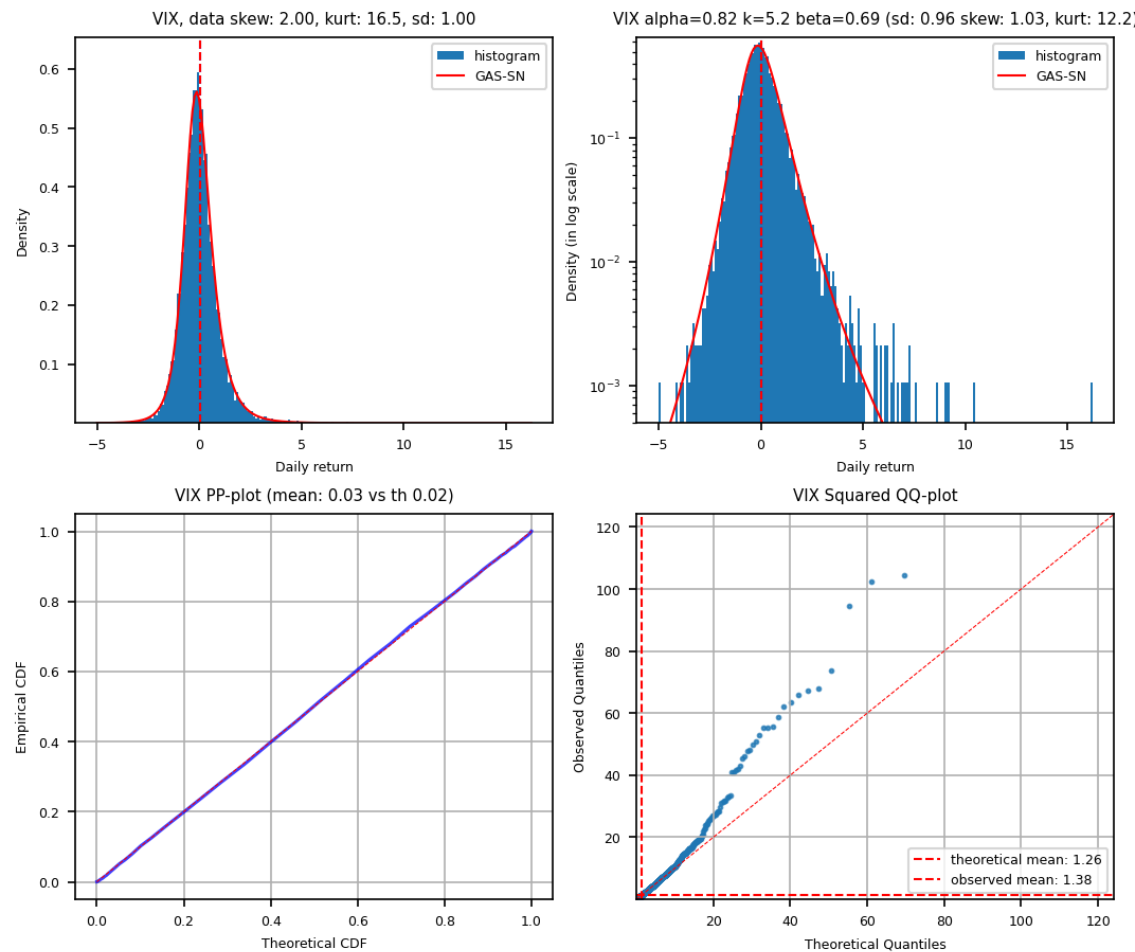


FIGURE 17.5. VIX Marginal from MLE fit of VIX/SPX daily log returns from 1990 to 2025 with the bivariate adaptive GAS-SN distribution. Data is standardized to one standard deviation on each axis.

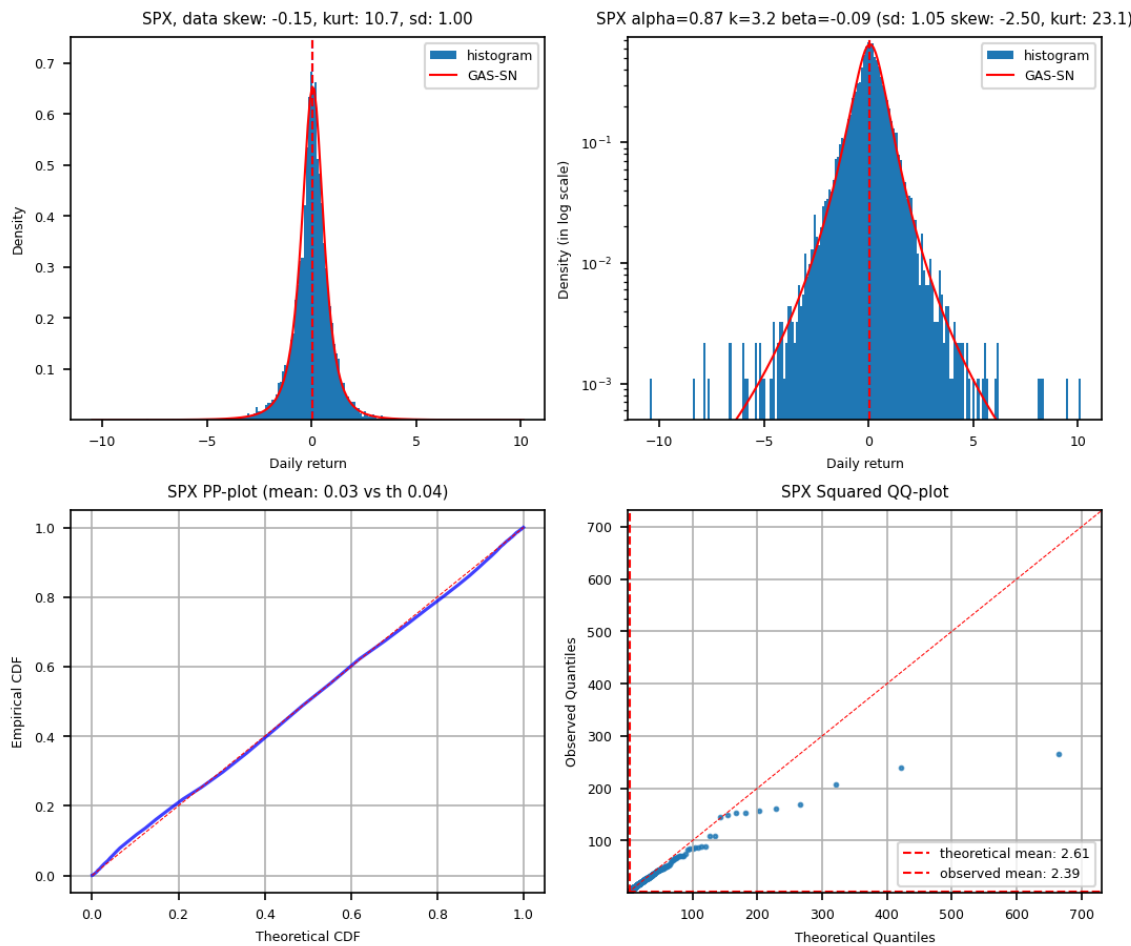


FIGURE 17.6. SPX Marginal from MLE fit of VIX/SPX daily log returns from 1990 to 2025 with the bivariate adaptive GAS-SN distribution. Data is standardized to one standard deviation on each axis.

APPENDIX A

1959

List of Useful Formula

1960

A.1. Gamma Function

1961 Gamma function is used extensively in this paper. First, note that $\Gamma(\frac{1}{2}) = \sqrt{\pi}$. Its **reflection**
 1962 **formula is**

$$(A.1) \quad \Gamma(z)\Gamma(1-z) = \frac{\pi}{\sin(\pi z)}$$

1963 And the **Legendre duplication formula** is

$$(A.2) \quad \Gamma(z)\Gamma(z+1/2) = 2^{1-2z}\sqrt{\pi}\Gamma(2z)$$

1964 **Gamma function Asymptotic:** At $x \rightarrow 0$, gamma function becomes

$$(A.3) \quad \lim_{x \rightarrow 0} \Gamma(x) \sim \frac{1}{x}$$

$$\lim_{x \rightarrow 0} \frac{\Gamma(ax)}{\Gamma(bx)} = \frac{b}{a} \quad (ab \neq 0)$$

1965 For a very large x , assume a, b are finite,

$$(A.4) \quad \lim_{x \rightarrow \infty} \frac{\Gamma(x+a)}{\Gamma(x+b)} \sim x^{a-b}$$

1966 **Sterling's formula** is used to expand the kurtosis formula for a large k , which is:

$$(A.5) \quad \lim_{x \rightarrow \infty} \Gamma(x+1) \sim \sqrt{2\pi x} \left(\frac{x}{e}\right)^x,$$

$$(A.6) \quad \text{or } \lim_{x \rightarrow \infty} \Gamma(x) \sim \sqrt{2\pi} x^{x-1/2} e^{-x}.$$

1967

A.2. Transformation

1968 Laplace transform of cosine is¹

$$(A.7) \quad \int_0^\infty dt \cos(xt)e^{-t/\nu} = \frac{\nu^{-1}}{x^2 + \nu^{-2}} = \frac{\nu}{(\nu x)^2 + 1}$$

1969 Gaussian transform of cosine is²

$$(A.8) \quad \int_0^\infty dt \cos(xt) e^{-t^2/2} = \sqrt{\frac{\pi}{2}} e^{-x^2/2}$$

Hence $\int_0^\infty dt \cos(xt) e^{-t^2/2s^2} = \sqrt{\frac{\pi}{2}} s e^{-(sx)^2/2}$

¹See https://proofwiki.org/wiki/Laplace_Transform_of_Cosine

²See <https://www.wolframalpha.com/input/?i=integrate+cos%28a+x%29+e%5E%28-x%5E2%2F2%29+dx+from+0+to+infty>

1970

A.3. Half-Normal Distribution

1971 The moments of the half-normal distribution (HN)³ are used several times. Its PDF is defined as

$$(A.9) \quad p_{HN}(x; \sigma) := \sqrt{\frac{2}{\pi}} \frac{1}{\sigma} e^{-x^2/(2\sigma^2)}, \quad x > 0$$

1972 which is a special case of GG with $d = 1, p = 2, a = \sqrt{2}\sigma$. Its moments are

$$(A.10) \quad E_{HN}(T^n) = \sigma^n \frac{2^{n/2}}{\sqrt{\pi}} \Gamma\left(\frac{n+1}{2}\right)$$

1973 which are the same as those of a normal distribution.

³See https://en.wikipedia.org/wiki/Half-normal_distribution

Bibliography

- 1975 [1] Adelchi Azzalini. *The Skew-Normal and Related Families*. Institute of Mathematical Statistics Monographs. Cambridge University Press, 2013.
- 1976 [2] H. Bateman and A. Erdélyi. *Higher Transcendental Functions*, volume 3 of *California Institute of Technology Bateman Manuscript Project*. McGraw-Hill Book Company., 1955.
- 1977 [3] Berndt Bruce C. *Ramanujan's Notebooks, Part I*. Springer New York, NY, 1985.
- 1978 [4] John C. Cox, Jonathan E. Ingersoll, and Stephen A. Ross. A theory of the term structure of interest rates. *Econometrica*, 53(2):385–407, 1985.
- 1979 [5] J.C. Crisanto-Neto, M.G.E. da Luz, E.P. Raposo, and G.M. Viswanathan. An efficient series approximation for the lévy α -stable symmetric distribution. *Physics Letters A*, 382(35):2408–2413, 2018.
- 1980 [6] NIST Digital Library of Mathematical Functions. <https://dlmf.nist.gov/>, Release 1.2.0 of 2024-03-15. F. W. J. Olver, A. B. Olde Daalhuis, D. W. Lozier, B. I. Schneider, R. F. Boisvert, C. W. Clark, B. R. Miller, B. V. Saunders, H. S. Cohl, and M. A. McClain, eds.
- 1981 [7] William Feller. Two singular diffusion problems. *Annals of Mathematics*, 54(1):173–182, 1951.
- 1982 [8] William Feller. On a generalization of marcel riesz' potentials and the semi-groups generated by them. *Meddelanden Lunds Universitets Matematiska Seminarium*, pages 73–81, 1952.
- 1983 [9] William Feller. *An Introduction to Probability Theory and its Applications (2nd Edition)*, volume 2. John Wiley & Sons, Inc., 1971.
- 1984 [10] Wikimedia Foundation. Inverse distribution, 2023. Retrieved December 1, 2023, from https://en.wikipedia.org/wiki/Inverse_distribution.
- 1985 [11] George Karagiannidis and Athanasios Lioumpas. An improved approximation for the gaussian q-function. *IEEE Communications Letters*, 11:644–646, 08 2007.
- 1986 [12] Paul Lévy. *Calcul des Probabilités*. Gauthier-Villars, 1925.
- 1987 [13] Xiaoyue Li and John M. Mulvey. Optimal portfolio execution in a regime-switching market with non-linear impact costs: Combining dynamic program and neural network. *arXiv preprint*, 6 2023. Available at arXiv: <https://arxiv.org/abs/2306.08809>.
- 1988 [14] Stephen H.T. Lihn. Stable count distribution for the volatility indices and space-time generalized stable characteristic function. *SSRN Working Paper*, 7 2020. Available at SSRN: <https://ssrn.com/abstract=3659383>.
- 1989 [15] Stephen H.T. Lihn. Generalization of the alpha-stable distribution with the degree of freedom. *arXiv preprint*, 5 2024. Available at arXiv: <https://arxiv.org/abs/2405.04693>.
- 1990 [16] F. Mainardi. *Fractional Calculus and Waves in Linear Viscoelasticity: An Introduction to Mathematical Models*. Imperial College Press, 2010. See Appendix F at <https://appliedmath.brown.edu/sites/default/files/fractional/36%20TheWrightFunctions.pdf>.
- 1991 [17] Francesco Mainardi and Armando Consiglio. The wright functions of the second kind in mathematical physics. *Mathematics*, 8(6), 2020.
- 1992 [18] Francesco Mainardi, Yuri Luchko, and Gianni Pagnini. The fundamental solution of the space-time fractional diffusion equation. *Frac. Calc. Appl. Anal.*, 4, 03 2007. See <https://arxiv.org/abs/cond-mat/0702419>.
- 1993 [19] Francesco Mainardi and Gianni Pagnini. Mellin-barnes integrals for stable distributions and their convolutions. *Fractional Calculus and Applied Analysis*, 11:443–456, 2008.
- 1994 [20] Arak Mathai and Hans Haubold. *Fractional and Multivariable Calculus: Model Building and Optimization Problems*. Springer Cham, 12 2017.
- 1995 [21] Hjalmar Mellin. Zur theorie zweier allgemeinen klassen bestimmter integrale. *Acta Societatis Scientiarum Fennicæ*, page 1–75, 1897.
- 1996 [22] The mpmath development team. *mpmath: a Python library for arbitrary-precision floating-point arithmetic (version 1.3.0)*, 2023. <http://mpmath.org/>.
- 1997 [23] Yuqi Nie, John M. Mulvey, H. Vincent Poor, Chenyu Yu, and Hao Huang. Deep generative models meet statistical methods: A generalized framework for financial regime identification. *SSRN*, 2024. Available at SSRN: <https://ssrn.com/abstract=5332057>.
- 1998 [24] John Nolan. *Univariate Stable Distributions, Models for Heavy Tailed Data*. Springer Cham, 01 2020.

- 2023 [25] Donald B. Owen. Tables for Computing Bivariate Normal Probabilities. *The Annals of Mathematical Statistics*, 27(4):1075 – 1090, 1956.
- 2025 [26] Richard B. Paris, Armando Consiglio, and Mainardi Francesco. On the asymptotics of wright functions of the second kind. *Fract. Calc. Appl. Anal.*, 24(1):54–72, 01 2021.
- 2027 [27] Dimiter Prodanov. Computation of the wright function from its integral representation. In *Advances in Nonlinear Dynamics*, volume 1, pages 421–431. Springer Nature Switzerland, 05 2024.
- 2029 [28] W. R. Schneider. Stable distributions: Fox function representation and generalization. In S. Albeverio, G. Casati, and D. Merlini, editors, *Stochastic Processes in Classical and Quantum Systems*, pages 497–511, Berlin, Heidelberg, 1986. Springer Berlin Heidelberg.
- 2032 [29] Y. Shu, C. Yu, and J.M. Mulvey. Downside risk reduction using regime-switching signals: a statistical jump model approach. *Journal of Asset Management*, 25:493–507, 2024.
- 2034 [30] E. W. Stacy. A generalization of the gamma distribution. *The Annals of Mathematical Statistics*, 33(3):1187 – 1192, 1962. See also https://en.wikipedia.org/wiki/Generalized_gamma_distribution.
- 2036 [31] Student. The probable error of a mean. *Biometrika*, 6:1–25, 1908. See also https://en.wikipedia.org/wiki/Student%27s_t-distribution.
- 2038 [32] Y.L. Tong. *The Multivariate Normal Distribution*. Research in Criminology. Springer New York, 1990.
- 2039 [33] Pauli Virtanen, Ralf Gommers, Travis E. Oliphant, Matt Haberland, Tyler Reddy, David Cournapeau, Evgeni Burovski, Pearu Peterson, Warren Weckesser, Jonathan Bright, Stéfan J. van der Walt, Matthew Brett, Joshua Wilson, K. Jarrod Millman, Nikolay Mayorov, Andrew R. J. Nelson, Eric Jones, Robert Kern, Eric Larson, C J Carey, İlhan Polat, Yu Feng, Eric W. Moore, Jake VanderPlas, Denis Laxalde, Josef Perktold, Robert Cimrman, Ian Henriksen, E. A. Quintero, Charles R. Harris, Anne M. Archibald, Antônio H. Ribeiro, Fabian Pedregosa, Paul van Mulbregt, and SciPy 1.0 Contributors. SciPy 1.0: Fundamental Algorithms for Scientific Computing in Python. *Nature Methods*, 17:261–272, 2020.
- 2046 [34] E. M. Wright. On the coefficients of power series having exponential singularities. *Journal London Math. Soc.*, s1-8, Issue 1 (1933):71–79, 1933.
- 2048 [35] E. M. Wright. The asymptotic expansion of the generalized bessel function. *Proc. London Math. Soc.*, s2-38, Issue 1 (1935):257–270, 1935.